

THESIS

TERTIARY LAKE SEDIMENTATION IN THE ELKO FORMATION, NEVADA—THE  
EVOLUTION OF A SMALL LAKE SYSTEM IN AN EXTENSIONAL SETTING

Submitted by

William H. Horner

Department of Geosciences

In partial fulfillment of the requirements

For the Degree of Master of Science

Colorado State University

Fort Collins, Colorado

Fall 2015

Master's Committee:

Advisor: Sven O. Egenhoff

Dennis Harry

Joe von Fischer

Robert Amerman

Copyright by William H. Horner 2015

All Rights Reserved

## ABSTRACT

### TERTIARY LAKE SEDIMENTATION IN THE ELKO FORMATION, NEVADA—THE EVOLUTION OF A SMALL LAKE SYSTEM IN AN EXTENSIONAL SETTING

The Lower to Middle Eocene Elko Formation of northeastern Nevada consists of basal coarse-grained siliciclastics and carbonates which are overlain by an organic-rich succession consisting of fine-grained siliciclastics, in places with fine-grained carbonates, and fine- to coarse-grained volcanoclastics at the top. Based on lithological and sedimentological characteristics in four documented localities arranged along a north-south transect, the succession shows fourteen facies, which are grouped into five facies associations (FAs): Siliciclastic mudstones and conglomerates (FA1); Massive coal-rich mudstones (FA2); Microbial-mat-bearing mudstones and carbonates (FA3); Microbial-mat-bearing mudstones and volcanoclastics (FA4); Carbonates and volcanoclastics (FA5).

The succession is interpreted to reflect deposition in a broad continental-lacustrine setting. FA1 rocks record sedimentation in the most proximal environment, consisting of alluvial-fluvial sedimentation. FA2 rocks reflect deposition in a marginal low-energy swamp environment, while FA3 rocks denote “open-water” lacustrine sedimentation in a limnetic setting that was highly sensitive to lake-level fluctuations. FA4 rocks record the onset of extrabasinal airfall tuff in the limnetic portion of the lake, and FA5 rocks record volcanoclastic sedimentation outpacing subsidence in the lake, ultimately “filling” up available accommodation space and ending lacustrine sedimentation.

The studied succession is subdivided into four vaguely chronostratigraphic intervals referred to as Stratigraphic Intervals 1 to 4, which record a lake system with significant lateral changes in accommodation space and resulting facies patterns in a north to south progression through time. Based on two recent  $^{40}\text{Ar}/^{39}\text{Ar}$  dates and four previous radiometric age dates, the northern outcrop, which is significantly older than the central and southern ones, records initial subsidence and the onset of lake sedimentation (Stratigraphic Interval 1). Subsidence varied over time causing the lacustrine depocenter and limnetic depozone to progressively shift southwards (Stratigraphic Intervals 2 through 4). Black shale source rocks in the measured sections therefore occur along the entire north-south transect of the studied lacustrine system, yet they represent rocks of different ages not correlatable throughout the Elko Formation. Coeval volcanism, which led to increased volcanoclastic sediment supply, followed black shale deposition and contributed to the north-south “filling in” of the lake system, ultimately culminating with the end of lacustrine sedimentation around 37.5 Ma.

The Elko Formation black shales have high source rock potential as an unconventional resource play, as their organic content consists almost entirely of Type-I (oil prone) kerogen. Contrary to deep-water, thermally-stratified anoxic-lake source rock models, long considered to be the only environments in which significant organic-matter preservation may have occurred, this study provides evidence for black shale deposition in the Elko lake to have occurred within a “shallow,” mostly *oxic* environment in the photic zone. Further, this research indicates that depositional environments in lacustrine settings may be scale-dependent. The Elko Formation is not merely a scaled-down version of large-lake systems, such as that in which the Green River Formation formed, but a unique type of system with its own set of controls. With increased industry attention being placed on this potential lacustrine petroleum system, this study provides a new source rock

model, as well as a temporal and spatial framework to be used as a predictive tool for the identification of rich source rock intervals in the Elko Basin.

## ACKNOWLEDGEMENTS

I am especially grateful for my advisor, Dr. Sven Egenhoff, for his continued feedback, insight, thought-provoking questions, and guidance throughout the duration of this project. More thanks are extended for the many hours he spent editing this thesis and improving my writing.

I have a great deal of gratitude to Noble Energy for funding this project, and for providing such a great team of people who collaborated with me and provided valuable guidance and insight along the way: Thanks to Rob Amerman, Morgan Hocker, Rick Stucker, Donald Burch, and Wendell Bond. Further thanks to Jon Bowman for arranging a track-hoe for field excavations.

Thanks to my thesis committee members, Dr. Sven Egenhoff, Dr. Dennis Harry, Dr. Joe von Fischer, and Dr. Rob Amerman, for their insightful suggestions and comments that helped me grow as a researcher and a writer.

My sincere gratitude to the Tomera family for allowing me to study the Elko succession and even camp on their beautiful ranch. A special thanks to Sven Egenhoff, Rob Amerman, Morgan Hocker, Rick Stucker, Erin McGowan, and Curtis Gaver for all their help, excitement, and encouragement in the field. A lot of fun was had in Elko, NV. A very special thanks to Lostra Brothers Towing Company in Elko, NV for locating me in the most dire of situations and towing my rental truck out of a bog, 30 miles deep into the middle of nowhere. I thought life as I knew it was over...

Thanks to the CSU Sedimentology working group for all the help, thought-provoking discussion, laughs, and cries (almost) over the past two years. Like the lake systems I studied, the CSU Sedimentology work group was dynamic; it constantly shifted with people as they started and graduated. I am pleased to have gotten to know Matt Petrowsky, Damien Borcovsky, Stacie Albert, Ketki Kolte, Lauren Droege, Ali Cigri, Curtis Gaver, Erin McGowan, Kathleen Masterson, Kathryn Schuller, Oguzhan Kendigelen, and Eda Celep. Thanks for making this such an awesome place to spend the day.

Finally, thanks to my family and to Kathryn Mullinax for their continued love, encouragement, and support.

## TABLE OF CONTENTS

ABSTRACT.....	ii
ACKNOWLEDGEMENTS.....	v
TABLE OF CONTENTS.....	vii
1.0 INTRODUCTION .....	1
2.0 GEOLOGICAL SETTING .....	4
3.0 METHODOLOGY .....	10
4.0 SEDIMENTOLOGY .....	13
4.1 Sedimentary Facies .....	14
4.2 Facies Associations.....	22
4.2.1 Facies Association 1: Siliciclastic mudstones and conglomerates .....	23
4.2.2 Facies Association 2: Massive coal-rich mudstones.....	23
4.2.3 Facies Association 3: Microbial-mat-bearing mudstones and carbonates.....	24
4.2.4 Facies Association 4: Microbial-mat-bearing mudstones and volcanoclastics .....	25
4.2.5 Facies Association 5: Carbonates and volcanoclastics .....	26
5.0 FACIES ARCHITECTURE .....	29
5.1 Stratal Architecture along the North – South Transect .....	31
5.1.1 Stratigraphic Interval 1 .....	31
5.1.2 Stratigraphic Interval 2 .....	32
5.1.3 Stratigraphic Interval 3 .....	32
5.1.4 Stratigraphic Interval 4 .....	33
6.0 DEPOSITIONAL MODEL AND BASIN EVOLUTION.....	35
6.1 Depositional Model.....	35
6.2 Lake Evolution.....	40
6.2.1 Time 1 .....	42
6.2.2 Time 2 .....	42
6.2.3 Time 3 .....	43
6.2.4 Time 4 .....	44
7.0 DISCUSSION .....	46
7.1 Elko Formation Source Rock Model and Kerogen Type.....	46
7.2 Differences in the Depozones: Small Lakes vs. Large Lakes.....	47
7.3 Differences and Contradictions in Elko Formation radiometric age dates .....	48

7.4 Distribution of Volcaniclastic Material and its Relationship to Source Rock Quality .....	49
7.5 Unconventional Petroleum Exploration Possibilities .....	51
8.0 CONCLUSIONS.....	52
REFERENCES .....	55
APPENDICES .....	61
APPENDIX 1: COMPILATION OF NEW AND PREVIOUSLY PUBLISHED AGES FOR THE ELKO FORMATION REFERENCED IN THIS STUDY .....	62
APPENDIX 2: MEASURED AND DIGITIZED SECTIONS OF THE UPPER ELKO FORMATION, NORTHEAST NEVADA .....	63
Coal Mine Canyon .....	65
Elko Hills A and B.....	71
Tomera Ranch.....	74
APPENDIX 3: OUTCROP SATELLITE VIEWS WITH WAYPOINTS .....	79
APPENDIX 4: SEM DATA OF MICROBIAL-MAT-BEARING ORGANIC-RICH MUDSTONE (F5) .....	83

## 1.0 INTRODUCTION

As pioneers in a newly unconventional age, the world is concerned with finding and exploiting black shales. These organic-rich shales are not merely restricted to marine depositional environments, and as competition for these resources continues, renewed interest has emerged in lacustrine systems (Katz and Lin, 2014). Black shales are the primary target for the lacustrine Elko Formation unconventional resource play in Nevada, USA, yet the depositional processes controlling black shales are not fully understood due to the difficulties in observing internal structure of rock with such extremely fine grain size. While detailed research on mudstones is beginning to provide insight and criticism of old models for depositional processes in marine settings (e.g. Bohacs, 1993; Macquaker et al., 1998; Schieber, 1998; Macquaker and Howell, 1999; Wignall and Newton, 2001; Macquaker et al., 2007; Egenhoff and Fishman, 2013), temporal and spatial variations of black shale units in lacustrine settings are not yet adequately explored, especially in small-lake settings such as the Eocene Elko succession.

Hundreds of papers focus on the coeval Green River lakes (Lake Gosiute and Lake Uinta) of Utah, Colorado and Wyoming, however these lakes differ significantly from the Elko lake as they feature an enormous geographic extent (~100,000 km<sup>2</sup>), evidence for basin-wide desiccation events (Eugster and Surdam, 1973), and long periods of bottom-water anoxia due to thermal stratification of the water column (Sullivan, 1980). Rather than regarding the Green River lakes as the standard-bearer for all lacustrine systems, this research allows for the unique perspective of understanding lacustrine depositional processes in small-lake systems. Whereas previous research on the Elko Formation (e.g. Solomon et al., 1979; Haynes, 2003) has provided a broad geological framework, any thorough understanding of Elko Formation sedimentology is in its infancy. The goal of the

present study is therefore to use a basin-wide facies and stratal architecture approach to build the first detailed depositional model of the lake-filling Elko succession for its 8-million-year depositional history. Topics addressed in this study include (1) a relationship between Elko lake evolution and formation of organic-rich deposits, (2) the validity of a deep-water anoxic source rock model for the Elko Basin as advocated by Haynes (2003), (3) evidence for a shifting basinal depocenter through time, and (4) a comparison between organic-rich deposits of the Elko Formation and the often cited Green River Formation (e.g. Carroll and Bohacs, 1999; Keighley et al., 2003; M. Smith et al., 2008; Tānavsuu-Milkeviciene and Sarg, 2012). Decimeter-scale outcrop descriptions, thin section analysis, and tuff age dates from four outcrops, representing a complete SSE-NNW transect of the Elko Basin (see Figure 1), are combined in this study to understand the processes controlling deposition and sediment architecture of the Elko Formation.

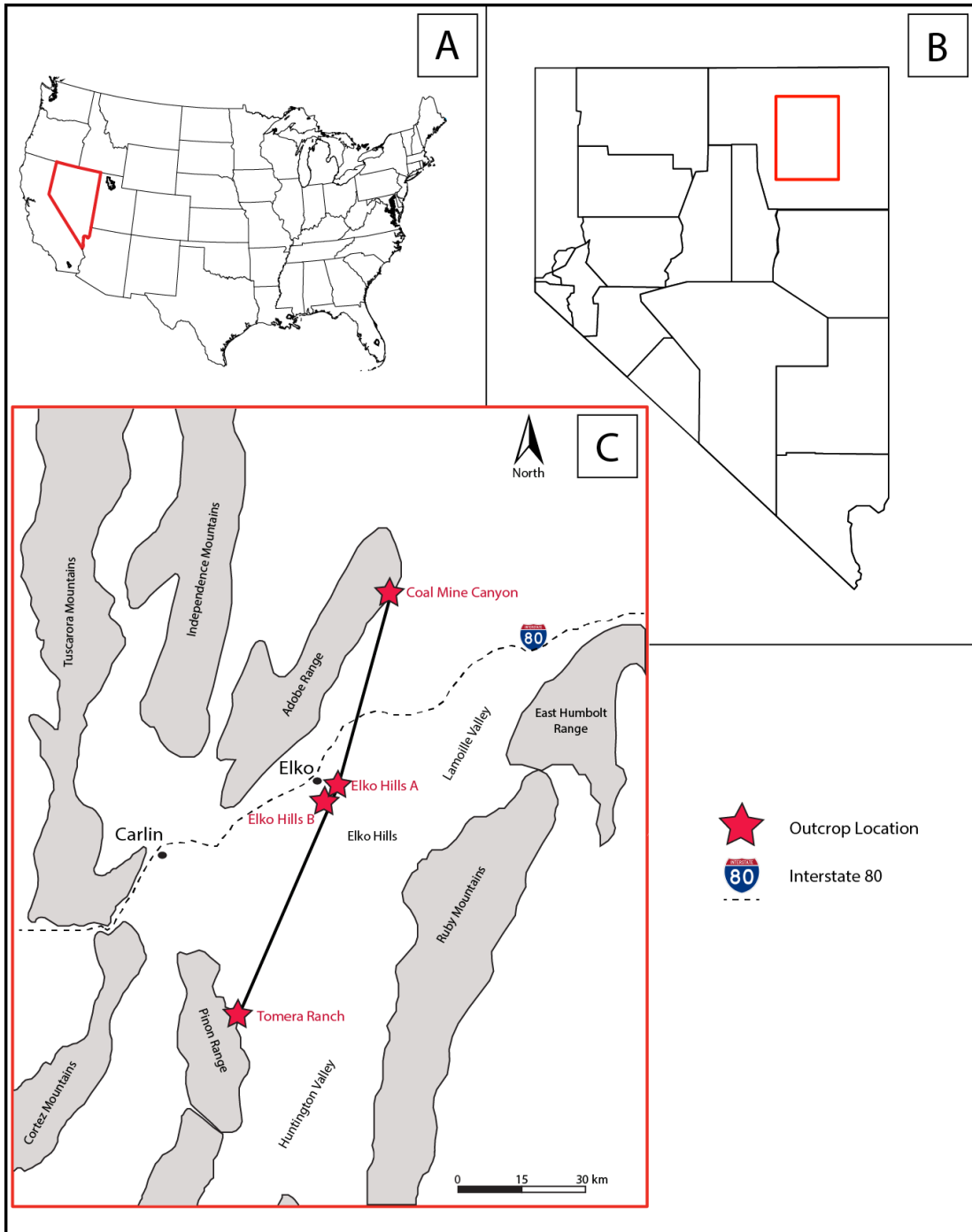


**Figure 1:** Map of the study area with outcrops and surrounding mountain ranges in northeastern Nevada, USA. Black line denotes transect incorporating the four Elko Formation successions used as part of this study (illustrated in appendix 1). Base map is modified from J. Smith et al., (1976).

## **2.0 GEOLOGICAL SETTING**

The Elko Basin represents a late to middle Eocene-age regional depression in northeastern Nevada. It formed during a period of extension and tectonic subsidence as an asymmetric half-graben in the hanging wall of the Ruby Mountains-East Humboldt Range (RMEH; Haynes, 2003). The fossil assemblage in the Eocene basin fill includes flora (sumac, redwood, swamp cypress, maple, and alder) that indicate a warm and temperate paleoclimate, allowing for swamps and extensive forests to ring the lake(s) throughout the basin (Wingate, 1983; Haynes, 2003).

### **2.1 Regional Tectonism and Volcanism**

Northeast Nevada underwent multiple episodes of contraction during the Antler Orogeny in the late Paleozoic and early Mesozoic and was succeeded by multiple episodes of extension beginning in the Eocene (Henry, 2008). The region was in the hinterland of the Late Cretaceous Sevier orogenic belt with continental crust around 50-60 km thick (Decelles, 2004). By the beginning of the Cenozoic, Northeast Nevada was part of an eroding plateau with elevations of at least 3 km due to thickening of the crust during the Sevier Orogeny (DeCelles, 2004).

Sedimentary basins began to form in this plateau in the Eocene from extensional processes including the Elko Basin, which began forming in the early Eocene with initial exhumation of the Ruby Mountains (McGrew et al., 2000). Another episode of Eocene extension tilted the Elko Formation strata 10 to 15 degrees southeast before 38.0 Ma (Ketner and Alpha, 1992; Haynes, 2003). This deformation may have caused a local angular unconformity between the Elko Formation and the Indian Well formation (J. Smith et al., 1976; Ketner and Alpha, 1992).

Major Basin and Range style extension commenced in Northeast Nevada during the middle Miocene resulting in pronounced uplift of the Ruby Range around 15.0 Ma (Colgan and Metcalf,

2006). Steep normal faults associated with this extension cut through the Elko basin to form a series of north-south trending mountain range fault blocks, characteristic of the distinct Basin and Range Province physiography that is evident today (J. Smith et al., 1976). Miocene deformation was the most impactful series of events in governing where the Elko Formation is exposed, eroded, and buried in the subsurface at present day. Middle to late Miocene extension stretched the upper crust by ~10% in northeast Nevada (Muntean et al., 2001), which may cause for estimations of Elko Basin extent and Elko Formation stratigraphic thicknesses to be much greater than actuality.

Magmatism began around 45.0 Ma in northeastern Nevada as part of a southward-trending belt that migrated from Washington and Idaho (Christiansen and Yeats, 1992; Henry, 2008). The middle Eocene magmatism was predominantly andesite to dacite lavas, however, rhyolitic ash-flow tuffs also erupted during this time (Haynes, 2003; Henry, 2008). This pulse of magmatism was contemporaneous with Eocene extension and ended by 35.0 Ma (Henry, 2008). A second pulse of volcanism in the region occurred in the Miocene around 16.5 Ma (Coats, 1964; Henry, 2008).

## **2.2 Basin Shape and Extent**

Solomon (1992) estimates the basin to have extended over 28,000 km<sup>2</sup>. However, basin size and shape are still being refined: While most researchers have interpreted the RMEH as the eastern boundary of the basin, studies largely disagree on the western extent. Some researchers suggest that the basin is bound to the west by the Adobe Range (e.g. J. Smith et al., 1976, Solomon and Moore, 1982; Figure 2A), though others postulate the presence of Eocene lacustrine strata west of the Adobe Range and suggest the Tuscarora Mountains as the westward cutoff for the Elko Basin

(Henry and Faulds, 1999; Haynes, 2003; Figure 2B). Even more uncertain is whether the Elko Basin represents a single, large basin (J. Smith et al., 1976; Solomon, 1992; Christiansen and Yeats, 1992; Wallace et al., 2008), a network of small, isolated basins (Nutt and Good, 1998), or a single, large basin separated into lithologically distinct eastern and western parts by a paleotopographic high (Haynes, 2003).

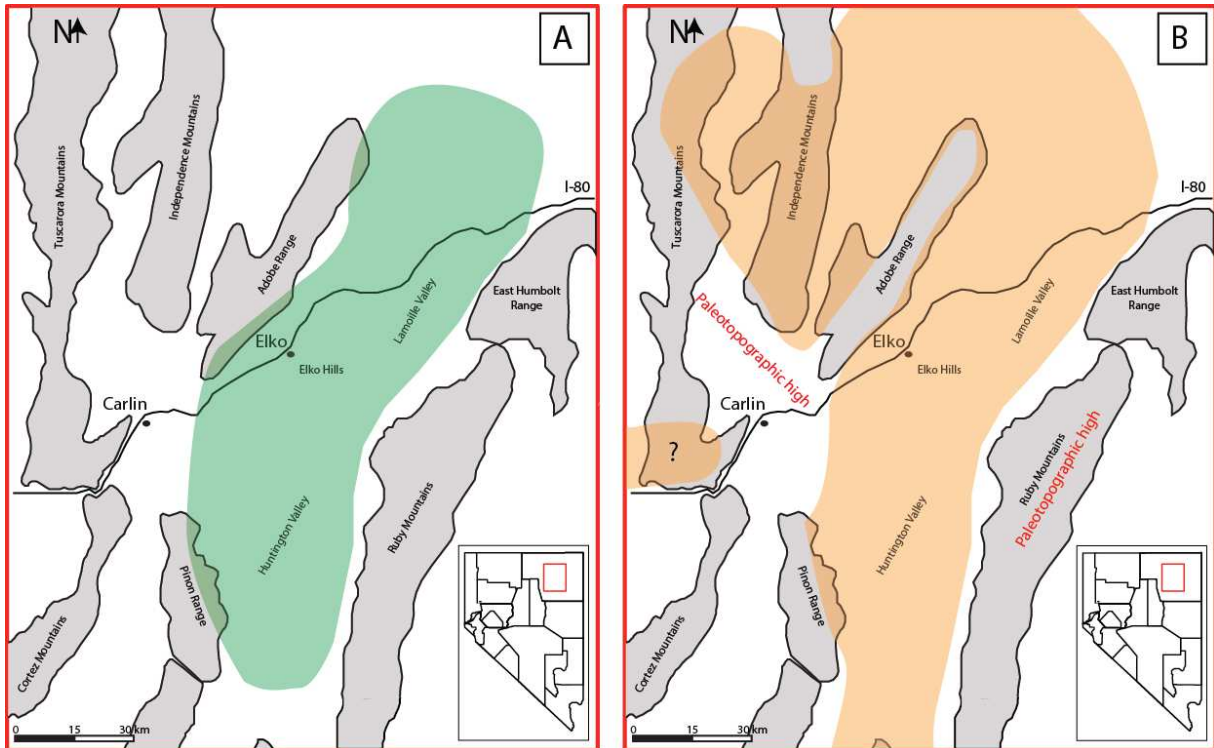


**Figure 2:** (A) Approximate lateral extent of the Elko Basin based on Elko Formation distribution in Solomon and Moore (1982); (B) Approximate lateral extent of the Elko Basin modified from Haynes (2003). Ruby Mountains and Adobe Range are thought to have been paleohighs in the Eocene (Haynes, 2003). Base map modified from J. Smith et al. (1976).

### 2.3 Elko Formation Stratigraphy

The lithologically diverse Eocene Elko Formation consists of conglomerate, sandstone, black shale, mudstone, siltstone, limestone, and tuff (e.g. J. Smith et al., 1976; Solomon et al., 1979). Initial lower member Elko Formation sediment deposition in the Elko Basin unconformably overlies Paleozoic rocks and consists of boulder-size conglomerates, which were deposited as

mixed alluvial-fluvial systems being shed from Eocene paleohighs (Haynes, 2003). With increasing basin subsidence, shallow lacustrine sediments consisting primarily of middle member cherty limestone were first deposited (Haynes, 2003). Regional subsidence continued east of the Adobe Range causing the lake(s) to deepen, allowing for deposition of the black shale that is diagnostic of the upper member of the Elko Formation. As the lake approached its maximum extent, coeval extrabasinal volcanism increased and basin-fill became predominately volcanoclastic (Haynes, 2003). The Eocene Indian Well Formation effectively filled the lake(s) and marked an end to Eocene lacustrine sedimentation (Solomon et al., 1979; Haynes, 2003). The Oligocene in this area records ash tuffs, but little non-volcanic deposition (Henry and Faulds, 1999). It probably represents a quiescent period with little siliciclastic deposition before a second episode of major regional extension commenced during Miocene time. Pronounced fluvial-lacustrine deposition with common vitric ash and tuff filled the basin from the Miocene (Humboldt Formation) to Pleistocene time (Hay Ranch Formation) (J. Smith et al., 1976).

Discrepancies in Elko basin scale can be in part attributed to conflicting opinions on Elko Formation nomenclature: J. Smith et al. (1976), Fouch et al. (1979), Solomon and Moore (1982), and Server and Solomon (1983) relegate the Elko Formation only to the oil shale-bearing successions that outcrop east of the Adobe and Piñon Ranges. Other Eocene sedimentary rocks in the area were mapped as “Tertiary conglomerate” and “Tertiary cherty limestone” (Coats, 1987). In contrast, Ketner and Alpha (1992) and Haynes (2003) include the “Tertiary cherty limestone” and “Tertiary conglomerate” units that outcrop both east and west of the Adobe Range to be part of the Elko Formation by designating the cherty limestone as the Elko Formation Middle Member and the conglomerate as the Elko Formation Upper

Member. In accordance with Ketner and Alpha (1992) and Haynes (2003), this paper marks the base of the Elko Formation with the, “Tertiary conglomerate unit,” or lower member, as it reflects the initial Eocene basin alluvial filling stage and is genetically associated with subsequent lacustrine deposition (Haynes, 2003).

The upper Elko Formation (the same interval sources previous to Ketner and Alpha (1992) and Haynes (2003) considered to be the *entire* Elko Formation), is the focus of this study, as it is the only Elko Formation member to contain organic-rich black shales. In the upper Elko Formation, many different facies names are used by various authors to describe the same groupings of strata. These previous subdivisions are based on lithostratigraphy at individual measured sections, but many are coeval in different portions of the Elko lake. The present paper uses facies associations, instead of a more traditional stratigraphic nomenclature. Figure 3 shows how previous facies subdivisions in the upper Elko Formation temporally relate to each other and to the facies associations proposed in this study.

Solomon et al., (1979) Elko Hills	Solomon and Moore (1982) Elko Hills	Wingate (1983) Coal Mine Canyon	Haynes (2003) Elko Hills	This study
Member 5 Tuff and rare shale and siltstone	Tuff shale and siltstone member	Unit 5 Claystones, siltstones, and coarse-grained sandstones	Tuffaceous shale facies	FA 5: carbonates and volcanoclastics
Member 4 Tuff, shale, and bituminous siltstone				FA 4: Microbial-mat-bearing mudstones and volcanoclastics
Member 3 Oil shale and rare limestones	Siltstone and oil shale member	Unit 4 Limestones and paper shales	Oil shale facies	FA 3: Microbial-mat-bearing mudstones and carbonates
Member 2 Oil shale, lignite, and tuff		Unit 3 Sandstones, siltstones, and shales		
		Unit 2 Claystones, siltstones, and coals		
Member 1 Chert-pebble conglomerates	Basal dolomite, oil shale, claystone, and conglomerate member	Unit 1 Chert-pebble conglomerates and siltstones	Calcareous shale facies	FA 1: Siliciclastic mudstones and conglomerates

**Figure 3:** Correlation chart of similar stratigraphic units (with different names) of upper Elko Formation strata throughout the history of Elko Formation research.

### 3.0 METHODOLOGY

This study incorporates data from four Elko Formation outcrop localities that form a transect in northeastern Nevada, here listed from north to south, and termed: (1) Coal Mine Canyon, (2) Elko Hills A (3), Elko Hills B, and (4) Tomera Ranch. Localities were intentionally chosen to correspond to trenches formed in Elko Formation rocks by the USGS in the 1970's for oil shale investigations (e.g. J. Smith et al., 1976; Moore et al., 1983). Outcrops of the Elko Formation are uncommon and only preserved at the surface along Miocene-age bounding faults (Haynes, 2003), so the chosen localities represent the only known oil-shale-bearing Elko Formation outcrops. Outcrop trenches were weathered and generally filled; therefore, a shovel and garden hoe were used to expose less weathered strata. The Tomera Ranch section was heavily weathered; here a track-hoe excavator was used to dig into the hillside up to 6 feet deep in effort to expose all possible strata (Figure 4).



**Figure 4:** A Track-hoe excavator was used to expose strata at the Tomera Ranch section. Picture is from the base of the section and is facing northeast.

At each outcrop, a detailed sedimentological section was measured by use of a 5.5-foot measuring stick with a leveling arm and mm to cm indentations, allowing for precise measurement of cm-scale stratigraphic features and lithological changes. Strike and dip were determined in areas of exposed bedding by using a Brunton compass and stratigraphic measurements were subsequently made by orienting the measuring stick at the angle of dip, perpendicular to strike. Some beds were highly weathered and contained no apparent bedding. In these instances, dip angles were approximated based on orientations of the beds directly under- and overlying the weathered interval. Along each measured section, GPS waypoints with WGS 1984 coordinates were taken at sample localities and significant facies changes. The four measured sections with descriptions and waypoint locations were drafted at decimeter scale using Adobe Illustrator® (Appendix 2).

80 samples were selected from the four outcrop localities for thin section analysis, and underwent different treatments depending on lithology. Mudstone thin sections were prepared by Wagner Petrographics in Lindon, UT where they were ground to 20- $\mu\text{m}$  thickness, impregnated with red fluorescent epoxy and polished. Thin sections consisting of coarse-grained (predominately silt, sand, and gravel-size) siliciclastics, volcanoclastics, and carbonates were prepared by Spectrum Petrographics in Vancouver, WA. Thin sections consisting of siliciclastics and volcanoclastics were ground to 30- $\mu\text{m}$  and carbonates were ground to 40- $\mu\text{m}$  thickness; both were impregnated with blue epoxy to display porosity and polished.

Thin sections were viewed in plane polarized and cross polarized light using a Leica DM 2500 P petrographic microscope and a Nikon H550S petrographic microscope at Colorado State University. Thin sections were used to delineate mineralogy and other critical components such as sub-mm scale sedimentary structures, organic matter, and any fossil content. These structures and

components were used to identify the origin of clastic materials and the sedimentary processes occurring at the time of and after deposition.

Eight thin section samples were further analyzed with a JEOL 5800LV scanning electron microscope (SEM) equipped with an energy dispersive spectrometer (EDS) at the United States Geological Survey in Denver, CO. The SEM was used to provide high-resolution images of grains and diagenetic cements with much higher focus than standard petrographic microscope can provide. EDS was used to understand elemental composition of grains, especially within the clay matrix, which is often indiscernible in a standard petrographic microscope. SEM data is attached as Appendix 4.

Two tephra samples were sent to the Oregon State University Geochronology Lab in Corvallis, OR to carry out  $^{40}\text{Ar}/^{39}\text{Ar}$  age analysis. A standard radiometric dating process was used where biotite phenocrysts were first separated from altered matrix by crushing, sieving, washing and drying, then passed through a Frantz magnetic separator. This was followed by mild acid cleaning (1 N acetic acid to remove carbonates, 1 N  $\text{HNO}_3$  to remove minor alteration), ultrasonic washing in DI water, drying, and a final hand-picking under a binocular microscope. After careful selection, unaltered biotite phenocrysts were analyzed using a Map 215-50 mass spectrometer equipped with the ArArCALC v 2.4 software package to determine their absolute age (Koppers, 2002).

#### **4.0 SEDIMENTOLOGY**

The Elko Formation is heterogeneous; its facies consist of varieties of all major sediment types including siliciclastics, organics, carbonates, and volcanoclastics. Detailed outcrop logging of four sections and petrographic observations of 80 thin sections allow the upper member of the Elko Formation to be subdivided into 14 distinct facies based on visual grain size estimates, lithology, and sedimentary structures (Table 1). Outcrop logs are presented in Appendix 2. Facies nomenclature is modified from Macquaker and Adams (2003) for fine-grained siliciclastics, and it follows Dunham (1962) for carbonates and Friedman et al. (1992) for volcanoclastics.

## 4.1 Sedimentary Facies

**Table 1:** Summary of facies attributes observed within the upper Elko Formation. Examples of each facies are illustrated in Figures 5 and 6.

	<b>Facies</b>	<b>Facies Thickness</b>	<b>Description and Sedimentary Structures</b>	<b>Composition</b>	<b>Interpretation</b>
<b>1</b>	Bituminous Coal	1-3 cm	Massive fabric with distinct “blocky” texture Beds are often lenticular (10-20 cm length) Vertically associated with lignite facies	90-95% terrigenous plant material or macrophytes 5-10% fine to medium silt-size detrital quartz	Fine grain size (clay and silt) suggests low energy conditions (initial suspension settling of plant material and <i>in situ</i> development of subbituminous coal?)
<b>2</b>	Lignite	15-125 cm	Massive fabric Broken or whole fossil leaves and woody detritus occur on bedding planes Locally contains slip surfaces with parallel striations (i.e. slickensides) Contains abundant root traces	60-80% terrigenous plant material or macrophytes 10-35% siliciclastic clay matrix 5-10% fine to medium silt-size detrital quartz	Fine grain size (clay and silt) suggests low energy depositional conditions (initial suspension settling and <i>in situ</i> development of lignite?) Broken or whole fossil leaves and woody detritus on bedding planes suggest deposition through suspension settling for organic matter Slickensides denote contracting and swelling of expansive clay minerals (e.g. Gray and Nickelsen 1989; Retallack, 1990)
<b>3A</b>	Massive siliciclastic mudstone	5-215 cm	No internal structure Variegated colors (grey, green, brown) Commonly unconsolidated Silt-rich clastic dykes commonly disrupt bedding Locally contains wispy organic material	70-85% siliciclastic clay matrix 5-15% fine to medium silt-size detrital quartz or volcanic lithoclasts 0-15% organic material	Fine-grain size (clay and silt) suggest low-energy conditions upon deposition Structureless fabric and dispersed silt grains indicate deposition after deceleration of fluid mud flows (Plint, 2014) or syndimentary liquefaction and/or fluidization, likely triggered by tectonism (Sims, 2013)
<b>3B</b>	Massive root-bearing siliciclastic mudstone	15-400 cm	Massive fabric with irregular, patchy distribution of clay-rich and organic-rich zones Commonly unconsolidated Contains abundant root traces Breaks apart in peds	60-70% siliciclastic clay matrix 20-30% fine to medium silt-size detrital quartz 0-10% organic material	Fine-grain size (clay and silt) suggests low-energy conditions upon deposition Subangular to subround silt grains indicate aeolian or water-lain deposition

			Locally contains slip surfaces with parallel striations (i.e. slickensides)		Peds and root traces suggest moderate to strong paleosol development in a terrestrial environment Massive fabric attributed to bioturbation and/or pedoturbation (Renaut and Gierlowski-Kordesch, 2010) Slickensides denote contracting and swelling of expansive clay minerals (e.g. Gray and Nickelsen 1989; Retallack, 1990)
4	Calcareous mudstone	0.1-200 cm	Discontinuous to continuous undulating to planar-laminations of uneven to even thickness mm apart Quartz silt is often dispersed in carbonate mud laminae Coarse silt to sand-rich laminae often scour underlying carbonate mud laminae Laminae contain no internal structures Clastic dykes, micro-normal faults, and water-escape structures commonly disrupt laminae and form convolute bedding Mm-scale stromatolites occur locally	60-90% carbonate mud and/ or microcrystalline dolomite matrix 10-40% fine to coarse silt-size detrital quartz (100% diagenetically altered to chert in middle member Elko Formation)	Non-erosive, planar-laminae of even thickness suggest phases of suspension-settling of carbonate mud Undulating to planar laminae of uneven thickness and basal erosional scours suggest instances bedload transport (Schieber et al., 2013) Clastic dykes, slumps, micro-normal faults, and water-escape structures indicate fluidization and/or liquefaction, likely triggered by a tectonic source (Sims, 2013)
5	Laminated microbial-mat-bearing mudstone	10-225 cm	Contain “wavy-crinkly” organic-rich laminae of sub-mm thickness and planar clay laminae of ~1-2 mm thickness Medium-silt to fine-sand grains are dispersed and often surrounded by sub-mm organic-rich laminae Clay generally occurs in lenses Locally contains ostracods (~1 mm), bivalves (3-5 mm), gastropods (~1 cm), fish (up to 1cm), leaves, wood detritus, and pollen spores Extremely fissile in outcrop	40-80% organic-rich mud mats 10-40% siliciclastic clay matrix 5-20% fine to medium silt-size detrital quartz and/ or volcanic lithoclasts	In-situ growth of benthic cyanobacterial microbial mats Lenticular clay laminae indicate instances of bedload transport of clay-sized material independent of microbial mats Microbial mats baffle isolated quartz silt, organic detritus, and volcanic silt grains from suspension and are most prevalent during periods of non-sedimentation
6	Massive ash-bearing mudstone	0.1-125 cm	No internal structure Locally contains fossil wood detritus and other amorphous organic detritus on bedding planes Vesicular in places	60-80% clay matrix 0-20% organic detritus 0-20% fine to coarse silt-size quartz	Fine grain size (clay and silt) suggests low-energy processes (suspension settling of ash, clay, and silt after volcanic events?)

			Vertically associated with microbial mat-bearing organic rich mudstone	0-20% fine to coarse silt-size plagioclase	Vesicular texture attributed to gas expansion formed during rapid cooling of ash Organic detritus on bedding planes suggest deposition of organic matter through suspension along with ash
7	Laminated silt- to sand-bearing siliciclastic mudstone	2-125 cm	Discontinuous to continuous planar laminae of uneven to even thickness (sub-mm to 3mm thick) Massive structure within laminae is predominant Coarse-tail grading of siliciclastic silt to sand locally occurs in 3mm thick, continuous, poorly sorted mudstone laminae	60-80% siliciclastic clay matrix 20-40% fine to medium silt-size detrital quartz 0-40% fine to medium sand-size detrital quartz	Sub-mm thick laminae of even thickness suggest periods of suspension settling Planar-laminae of uneven thickness with silt to sand-size grains suggest some bedload transport Few continuous laminae of coarse-tail graded, poorly sorted silt in a mud matrix indicates debris flows as a possible transport mechanism (Fisher, 1971)
8	Fossiliferous wackestone	5-60 cm	Massive fabric Contains broken to whole ostracods (~1 mm) and/ or gastropods (~1 cm) Clastic dykes (consist of massive siltstone) and water-escape structures in places Commonly interbedded with microbial mat-bearing organic-rich mudrock (F5)	70-90% micrite and/or microcrystalline dolomite matrix 10-30% carbonate shells 0-10% medium to coarse silt-size detrital quartz	Transport of carbonate mud either through suspension (Flügel, 2010), or bedload processes (Schieber et al., 2013)
9	Siliciclastic sandstone	0.2-50 cm	No internal structure Commonly occurs as distinct sandstone laminae (~5 mm thick) in carbonaceous mudstone facies Poorly-sorted with angular to sub-angular grains Scours underlying mudrock units Lenticular in places Contains clastic dykes and vertical water escape structures	40-80% fine to coarse sand-size detrital quartz 0-30% fine to coarse sand-size volcanoclastic lithoclasts 20-60% siliciclastic clay matrix	Erosional scours of underlying sediment, local lenticular bedding, and sand-size grains suggest high-energy, bedload transport Clastic-dykes and water-escape structures suggest fluidization and/or liquefaction, likely triggered by tectonic activity (Sims, 2013)
10	Vitric tuff	10-350 cm	Massive fabric Remnant gas bubbles between triple junctions of glass shards Vitric groundmass alters to clay in places Skeletal plagioclase in places (selective dissolution) Contains broken or whole fossil leaves and charcoal fragments on bedding planes in places	60-80% vitric groundmass 10-20% plagioclase phenocrysts 0-5% quartz phenocrysts 0-5% biotite phenocrysts	Vitric groundmass indicates rapid-cooling of volcanic material (air-fall deposition into lake) Rare welding features that are also associated with fossil leaves and charcoal denote

			Rarely contains welding features		instances of air-fall deposition onto subaerial areas
<b>11</b>	Crystal tuff	1-225 cm	No internal structure Vitric groundmass often partly altered to clay Skeletal plagioclase in places (selective dissolution) Rarely contains siliceous spherulite crystals (~1mm)	30-50% vitric to bentonite groundmass 30-40% plagioclase phenocrysts 15-25% quartz phenocrysts 0-5% biotite phenocrysts 0-5% sand-size lithoclasts	Initial air-fall transport and rapid deposition from suspension as indicated by massive fabric Spherulites likely formed from devitrification of volcanic glass (Lofgren, 1971)
<b>12</b>	Lithic tuff	25-300 cm	Massive fabric Groundmass almost entirely altered to clay Skeletal plagioclase in places (selective dissolution) Locally contains gravel-size lithoclasts	50-80% bentonite matrix 20-40% lithoclasts 0-10% plagioclase phenocrysts 0-5% biotite phenocrysts 0-5% charcoal and organic detritus	Initial air-fall transport and rapid deposition from suspension as indicated by massive fabric Charcoal fragments and local gravel-size lithoclasts indicate instances of reworking of sediments
<b>13</b>	Clast-bearing packstone	10-50 cm	Massive fabric Contains clasts of massive to well-laminated carbonate mudstone in places (1-2 cm) Contains shell-debris and lithoclasts in places Commonly heavily dolomitized	20-50% carbonate mud and/ or microcrystalline dolomite matrix 0-40% indistinguishable, round, dolomitized grains with dark rims 0-10% bioclasts (broken ostacods) 0-10% silt to sand-size detrital quartz	Overall coarse grain size suggests high-energy conditions Massive to well-laminated carbonate mudrock clasts represent rip-up clasts Poorly sorted bioclasts and rip-up clasts suspended in matrix suggest high-energy, erosive currents, likely storm or tectonically driven, as possible modes of transport Lack of internal structure indicates rapid deposition and/or liquefaction
<b>14</b>	Siliciclastic conglomerate	50-90 cm	Poorly-sorted angular to sub-rounded grains Unconsolidated in outcrop No internal structure No matrix or cement	40-60% pebble-size lithoclasts 20-40% sand-size detrital quartz 10-30% sand to pebble-size chert *Clasts are boulder-sized in lower Elko Member	Sand to pebble-size grains suggests high energy, bedload transport

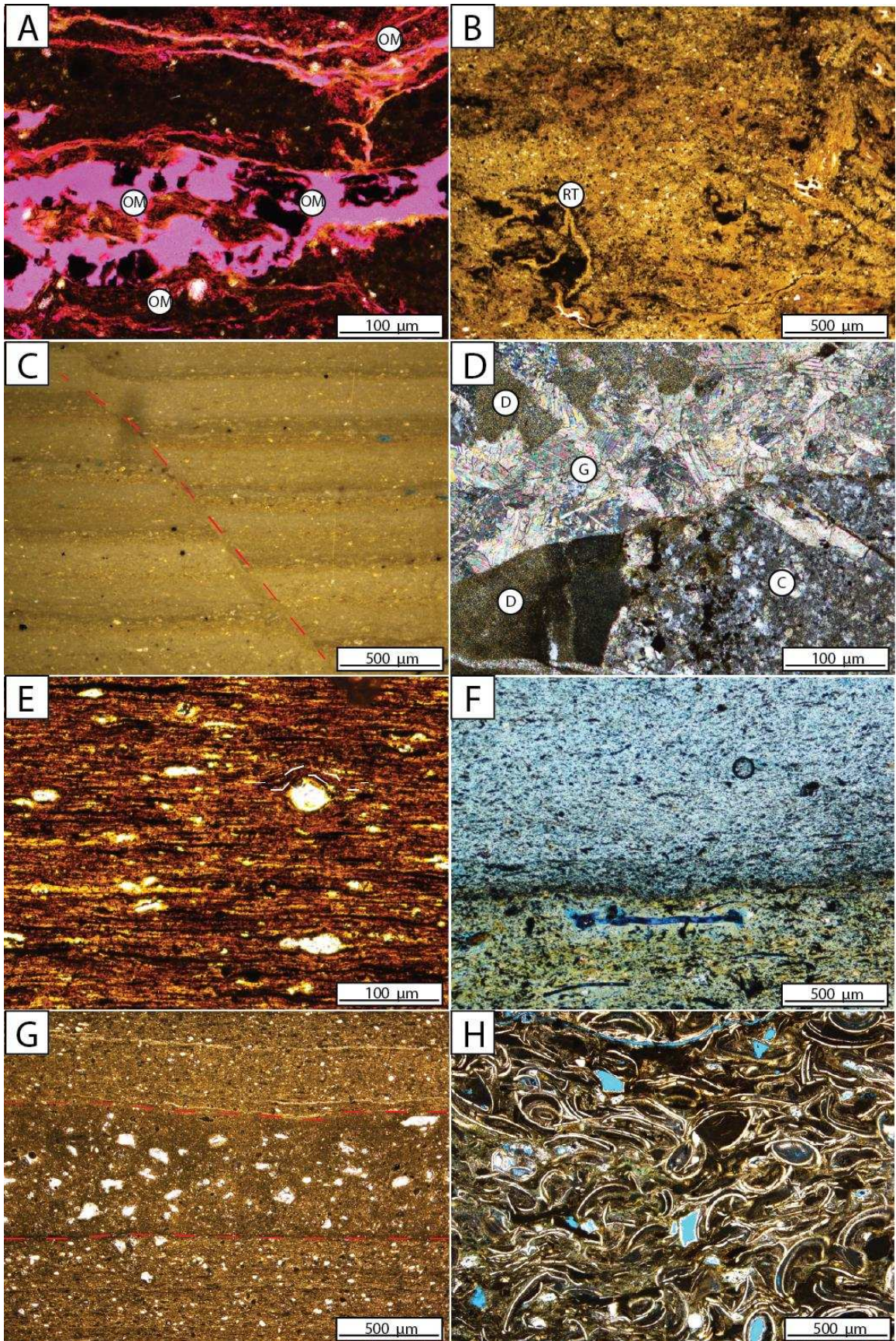


**Figure 5:** Thin section photomicrographs of the Upper Elko Formation. Facies is abbreviated as ‘F’ in annotations and captions: **(A)** Lignite (F2) (Coal Mine Canyon, 190.5 ft.) Organic material makes up more than 60% of the rock volume and preferentially weathers. Pink portion is porosity. **(B)** Massive root-bearing siliciclastic mudstone (F3B) (Coal Mine Canyon, 79.6 ft.). **(C)** Laminated calcareous mudstone (F4) (Coal Mine Canyon, 267.5). Micro-normal fault is traced out with red dashed line. **(D)** Calcareous mudstone (F4) that has been 100% diagenetically altered with cement. ‘D’ represents microcrystalline dolomite, ‘G’ is gypsum and ‘C’ is chert (Tomera Ranch- “cherty limestone”). **(E)** Microbial-mat-bearing organic-rich mudstone (F5) (Elko Hills A, Elko Hills, 1.5ft.). Microbial mats (black, wavy laminae) make up ~80% of this sample. White dashed lines trace mats building around a volcanoclastic silt grain. **(F)** Massive ash-bearing mudstone (F6) (Elko Hills A, Elko Hills, 35 ft.). The bottom bed contains more terrigenous organic material (~15%) than the top (~1–3%). **(G)** Laminated, silt to sand-bearing siliciclastic mudstone (F7). Laminae within dashed red lines are interpreted to be a debris flow, indicated by non-graded, subangular volcanoclastic silt grains “floating” in clay-rich matrix. **(H)** Fossiliferous wackestone (F8) (Tomera Ranch, 69.8 ft.). All white shell debris are ostracods that have undergone secondary compaction.

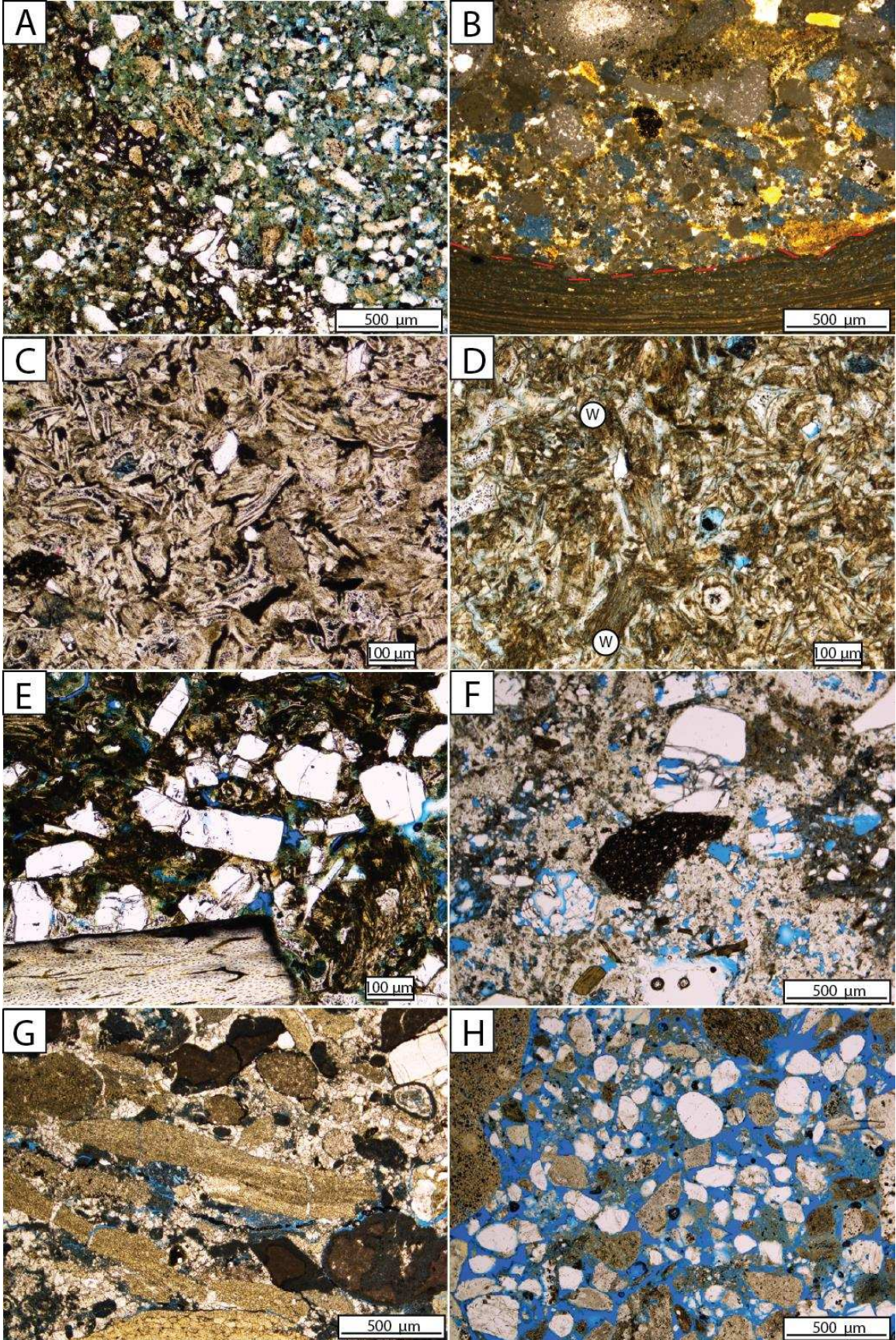


**Figure 6:** Thin section photomicrographs of the Upper Elko Formation (continued): **(A)** Siliciclastic sandstone (F9) (Coal Mine Canyon, 35 ft.). This sandstone is argillaceous and contains bitumen (black material). **(B)** Siliciclastic sandstone (F9) laminae overlying and scouring calcareous mudstone (F4) (Coal Mine Canyon, 268 ft.). Contact is noted in dashed red lines. The sandstone is interpreted to represent deposition from a high-energy current, likely triggered by storms or tectonic events. **(C)** Vitric tuff (F10) (Elko Hills A, Elko Hills, 74 ft.). Glass shards are white, but appear completely black under cross-polarized light. **(D)** Vitric tuff (F10) that was sufficiently hot to produce fiamme welding features, denoted by an encircled 'W' (Elko Hills B, Elko Hills, 51 ft.). **(E)** Crystal tuff (F11) (Tomera Ranch, 64 ft.). Phenocrysts are dominantly plagioclase feldspar. **(F)** Lithic tuff (F12) (Tomera Ranch, 260 ft.). A volcanic lithoclast is apparent as the black clast near the center of the image. **(G)** Clast-bearing packstone (Coal Mine Canyon, 494 ft.). Massive individual clasts are heavily dolomitized (nearly 100%). **(H)** Siliciclastic conglomerate (F14) (Coal Mine Canyon, 40.0 ft.).

## 4.2 Facies Associations

The 14 facies (“F” + number in text) described in Table 1 are grouped into five facies associations (“FA” + number in text) based on temporal and spatial relation of facies throughout measured sections (Table 2). The five facies associations, which represent unique depositional zones with little overlap, are described in detail below. Facies groupings are based primarily on grain size and composition because few sedimentary structures are recorded in Elko Formation sediments.

**Table 2:** Summary of Facies Associations and their corresponding facies in the Upper Elko Formation. Corresponding facies are arranged in order of abundance, top to bottom, per Facies Association.

Facies Association	Facies
<b>Facies Association 1</b> Siliciclastic mudstones and conglomerates	<b>Facies 3A:</b> Massive siliciclastic mudstone <b>Facies 14:</b> Siliciclastic conglomerate <b>Facies 9:</b> Siliciclastic sandstone
<b>Facies Association 2</b> Massive coal-rich mudstones	<b>Facies 2:</b> Lignite <b>Facies 3A:</b> Massive siliciclastic mudstone <b>Facies 3B:</b> Massive root-bearing siliciclastic mudstone <b>Facies 1:</b> Bituminous coal
<b>Facies Association 3</b> Microbial-mat-bearing mudstones and carbonates	<b>Facies 5:</b> Laminated, microbial-mat-bearing mudstone <b>Facies 3A:</b> Massive, siliciclastic mudstone <b>Facies 4:</b> Calcareous mudstone <b>Facies 8:</b> Fossiliferous wackestone <b>Facies 7:</b> Laminated, silt- to sand-bearing siliciclastic mudstone <b>Facies 13:</b> Clast-bearing packstone <b>Facies 9:</b> Siliciclastic sandstone <b>Facies 10:</b> Vitric tuff
<b>Facies Association 4</b> Microbial-mat-bearing mudstones and volcanics	<b>Facies 5:</b> Laminated microbial-mat-bearing mudstone <b>Facies 6:</b> Massive ash-bearing mudstone <b>Facies 3A:</b> Massive siliciclastic mudstone <b>Facies 4:</b> Calcareous mudstone <b>Facies 10:</b> Vitric tuff <b>Facies 4:</b> Calcareous mudstone <b>Facies 10:</b> Vitric tuff
<b>Facies Association 5</b> Carbonates and volcanics	<b>Facies 11:</b> Crystal tuff <b>Facies 12:</b> Lithic tuff <b>Facies 13:</b> Clast-bearing packstone

#### **4.2.1 Facies Association 1: Siliciclastic mudstones and conglomerates**

The siliciclastic mudstones and conglomerates facies association (FA1) are uncommon in the observed transect being present only Coal Mine Canyon, where it forms a continuous vertical succession approximately 10 meters thick. In outcrop, FA1 is unconsolidated and sediments are variegated with grey and brown colors (Figure 7-A). It consists solely of massive rocks, including massive siliciclastic mudstone (F3A) and siliciclastic sandstone (F9; Figure 6-A), which are intercalated with siliciclastic conglomerate (F14; Figure 6-H). F3A dominates the facies association (~80%), while 30–90 cm beds of F14 and F9 make up smaller respective portions. In places, the conglomerate (F14) scours underlying beds of sandstone (F9). In general, the amount of detrital siliciclastic material is higher in FA1 than in any other facies association; carbonates and volcanoclastics are noticeably absent. FA1 is laterally discontinuous and represents only 5% of observed Upper Elko Formation bulk rock volume. No macrofossils or trace fossils are observed in this facies association.

#### **4.2.2 Facies Association 2: Massive coal-rich mudstones**

The massive coal-rich mudstone facies association (FA2) forms vertically continuous units that range in thickness from 2–50 meters. In outcrop, it appears unconsolidated and variegated with grey, green, brown, and black colors (Figure 7-B). It is comprised completely of siliciclastic and organic fine-grained (clay- to silt-size) rocks with massive fabrics including massive siliciclastic mudstone (F3A), massive root-bearing siliciclastic mudstone (F3B; Figure 5-B), lignite (F2) (Figure 5-A), minor calcareous mudstone (F4) and bituminous coal (F1). Alternating beds of lignite (F2) and siliciclastic mudstones (F3B) dominate the facies association; bituminous coal (F1) only occurs in thin (1–3-cm thick) lenses (Figure 7-B). FA2 contains more terrigenous

organic material than any other upper Elko Formation facies association. Wood detritus and broken to whole fossil leaves are the most common types of organic material. Leaves include the conifer *Glyptostrobus*, alder, pine, cone, and other undistinguishable angiosperms (Daniel Peppe pers. comm., August, 2013; Ian Miller pers. comm., April, 2014). Locally, angiosperm leaves show signs of insect damage. Massive clay-dominated mudstones (F3B) are generally poorly developed as soils, but locally contain root traces (1–5-mm length; Figure 5-B). FA2 is present at Coal Mine Canyon and in minor amounts at the Elko Hills A and Elko Hills B outcrop localities; it represents approximately 15% of the measured Upper Elko Formation bulk rock volume.

#### **4.2.3 Facies Association 3: Microbial-mat-bearing mudstones and carbonates**

The microbial-mat-bearing mudstones and carbonates facies association (FA3) is characterized by intervals of those two lithofacies that are 15–30 meters thick. FA3 is the most lithologically diverse facies association in the upper Elko Formation. It has a structureless to well-laminated fabric and consists of laminated microbial-mat-bearing mudstone (F5; Figure 5-E), fossiliferous wackestone (F8), calcareous mudstone (F4) (Figure 5-C), massive siliciclastic mudstone (F3A), laminated, silt- to sand-bearing siliciclastic mudstone (F7; Figure 5-G), clast-bearing packstone (F13; Figure 6-G), minor siliciclastic sandstone (F9; Figure 6-B), and minor vitric tuff (F10; Figure 6-C). Cyclic interbedding of organic-rich mudstones (F5) and carbonates (F8 and F13) are most diagnostic of this facies association (Figure 7-C), where each organic-rich mudstone - carbonate cycle ranges from 0.2 to 1 meters. Thin-shelled *Candona* ostracods (Figure 5-H) and gastropod (*Lymnaea*?) macrofossils are prevalent in both facies throughout these cycles. Overall, gastropods are more common in the carbonates, and ostracods are more common in the organic-rich mudstones. In the carbonates, fossils show no clear orientation and are randomly dispersed, but in organic-rich mudstones they exclusively occur along bedding planes. One single fossil fish of the Elko

Formation was retrieved in FA3 at the Coal Mine Canyon outcrop. Rarely, leaves and wood detritus are present in FA3, though they are not as common as in FA2. Leaves include the conifer *Glyptostrobus*, alder, pine, cone, and other undistinguishable angiosperms (Daniel Peppe pers. comm., August, 2013; Ian Miller pers. comm., April, 2014). No burrows are observed in FA3.

After intervals of cyclic microbial-mat-bearing mudstone (F5) and limestone (F8), massive to laminated calcareous mudstone (F4) and massive siliciclastic mudstone (F3A) are the next most common lithofacies. These lithofacies form vertically continuous intervals up to 5 meters thick, and are only interrupted by silt- to sand-bearing siliciclastic mudstone (F7) laminae or siliciclastic sandstone (F9) laminae. In places, the calcareous mudstone (F4) is comprised of extremely fine (<1mm) rhythmic light and dark laminae. Rarely, coarse-clast-bearing packstones (up to 0.5 meter thick; F13) occur in predominantly calcareous mudstone intervals (F4).

Soft-sediment deformation is widespread in this facies association and generally occurs in calcareous mudstones (F4) and less commonly in microbial mat-bearing mudstones (F5). The syndimentary deformation structures include micro-normal faults (1–5-mm offset; Figure 5-C), sedimentary dykes that generally contain much higher silt concentrations than the substrate they intrude, vertical water-escape structures, and slumps (e.g. flow folds). FA3 occurs at the Coal Mine Canyon and Tomera Ranch outcrop localities and represents 25% of the Upper Elko Formation bulk rock volume.

#### **4.2.4 Facies Association 4: Microbial-mat-bearing mudstones and volcanoclastics**

The Microbial-mat-bearing mudstones and volcanoclastics facies association (FA4) forms units that are 2–25 meters thick. It is perhaps the most distinguishable facies association in outcrop due to distinct repeated decimeter-scale interbedding of laminated microbial-mat-bearing organic-rich

mudstone (F5) and white, massive to laminated, ash-bearing mudstone (F6) (Figure 5-F; Figure 7-D). In general, FA4 contains up to 50% ash, much more than the preceding facies associations. Rarely, leaves, wood detritus, *Candona* ostracods and *Sphaeriidae* fingernail clams are evident in the microbial-mat-bearing siliciclastic mudstone (F5), but they never occur in the other facies that comprise this association. No burrows are observed in FA4.

Although cycles of organic-rich mudstone (F5) and ash-bearing mudstone (F6) dominate FA4, vitric tuff (F10) and calcareous mudstone (F4) are also present. Calcareous mudstone (F4) commonly forms continuous intervals (1–5 meters thick) between cycles of interbedded microbial-mat-bearing organic-rich mudstone and ash-bearing mudstone. These intervals are commonly dolomitized (Figure 5-D). Vitric tuff (F10) occurs in distinct beds 1–3-m thick throughout FA4 and is generally overlain and underlain by F4. Overall, FA4 occurs frequently at the Coal Mine Canyon and the Elko Hills outcrop localities, and in limited intervals at the Tomera Ranch measured section. FA4 represents 20% of the observed Upper Elko Formation bulk rock volume in all outcrops combined.

#### **4.2.5 Facies Association 5: Carbonates and volcanoclastics**

The Carbonates and volcanoclastics facies association (FA5) forms units that are 5–30 meters thick. FA5 contains a structureless to well-laminated fabric and is comprised of vitric tuffs (F10; Figures 5-C and 7-D), crystal tuffs (F11; Figure 5-E), and lithic tuffs (F12; Figure 5-F) with intercalated calcareous and/or ash-bearing massive mudstones (F4 or F6). All tuffs throughout FA5 contain the same four principal phenocrysts and clasts: (1) plagioclase; (2) quartz; (3) biotite; (4) and siliciclastic lithoclasts. Siliciclastic lithoclasts can be sand to gravel size. In the Elko Hills sections, vitric tuffs (F10) frequently contain a strong organic component (2–5% rock volume) and yield

partial to whole fossil leaves and charcoal fragments (1–10 mm in size). Lithic tuffs rarely show welding features, which are only locally observed in vitric tuff (F10; Figure 5-D). Volcaniclastics (F10, F11, and F12) are the dominant lithology of this facies association; they make up approximately two thirds of the sediment stack.

Minor lithofacies include calcareous mudstones (F4) and clast-bearing packstones (F13). Calcareous mudstones (F4) form continuous intervals 1–10 m thick. Clast-bearing packstones (F13) are rare and occur as beds less than a meter thick. These two carbonate facies in FA5 show two important distinctions from other facies associations with carbonates (FA3 and FA4) are observed: (1) in FA5 synsedimentary deformation is absent; (2) dolomite is much more prevalent than in FA3 and FA4. Dolomite accounts for approximately 50% of the FA5 bulk rock volume and is especially common as microcrystalline cement in calcareous mudstones (F4). Clast-bearing packstones (F13) are heavily cemented with dolomite and calcite; they contain abundant well-rounded dolomite lithoclasts (2–5 mm diameter) with dark dolomitic rims. FA5 is present in all measured outcrop localities. It represents approximately 35% of the measured Upper Elko Formation bulk rock volume.

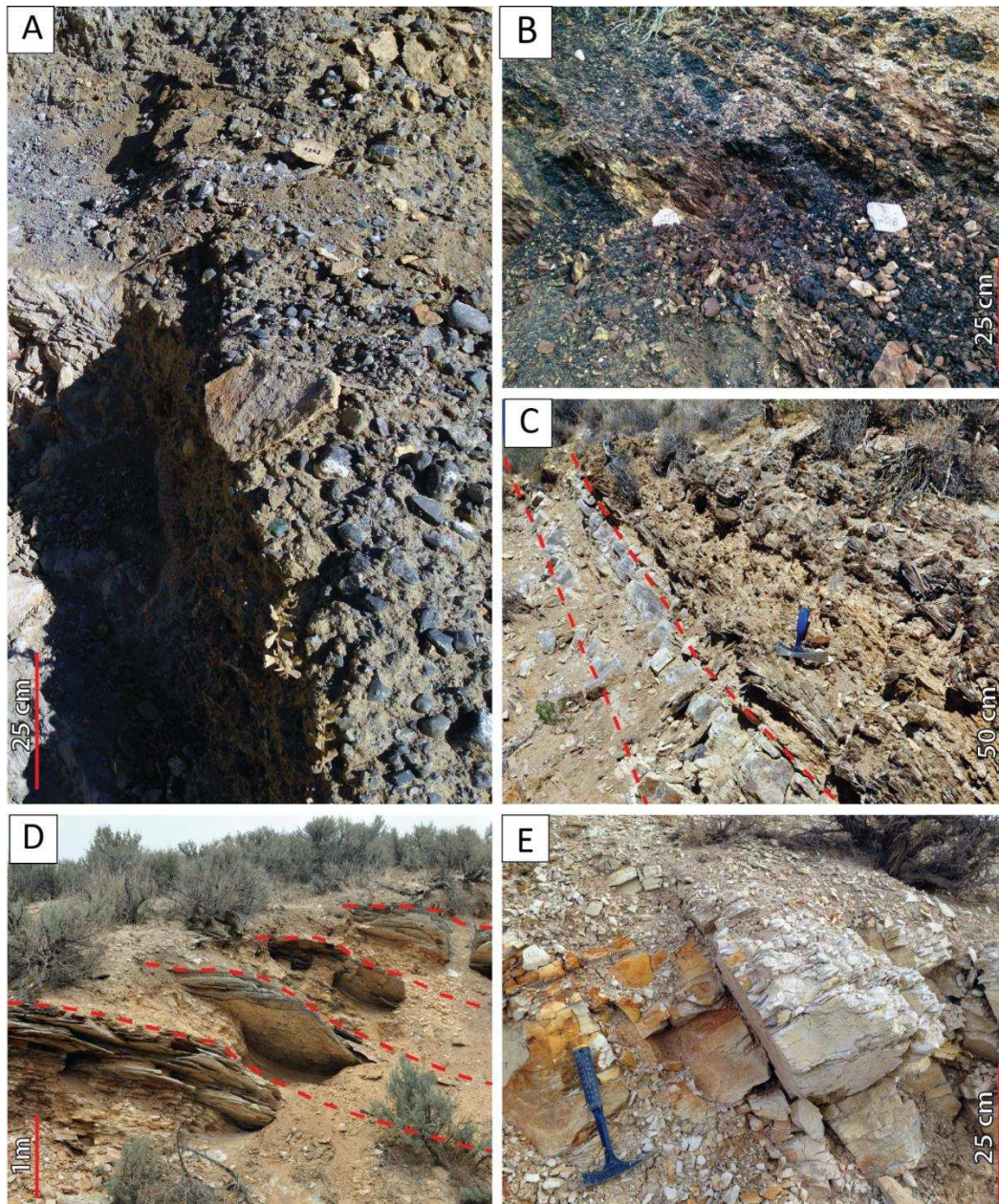


**Figure 7:** Facies Associations of the Elko Formation as they appear in outcrop: **(A)** Siliciclastic conglomerate (F14) of FA1 (Coal Mine Canyon). Notice the massive and unconsolidated texture. **(B)** Lignite (F2) and bituminous coal (F1) of FA2 (Coal Mine Canyon). Notice the variegated color and massive and unconsolidated texture of FA2 sediments. White rocks placed on the outcrop were used as markers when measuring stratigraphy. **(C)** Microbial-mat-bearing mudstone (F5) and interbedded fossiliferous wackestone (F7) (Coal Mine Canyon). Red lines denote contacts of two fossiliferous wackestone beds with the microbial mat-bearing mudstone in the frame. **(D)** Interbedding of microbial mat-bearing mudstone (F5) and ash-bearing mudstone (F6) of FA4 as it appears at Elko Hills A (Elko Hills). Red lines signify the contacts of resistant organic-rich mudstone with overlying easily weathered, ash-rich mudstone. **(E)** Resistant vitric tuff (F10) of FA5 near the top of Elko Hills A (Elko Hills). This unit produces abundant fossil leaves and charcoal fragments.

## 5.0 FACIES ARCHITECTURE

The upper Elko Formation in Nevada is represented by four detailed sections in the study area that are arranged along a north-south transect (Appendix 2; Figure 8). Lateral traceability of outcrops is extremely limited, and no distinct marker beds were observed across this transect. Therefore, Elko Formation sedimentary rocks can only be grouped into four vaguely chronostratigraphic intervals, here referred to as “Interval 1” to “Interval 4” based on existing (Solomon et al. 1979; Haynes, 2003) and new radiometric age dates. The Elko Formation stratigraphic columns in Figure 8 do not only show the measured sections from this study but also incorporate data from Haynes (2003) in order to provide a more complete picture of the succession, especially at the bottom of the unit, which is not exposed.

While previous authors (Solomon, 1992; Haynes, 2003) used a lithostratigraphic framework for correlation across the Elko Basin, growing evidence suggests lithological variability from north to south at contemporaneous times. An  $\text{Ar}^{40}/\text{Ar}^{39}$  radiometric age date of a biotite-rich tuff interbedded with black shale (FA4) at Coal Mine Canyon has an age of  $48.2 \pm 0.02$  Ma, while a sample of biotite-rich tuff interbedded with black shale (FA4) at Tomera Ranch, previously envisioned to represent the same chronostratigraphic interval, is dated  $43.5 \pm 0.02$  Ma. This indicates a time-transgressive relationship of Elko formation sedimentation across the transect: the Elko Formation is oldest at the northern Coal Mine Canyon outcrop and youngest at the southern Tomera Ranch section. The time-transgressive relationship is also reflected by previous age dates from the upper Elko Formation-Indian Well Formation contact, which is oldest ( $41.1 \pm 0.2$  Ma) at Coal Mine Canyon and youngest ( $37.5 \pm 0.1$  Ma) at Tomera Ranch (Haynes, 2003).

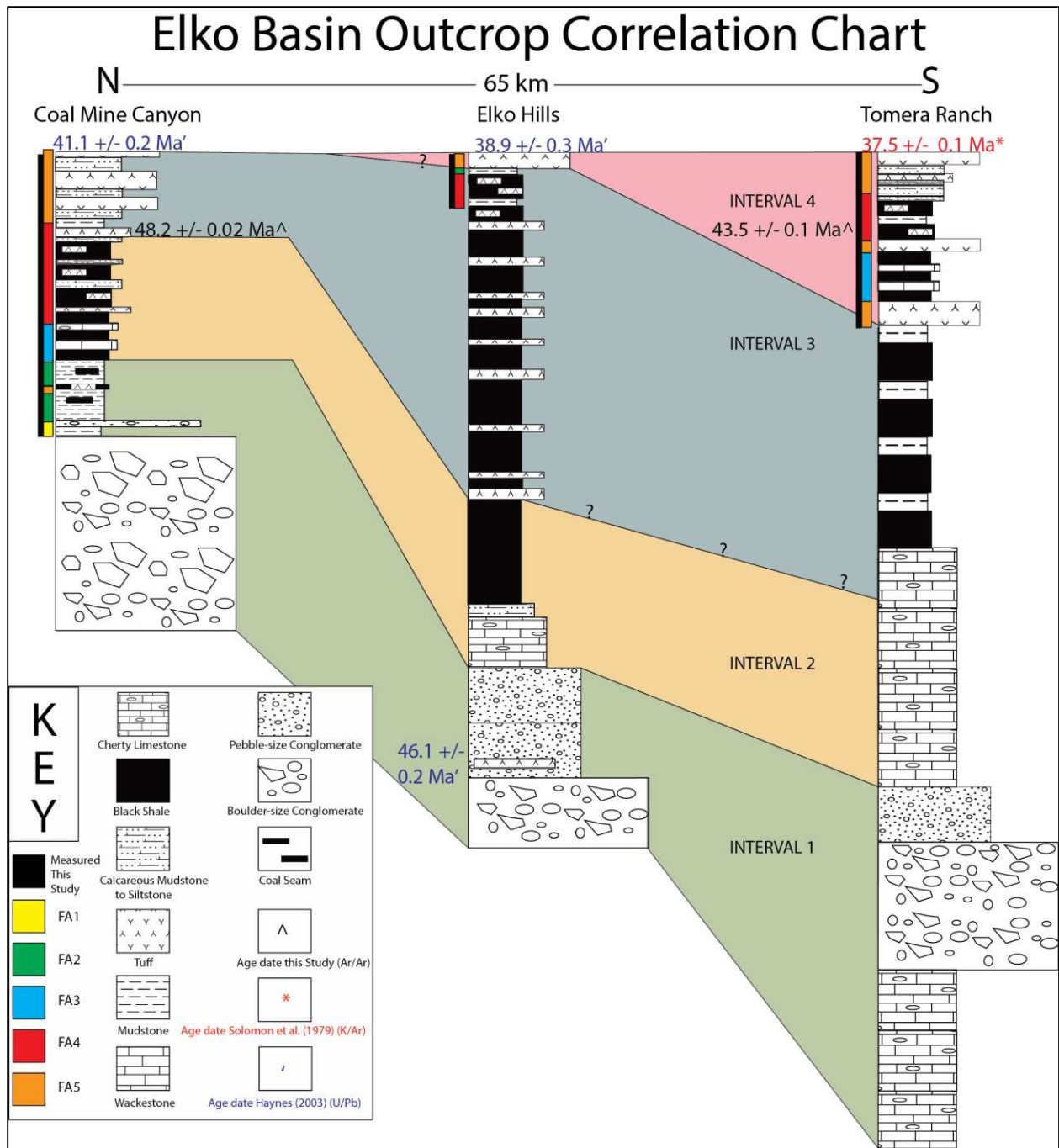


**Figure 8:** Elko Basin correlation chart with generalized stratigraphy showing the diachronous nature of Elko Formation strata from north to south. Four broad time intervals termed “Interval 1”, “Interval 2”, and “Interval 3”, and “Interval 4” are defined based on radiometric age dates of this study.

## **5.1 Stratal Architecture along the North – South Transect**

### **5.1.1 Stratigraphic Interval 1**

Interval 1 consists of sediments making up the basal portion of the Elko Formation. At all three study area localities, Interval 1 consists of basal conglomerates that grade from boulder- to pebble-size. At Coal Mine Canyon, Interval 1 fines upward more into 160 feet of lignite (F2), bituminous coal (F1), and massive mudstones (F3A, F3B), but at the central and southern localities it consists exclusively consist of conglomerates. Thicknesses of the boulder-size basal conglomerates vary along the transect; they are thinnest in the central part of the study area, in the Elko Hills (~130 feet), and increase in thickness outward towards the north (550 feet at Coal Mine Canyon) and south (325 feet at Tomera Ranch). Conglomerates vary across the transect; consisting almost entirely of boulder-size clasts (1.5 meter diameter) in the north; dominated by pebble-size conglomerates in the center; and consisting of limestone-clast conglomerates, smaller boulder-size (0.5 meter diameter) conglomerates, and sandy pebble-size conglomerates (Haynes, 2003) in the south. Tuffs are rare in Interval 1 and only two occurrences were observed: (1) Ash is found interlayered in a single bed (~5 feet) of lignite (F2) at Coal Mine Canyon; and (2) a 6-foot-thick lenticular airfall tuff near the base of the Elko Hills sandy pebble-clast conglomerate was identified by Haynes, (2003) and dated  $46.1 \pm 0.2$  Ma. Black shale is not observed along the north-south transect in stratigraphic Interval 1.

### **5.1.2 Stratigraphic Interval 2**

Interval 2 represents the lower central portion of the Elko Formation succession. A major shift in lithology occurs across the north-south transect in this interval. In the north, at Coal Mine Canyon, the succession consists of 50 feet of highly cyclic interbedded microbial-mat bearing shale (i.e., black shale; F5) and fossiliferous wackestone (F7; FA3); is overlain by 250 feet of interbedded, microbial-mat-bearing mudstone (F5; 0.2–5 feet), ash (~1 cm), and calcareous mud- to siltstone (F4; 2.0–10 feet) (FA4). At the Elko Hills sections, Interval 2 is comprised of 150 feet of cherty limestone, overlain by 170 feet of calcareous shale and siltstone (Haynes, 2003) that fines upwards into a thick (~300-foot) interval of continuous black shale (Haynes, 2003). In the south, at Tomera Ranch, Interval 2 consists entirely of cherty limestone, possibly up to 800 feet thick (Haynes, 2003). Black shale units in Interval 2 vary in thickness and interbedded lithologies along the transect: they are thick at Coal Mine Canyon and commonly interbedded with carbonates, equally thick at the Elko Hills outcrops, but not interbedded with carbonates (Haynes, 2003), and completely absent at Tomera Ranch. Ash content decreases in abundance along the north-south transect and only occurs at Coal Mine Canyon (Haynes, 2003).

### **5.1.3 Stratigraphic Interval 3**

Stratigraphic Interval 3 represents the central to upper portion of the Elko Formation. In the north, at Coal Mine Canyon, sediments of Interval 3 are much coarser-grained than Interval 2, as indicated by a 250-foot succession consisting of coarse-grained volcanoclastics (F10, F11, F12), wackestone (FA8), and clast-bearing packstone (F13). A tuff (F10) at the base of this succession has an age of  $48.2 \pm 0.02$  Ma. The amount of volcanoclastic material increases upwards in this part of the Elko Formation succession, which is overlain by Indian Well Formation conglomerates and

tuffs. The Elko Formation-Indian Well Formation contact at Coal Mine Canyon is dated at  $41.1 \pm 0.2$  Ma (Haynes, 2003). In the central Elko Hills, Interval 3 consists predominantly of microbial-mat-bearing mudstone (0.2–4.0 foot-thick beds; F5) that is interbedded with massive, ash-bearing mudstone (~1 cm–5.0 feet; F6), and tuff (1.0–7.0 feet; F10, F11, and F12) with increasing ash content up-section. In the southern section at Tomera Ranch, Interval 3 consists of approximately 100 feet of cherty limestone that is overlain by roughly 800 feet of black shale (F5) and non-organic-rich mudstone (Haynes, 2003). Microbial-mat bearing mudstone (i.e. black shale; F5) varies in thickness along the transect in Interval 3. It is completely absent at Coal Mine Canyon, thickest in the Elko Hills, and thins towards the south at Tomera Ranch. Ash content decreases in abundance along the north-south transect; it is dominant at Coal Mine Canyon, prevalent in the Elko Hills, and absent at Tomera Ranch.

#### **5.1.4 Stratigraphic Interval 4**

Interval 4 is not present at Coal Mine Canyon. At Tomera Ranch, it is denoted by the first occurrence of volcanoclastic material, indicated by a 35-foot succession of coarse-grained volcanoclastics (F10, F11, and F12; FA5). This tuff is tentatively correlated with a 25-foot succession of biotite-rich tuff (F10, F11, and F12; FA5) at the top of the Elko Hills sections. However, radiometric age dates of these two tuffs are not available for this study. Above the 35-foot tuff succession, the Tomera Ranch section consists of 100 feet of interbedded microbial-mat-bearing mudstone (F5; 0.5 to 3.0 foot beds) and wackestone (F8; 0.2–5.0 foot beds) (FA3), which is overlain by 47 feet of volcanoclastics (F10, F11, F12), then fines into a series of interbedded microbial-mat-bearing mudstones (F5), non-organic-rich mudstones (F3A), calcareous mudstones (F4) and ash-bearing mudstones (F6) (FA4). All four of these facies are interbedded at a 0.1-foot to 4.0-foot scale. A tuff interbedded with black shale (FA4) in the central part of this interval at

Tomera Ranch denotes an age of  $43.5 \pm 0.02$  Ma. Ninety feet of coarse-grained volcanoclastics (F10, F11, and F12; FA5) overlie the interbedded black shale interval and are capped by an Indian Wells Formation ignimbrite, which is dated  $37.5 \pm 0.1$  Ma (Haynes, 2003). Black shales vary along the north-south transect in stratigraphic Interval 4; they are absent at the Coal Mine Canyon and Elko Hills outcrops and thickest at Tomera Ranch.

## 6.0 DEPOSITIONAL MODEL AND BASIN EVOLUTION

### 6.1 Depositional Model

Within the study area, the Elko Formation comprises facies deposited in a broad continental-lacustrine environment. Common spatial and temporal heterogeneity of upper Elko Formation sediments in cyclicity, composition, grain size, and fossil content suggest: (1) Elko Formation sediments were laid down in a variety of continental–lacustrine depozones including alluvial-fluvial, palustrine-lacustrine, littoral-lacustrine and limnetic-lacustrine (Figure 9); (2) the Elko Formation records deposition of a lacustrine system with fluctuating lake levels through time and constantly influenced by changes in climate, tectonics, and/or volcanoclastic input (Figures 10 and Figure 11).

The facies associations discussed in this study represent four spatially distinct depositional zones, which, ordered from proximal to distal, include (1) alluvial-fluvial, (2) palustrine-lacustrine, (3) littoral-lacustrine, and (4) limnetic-lacustrine (Figure 9). The preponderance of large (gravel to pebble) and predominant subangular clasts in the alluvial-fluvial depozone (FA1) reflects a proximal position to the source area of these sediments. Based on the predominantly subangular coarse-sized grains, deposition likely occurred in a braided-river system, probably linked to an alluvial-fan environment (see Figure 11-1). Energy levels were sufficient in the braided channels to erode underlying strata, as evidenced by common scour and attenuation features. This alluvial-fluvial depositional environment is interpreted to represent the highest energy-transport levels throughout the Elko Formation succession. The alluvial-fluvial depozone is prevalent across the studied transect at the bases of all localities, suggesting proximal fluvial-alluvial deposition was

most dominant in the early stages of Elko Basin development. Like Haynes (2003), this study interprets the fans as being derived from a north-south trending paleohigh to the west and north-west of the measured sections (modern Adobe Range for Coal Mine Canyon and Elko Hills; modern Piñon Range for Tomera Ranch?). Coal Mine Canyon contains the coarsest basal boulder conglomerate (up to 1.5 meters in diameter) suggesting it represents the most proximal outcrop to the paleohigh in the study area. Tomera Ranch is the only measured section to contain limestone clasts in its basal conglomerate (Haynes, 2003; this study) indicating a limestone source in the south of the study area. These limestone clasts were likely sourced from a local assemblage of Paleozoic marine carbonates.

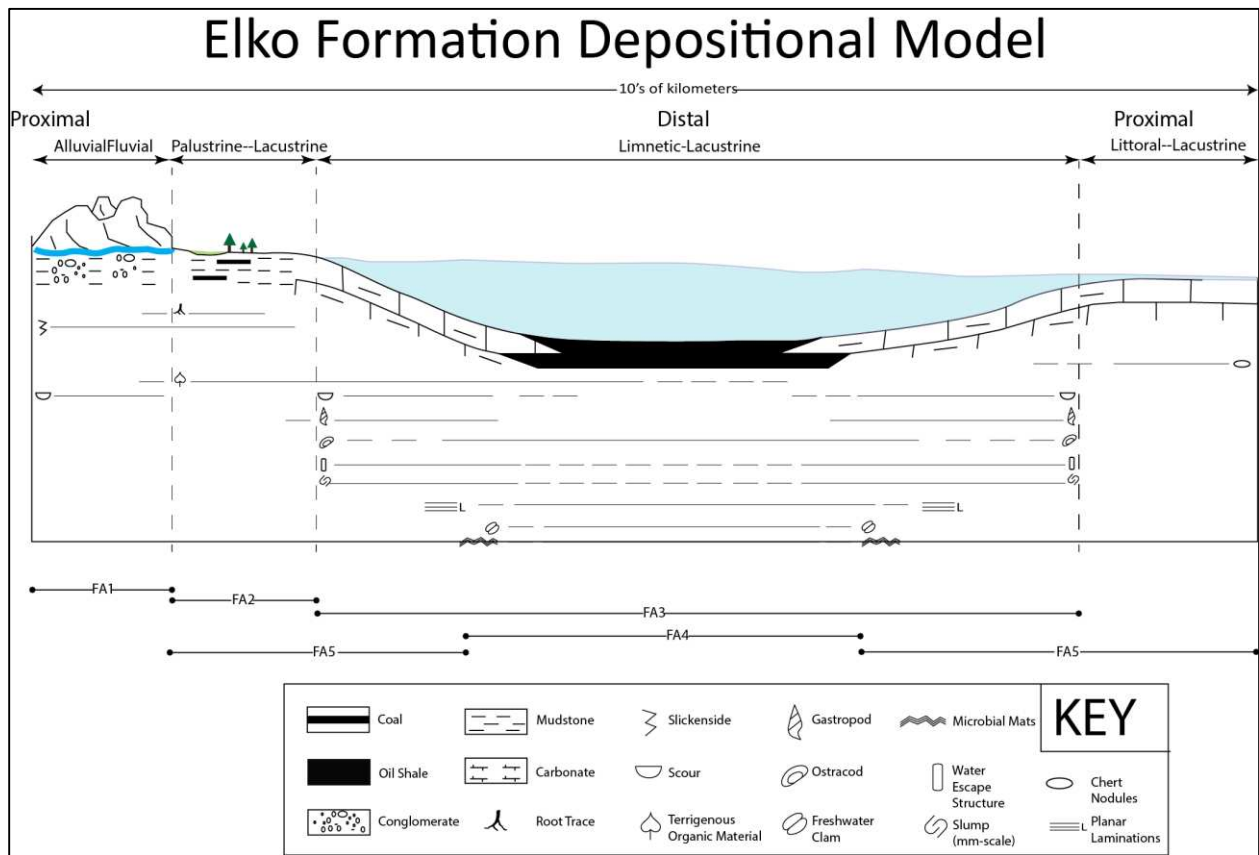


**Figure 9:** Conceptual depositional model for the Elko Formation.

The palustrine-lacustrine environment (FA 2) is interpreted as a shallow restricted-swamp system (see Figure 11-2). Paleosols and coal beds denote the marginal position of this depozone, as paleosols reflect subaerial exposure and coal beds, deriving from buried terrigenous material, have commonly been recognized as indicators for marginal, palustrine settings in lacustrine systems (Renaut and Gierlowski-Kordesch, 2010). This portion of the Elko Basin experienced tranquil energy conditions, as indicated by a preponderance of mudstones with no energy-driven sedimentary structures. The complete lack of sedimentary structures in this depozone suggests that deposition in the swamps was through suspension, and high-energy currents never interrupted the prevailing quiescent conditions. The palustrine-lacustrine swamp depozone exclusively occurs at the Coal Mine Canyon section, suggesting that swamps dominated lake margins to the north and may have been limited or absent in other portions of the study area.

The littoral-lacustrine carbonate depozone, comprised entirely of cherty limestone during the early to middle stages of basin evolution and of interbedded volcanoclastics and carbonates (FA5) during late basin evolution (see Figure 11-5), is envisioned to represent a marginal lacustrine environment of the Elko lake. A lack of evaporate minerals or mudcracks suggest this depozone was subaqueous and never occupied a desiccated environment. Thick cherty limestone successions of this depozone occur exclusively at the Elko Hills and Tomera Ranch sections, suggesting that expansive littoral carbonates only precipitated towards the central and southern portions of the study area. Cherty limestones are mostly absent at Coal Mine Canyon except for a single 3.0-foot thick bed in stratigraphic Interval 2; there, it is likely that the swamp environment and fluvial input(s) in the northern portion of the Elko Basin inhibited carbonate zones in the north due to siliciclastic discharge from the river mouth(s) diluting the water budget and thereby precluding carbonate precipitation.

The limnetic-lacustrine depozone (FA3 and FA4) represents the most distal environment in the Elko Basin. It reflects an “open-water” portion of the Elko lake. Distinct cycles of laminated, microbial-mat-bearing organic-rich mudstone (F5) and fossiliferous wackestone (F8) are common at Coal Mine Canyon and Tomera Ranch; they are interpreted to represent entirely subaqueous lacustrine deposition (see Figure 11-3), with organic-rich mudstone beds deposited during highstands and fossiliferous wackestone beds deposited during lowstands. This cyclic pattern represents a rapidly fluctuating lake level, or “balance-filled” lake (e.g. Carroll and Bohacs, 1999; Renault and Gierlowski-Kordesch, 2010; Tänavsuu-Milkeviciene and Sarg, 2012), with climatic and/or tectonic factors (Bohacs et al., 2000) seen as the dominant contributors to the lake-level changes. In contrast to Coal Mine Canyon and Tomera Ranch, the organic-rich shales at the Elko Hills outcrops are not interbedded with carbonates, suggesting that the Elko Hills succession occupied the most basinward position of the Elko lake and was less sensitive to falls in lake-level. Consequently, the Elko Hills sections also record the thickest organic-rich black-shale intervals in the study area. The microbial mats at all study area localities are most common in laminae of siliciclastic mudstones with little silt content, indicating that they likely thrived during periods of little siliciclastic and carbonate sedimentation in distal sediment-starved portions of the Elko lake (cf. Schieber, 1999; Egenhoff et al., 2013).

Beds consisting of coarse material (i.e. siliciclastic sandstone (F10) and clast-bearing packstone (F13)) only rarely occur in the limnetic-lacustrine depozone. They reflect periodic high-energy events (likely storms) and are vertically associated with calcareous mudstone (F4) intervals. The storm-driven bottom-water flows are erosive, as indicated by 1–3 cm rip-up clasts of F4 sediments observed in F13, and erosional scouring into underlying substrate of both F10 and F14. Rarely,

sediments of F10 are coarse-tail graded in a mud matrix, suggesting transport to distal portions of the lake via debris flows.

The abundant soft-sediment-deformation features (i.e. syndimentary injection dykes, water-escape structures, and convolute bedding) exhibited in the Elko Formation lacustrine-limnetic depozone are associated with abundant normal micro-faulting, hinting at the role of extensional tectonism in the evolution of the Elko lake. As such, their origin is attributed to two tectonically induced processes: (1) liquefaction, where grains are suddenly and temporarily converted from a solid state into a liquefied state (Obermeier, 1996); or (2) fluidization, where fluid suddenly moves upward in nearly vertical pathways and produces a fluid drag on overlying sediments (e.g. Levi et al., 2006; Sims, 2013). Frequent liquefaction and/or fluidization events in this depozone are interpreted to be the catalyst for the ubiquitous massive fabric occurring in the calcareous mudstone (F4) facies so commonly recorded in the Elko Formation limnetic-lacustrine depozone. The “cherty limestone,” originally thought to exclusively encompass a middle member of the Elko Formation (J. Smith et al., 1976; Ketner and Alpha, 1992; Haynes, 2003), most likely represents a lithology that combines depositional with diagenetic characteristics. Because microcrystalline silica or chert in this unit occurs only as pore-filling, fracture-occluding, or overgrowth cement it seems most probable that the “cherty limestone” was originally deposited as a limestone similar to the calcareous mudstone (F4) based on its overall fine carbonate grain size, and therefore reflects deposition in a shallow lake environment (Renaut and Gierlowski-Kordesch, 2010). The silica required to precipitate the chert cement is interpreted to derive from the alteration of volcanic glass (Tucker, 2009). However, it may also have been derived from slightly alkaline lake-waters, which can precipitate chert through periodic input of freshwater biogenic production of carbon dioxide,

and/or evaporative concentration (Schubel and Simonson, 1990). This same effect is also observed in upper Elko Formation calcareous mudstones (F4).

## **6.2 Lake Evolution**

Recent  $^{40}\text{Ar}/^{39}\text{Ar}$  and past  $^{40}\text{K}/^{40}\text{Ar}$  (Solomon et al., 1979) and  $^{235}\text{U}/^{207}\text{Pb}$  (Haynes, 2003) absolute age dates suggest that deposition of lacustrine rocks in the four studied outcrops did not occur at the same time, but instead diachronously (Figure 10; Figure 11). The thickest accumulations of organic-rich black shale change spatially along the transect through time, indicating a shifting depocenter within the Elko lake (Figure 10). Different timespans, here interpreted to reflect different phases of lake evolution, are termed “Time 1” which represents an early timespan in Elko Basin evolution, “Time 2,” denoting an early–medial timespan, “Time 3,” which represents a medial–late timespan, and “Time 4,” which reflects the final phase in Elko lake evolution (Figure 10).

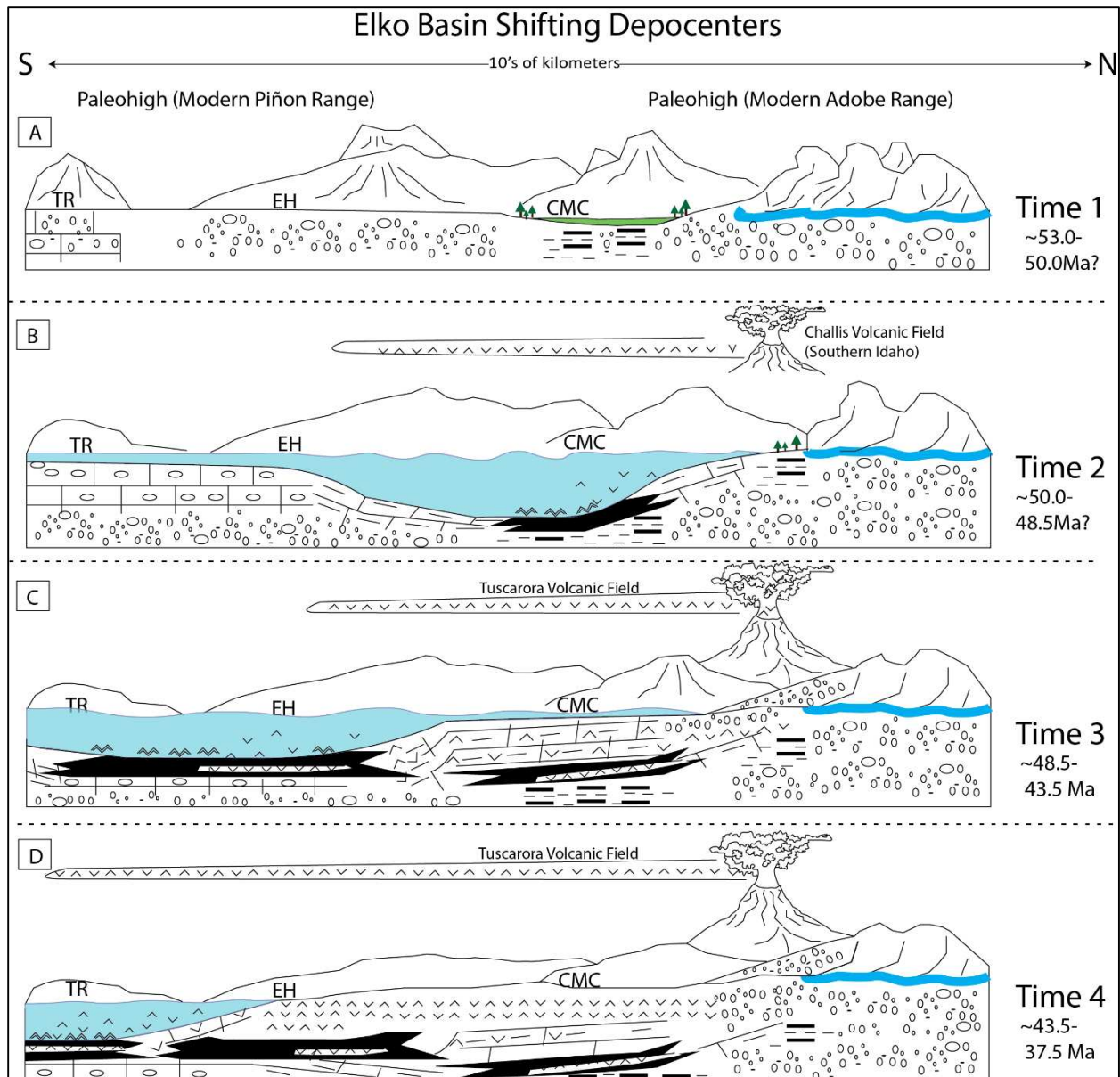


**Figure 10:** Shifting Elko Basin depocenter during the Eocene. The depocenter migrates from the northern portion of the study area to the south through time.

### **6.2.1 Time 1**

Time 1 (Figure 10-A; ~53.0–50.0 Ma?) encompasses stratigraphic Interval 1. Subsidence was high only in the northern portion of the basin, as indicated by a succession of fine-grained rocks of the palustrine-littoral depozone (FA2) including lignite (FA2), bituminous coal (F1), and siliciclastic mudstones with and without root traces (F3B and F3A) at Coal Mine Canyon. Even though no equivalent age dates could be obtained, it is likely that subsidence was relatively low in the central and southern portions of the basin, indicated by coarse-grained boulder- to pebble-size conglomerate deposition through alluvial-fluvial (FA1) processes in the Elko Hills outcrops and at Tomera Ranch. The interplay between subsidence and sediment supply was not sufficient anywhere in the basin to form a deep-water limnetic-lacustrine depozone and consequently no black shale facies were deposited at this time (see Figure 10-A; Figure 11-1; Figure 11-2).

### **6.2.2 Time 2**

Time 2 (Figure 10-B; ~50.0–48.5 Ma?) encompasses stratigraphic Interval 2, expressed by a major depocenter in the northern portion of the Elko Basin as indicated by deep-lake organic-rich limnetic-lacustrine deposition (FA3 and FA4) at the Coal Mine Canyon outcrop. It is likely that time-equivalent shallow littoral-carbonates were deposited in the central and southern portions of the basin (Elko Hills and Tomera Ranch, respectively) during this time, suggested by significant accumulations of cherty limestone. Only minor volcanic pulses occurred during this stage of basin evolution, indicated in outcrop by sparse ash beds interbedded with organic-rich black shales at Coal Mine Canyon (see Figure 10-B; Figure 11-3). Ash beds are not present at the Elko Hills and southern Tomera Ranch localities during this time (Haynes, 2003), suggesting that airfall volcanism exclusively influenced the northern part of the lake before progressively affecting also

the central and southern portions of the Elko Basin. These early tuff beds were probably sourced by explosive eruptions of the Challis Volcanic Field of southern Idaho (McIntyre et al. 1982; Janecke et al. 1997).

### **6.2.3 Time 3**

Time 3 (Figure 10-C; ~48.5–43.5 Ma) encompasses stratigraphic Interval 3. During this time, the Elko Basin contained a central to southern basin depocenter, indicated by organic-rich limnetic-lacustrine deposition (FA3 and FA4) at the Elko Hills and Tomera Ranch outcrops, and a shallow northern portion of the basin, indicated by shallow-water carbonates and mixed alluvial-volcaniclastic rocks (FA5) in the north at Coal Mine Canyon. During this time, the central Elko Basin (Elko Hills area) probably represented the deepest portion of the Elko Basin, as these outcrops show a thick accumulation of black shale with no significant interbedded carbonates or non-organic mudstones, as opposed to Tomera Ranch, which exhibits interbedded black shales and non-organic-rich mudstones (Haynes, 2003). The Elko Basin recorded a dramatic increase in extrabasinal volcanism during Time 3, indicated by a coarsening-upward succession mostly comprised of volcaniclastic beds (FA5) at Coal Mine Canyon. The volcanism interrupted predominantly black shale deposition in the limnetic-lacustrine depozone at Elko Hills during this time; however, it did not have a significant influence on southern Elko Basin sedimentation, as indicated by a dearth of volcanic rocks recorded at Tomera Ranch. Ash-flow and airfall tuffs deposited in this phase of basin evolution likely originated from the Tuscarora Volcanic Field of northeastern Nevada and filled the Elko Basin progressively from north to south (Haynes, 2003; see Figure 10-C; Figure 10-D; Figure 11-4).

#### **6.2.4 Time 4**

Time 4 (Figure 10-D; ~43.5–37.5 Ma) is a timespan enveloping stratigraphic Interval 4. During this time, the depocenter of the basin and resulting deep-lake limnetic-lacustrine facies had migrated southward to the Tomera Ranch area. Any sedimentation in the northern Coal Mine Canyon area was likely mixed alluvial conglomerates and volcanoclastics of the Indian Well Formation, as indicated by the Elko Formation-Indian Well Formation contact dated at 41.1 Ma (Haynes, 2003). The central Elko Hills successions contained significant airfall-tuff accumulations (FA5) and a lack of any organic-rich black shales, as indicated in outcrop by a 25-foot interval of tuff (F10). The tuff (F10) at the Elko Hills during this time is locally welded and contains pieces of woody debris and charcoal, suggesting the Elko Hills area did not experience subaqueous deposition during this time, as otherwise the tuff would rapidly cool down upon deposition and not form any welding features. The Elko Formation-Indian Well Formation contact in the Elko Hills area is dated 38.9 Ma (Haynes, 2003). At this stage of Elko Basin evolution, extrabasinal ashes (likely of the Tuscarora Volcanic Field; Haynes, 2003) spread across the entire basin as it is recorded even in the southern portions of the study area, as indicated by several tuffs (0.1 to 4.0 feet thick) interbedded with organic-rich black shales at Tomera Ranch. Deposition became exclusively volcanoclastic across the entire basin towards the end of Time 4, indicated by abundant airfall and ashflow tuffs. An Indian Well Formation ignimbrite was laid down at the end of Time 4 and is dated at 37.5 Ma (Haynes, 2003). The airfall and ashflow tuffs, brought about by a southward-migrating magmatic front (Haynes, 2003), are interpreted as having caused the “filling-in” style of this lacustrine system by the end of Time 4 (Figure 10-D; Figure 11-5).

# Elko Lake Evolution

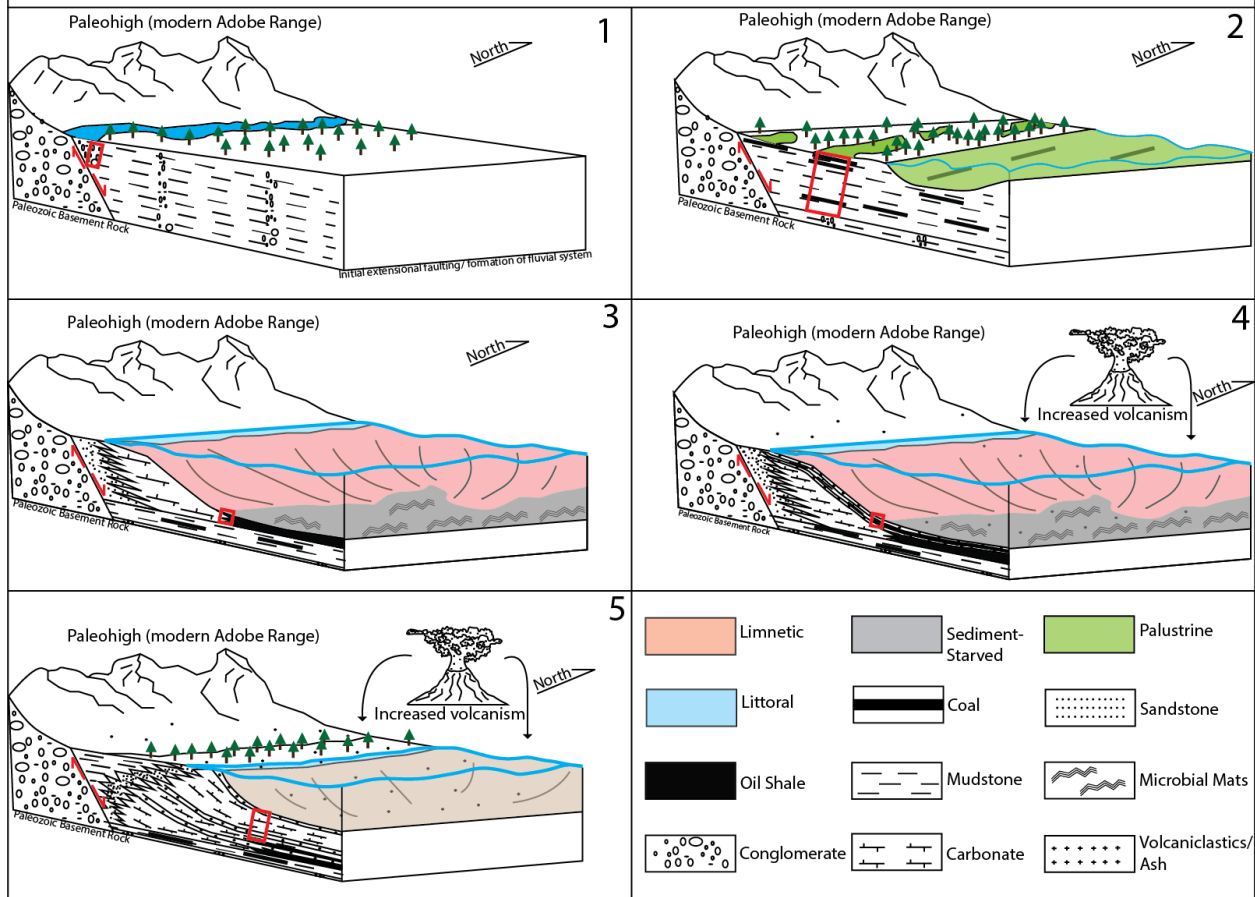


**Figure 11:** Five-stage Elko lake evolution. (1) Initial extensional faulting and creation of an alluvial-fluvial system; (2) Minor subsidence through ongoing extension and formation of lowlands, swamps, and shallow lake; (3) Increasing subsidence through ongoing extension and formation of an open-water lake with a limnetic zone; (4) Stable subsidence and onset of volcanism; (5) Decrease in subsidence and dominant volcanism lead to infilling of the lake and shallowing waters. Red boxes denote lithology observed for each stage in the Coal Mine Canyon section.

## 7.0 DISCUSSION

### 7.1 Elko Formation Source Rock Model and Kerogen Type

Perennially thermally stratified lakes with an anoxic profundal zone have long been considered prerequisites for the formation and preservation of source rocks in lacustrine systems (Renaut and Gierlowski-Kordesch, 2010) and such a model has been used in interpreting the prevalent organic-rich black shales in the Elko Formation (Solomon et al., 1979; Haynes, 2003). Thin section microscopy used in this study, however, shows that the Elko lake source rocks may not be exclusively derived from a deep-water, thermally stratified, anoxic layer. The organic-rich source rocks (microbial-mat-bearing organic-rich mudstones; F5) found in the limnetic-lacustrine depozone of the Elko Formation contains abundant cyanobacterial mats ranging up to 90% of the bulk rock volume. Therefore, most of the F5 organic material is interpreted to derive from the buried *in-situ* microbial mats themselves, rather than a planktonic “rain” of organic matter to anoxic bottom-waters. The cohesive film-like matrix of the cyanobacterial mats acts as an “ecological membrane” at the sediment-water interface, allowing for reducing to anoxic conditions in the sediments under the mats (Bauld, 1981), even during times of well-oxygenated lake waters. Though certain cyanobacterial communities can survive even in anoxic waters (Seckbach and Oren, 2010), they are often found throughout the limnetic-lacustrine depozone with oxic *Candona* ostracods. These benthic *Candona* ostracods show no evidence of additional transport, suggesting they were buried *in-situ*. This suggests available benthic oxygen at times even in distal portions of the Elko lake. Additionally, the ubiquity of the benthic cyanobacterial microbial mats in F5 organic-rich mudstones suggests that lake depths were likely not sufficient to form a true profundal (sunlight-deprived) zone, as Brock and Gustafson (1976) demonstrated the maximum water-depth

limit for cyanobacterial mats to survive to be ~50 m. As such, this number can be used as a crude maximum depth for the limnetic depozone in the Elko lake. Because cyanobacterial mats are so frequently observed in the lacustrine-limnetic zone (FA3 and FA4) black shales (F5), the organic matter type in Elko Formation source rocks is interpreted to consist almost entirely of algal Type-I, oil-prone kerogen. Trace amounts of terrigenous organic material intermixed with F5 black shales likely provides a slight Type-III kerogen (gas-prone) signature to the Elko Formation source rocks.

## **7.2 Differences in the Depozones: Small Lakes vs. Large Lakes**

Lacustrine systems of all shapes and sizes are dynamic (Renaut and Gierlowski-Kordesch, 2010); like their marine counterparts, lakes feature depozones that spatially expand and contract due to rises (i.e. highstands) and falls (i.e. lowstands) in base level (Bohacs et al., 2000). In the case of large lake systems (e.g., Green River Formation, modern Great Lakes, USA), these depozones seem to mimic marine environments. For example, major well-sorted, wave-rippled sandstone shoreline deposits are recognized in Green River Formation stratigraphy (Surdam and Stanley, 1979; Tänavsuu-Milkeviciene and Sarg, 2012), and well-sorted-sandstone shorelines are observed at the Great Lakes, USA today. Turbidites are recorded in many large lake systems including the Eocene Green River Formation (Dyni and Hawkins, 1981), the Jurassic Anyao Formation lakes in China (Buatois et al., 1996), and the Holocene Lake Tahoe in the USA (Osleger et al., 2009), and give evidence that these large lakes contain a “slope” depozone similar to marine environments. These large lakes systems even record wave activity as major depositional contributors, indicated by symmetrical wave ripples and hummocky cross stratification (Surdam and Wolfbauer, 1975; Keighley et al., 2003) that, as in marine systems, are interpreted to occur between fair-weather and storm-weather wave bases. These findings, especially in economically important and often-cited

lacustrine systems such as the Green River Formation and Great Lakes, give the impression that lakes behave exactly like their marine counterparts and their depositional environments are just “mini” versions of marine environments. However, in the case of the Elko Formation, these shoreline deposits, lacustrine turbidites, and diagnostic wave-induced sedimentary structures are not observed in the study area. Although syndepositional tectonic activity in the Elko Basin may have hampered the preservation of these sedimentary structures, the rarity of them both spatially and temporally suggests differences between small and large lake systems. While depositional processes in large lakes may behave similarly to marine systems, the same does not always hold true for “small” lakes like the one that formed the Elko Formation. Instead of a typical large lake or marine progression of depozones (i.e. wetland, backshore, foreshore, offshore slope, etc.) the Elko Formation grades vertically from a swamp environment (FA2) to an open-water limnetic environment (FA3 and FA4) with no intervening distinct shoreline or slope depozone. This suggests that lacustrine depositional environments in small vs. large lake systems may be scale-dependent and their interpretation should take this possibility into account.

### **7.3 Differences and Contradictions in Elko Formation radiometric age dates**

While this study provides two new age dates, more are clearly needed to better constrain correlation of outcrops in the Elko Basin. Previous ages reported by Solomon et al. (1979) and Haynes (2003) are inconsistent, and contradict the ages presented here. Solomon et al. (1979) report a tuff near the Elko Formation-Indian Well Formation contact at the Elko Hills as  $37.1 \pm 1.0$  Ma, while Haynes (2003) records an age of  $38.9 \pm 0.3$  Ma for the same tuff bed. In another instance, Solomon et al. (1979) report the oldest tuff in the Elko Formation (tuff interbedded with the basal boulder conglomerate in the lower member Elko Hills; Stratigraphic Interval 1) as  $43.3 \pm 0.4$  Ma, while Haynes (2003) reports an age of  $46.1 \pm 0.2$  Ma for the exact same tuff bed. More

perturbing is that a tuff interbedded with oil shale in the Coal Mine Canyon upper member (Stratigraphic Interval 2; several thousand feet higher stratigraphically from the previous Stratigraphic Interval 1 “oldest tuff”) was dated as part of this study as  $48.2 \pm 0.02$  Ma. If the new  $^{40}\text{Ar}/^{39}\text{Ar}$  dates are correct, this suggests lacustrine deposition in the Elko Basin occurred at least two million years earlier than previously envisaged. Still, although the previous age dates are partly inconsistent with this study, they do support the same overall trend: the Elko Formation is oldest to the North at Coal Mine Canyon and youngest to the south at Tomera Ranch.

Differences in age dates, especially of the same source material, may relate to different methods in dating. Three different parent/daughter isotope combinations were used in the dating of Elko Formation tuffs:  $^{40}\text{K}/^{40}\text{Ar}$  (Solomon et al., 1979),  $^{235}\text{U}/^{207}\text{Pb}$  (Haynes, 2003), and  $^{40}\text{Ar}/^{39}\text{Ar}$  (this study). Another possibility stems from the intense weathering at all outcrops across the study transect. Biotite and zircon, the two phenocrysts used by all authors for radiometric age dates, may have experienced argon (biotite) or uranium (zircon) loss due to weathering processes. In the case of the Elko Formation, both Solomon et al. (1979) and Haynes (2003) may have used more weathered samples for dating than this study. Future chronostratigraphic studies on the Elko Formation would be best served to use the “freshest” possible samples, from core if feasible, to help resolve these differences.

#### **7.4 Distribution of Volcaniclastic Material and its Relationship to Source Rock Quality**

Throughout the Elko Formation, volcaniclastic sedimentation and organic-rich source rock intervals share an inverse relationship. The volcaniclastic sedimentation occurs in several pulses throughout Elko Formation sedimentation but clearly becomes more pronounced towards the stratigraphic top of each measured section (Stratigraphic Interval 2 at Coal Mine Canyon,

Stratigraphic Interval 3 at Elko Hills, and Stratigraphic Interval 4 at Tomera Ranch). All measured sections show an interval (FA4) consisting of organic-rich black shale and interbedded airfall tuff (205 feet at Coal Mine Canyon, 40 feet in the Elko Hills, and 140 feet at Tomera Ranch), however, these FA4 intervals are always overlain by FA5 intervals that contain abundant ashes but completely lack organic-rich black shale. This suggests that the cyanobacterial mats which prefer sediment starved conditions (e.g. Schieber, 1999; Egenhoff et al., 2013) and make up a significant portion of organic-rich black shales, could only withstand input of volcanoclastic ash for a limited amount of time before ceasing.

Spatially, the sweeping volcanoclastic sedimentation occurs progressively in a north to south fashion along the study transect, initiating at Coal Mine Canyon and ending at Tomera Ranch. Organic-rich source rock deposition mimics this same trend by shifting spatially from the northern portion of the study area (Coal Mine Canyon; Stratigraphic Interval 2) to the central portion (Elko Hills; Stratigraphic Interval 3) to the southern portion (Tomera Ranch; Stratigraphic Interval 4) throughout the evolution of the Elko Basin. Interestingly, organic-rich source rock deposition is always most pronounced southward of the locus of volcanoclastic sedimentation: when volcanoclastic deposition is at its maximum at Coal Mine Canyon (Stratigraphic Interval 3) black shales are thickest at the Elko Hills, and when volcanoclastic sedimentation is dominant at the Elko Hills (Stratigraphic Interval 4), black shale deposition exclusively occurs to the south at Tomera Ranch. This suggests that conditions necessary for black shale deposition, particularly those with a strong algal mat component, cannot exist in the same area as the abundant volcanoclastic input, but instead thrive southward of the north-south sweeping volcanic belt. In the case of the Elko Basin, this volcanoclastic sediment supply likely successively outpaced the accommodation space

necessary for black shale deposition from north to south, enhancing tectonic factors that caused the basin depocenter and black-shale environment to shift southward over time.

### **7.5 Unconventional Petroleum Exploration Possibilities**

Organic-rich black shales were observed at every measured section in the study area, suggesting petroleum potential in the Elko Basin is high where the shales were sufficiently buried and are therefore thermally mature. The measured sections of this study, along with the measured stratigraphy of Haynes (2003), show that organic-rich black shales are thickest in the central Elko Hills area. This suggests that for the majority of the Elko Basin's history, the central Elko Hills area was the deepest and most strongly sediment-starved portion of the Elko Basin, and consequently black shales at those localities likely feature the highest TOC content. Because of its basinal position, however, the vertically continuous black shales encountered in the Elko Hills are less sensitive to lake-level fluctuations and thus do not show the decimeter-scale interbedding with fossiliferous wackestones (F8; FA3) that occurs at Coal Mine Canyon and Tomera Ranch. The black shales of this study frequently contain up to 20% siliciclastic and/or volcanoclastic silt-size material, but if the shales prove to be too ductile for hydraulic fracturing, the marginal positions of the Elko Basin may be more economically viable because of their interbedded limestone beds. As an unconventional resource play, hydraulic fracturing is essential for hydrocarbon production; the black shale intervals in more marginal positions of the Elko Basin (Coal Mine Canyon and Tomera Ranch), though probably lower in TOC than the Elko Hills, contains essential brittle and "fraccable" limestone beds.

## 8.0 CONCLUSIONS

1. The Eocene Elko Formation in Nevada, USA, consists of fourteen facies, eight of which are siliciclastic, three carbonate, and three volcanoclastic. The facies can be grouped into five facies associations: siliciclastic mudstones and conglomerates (FA1), massive coal-rich mudstones (FA2), microbial-mat-bearing mudstones and carbonates (FA3), microbial-mat-bearing mudstones and volcanoclastics (FA4), and carbonates and volcanoclastics (FA5).
2. The studied succession is poorly exposed in four outcrops along the study transect. Measured sections of this study likely show little chronostratigraphic continuity for any given facies association with no distinct marker beds. Therefore, the Elko Formation is subdivided into four vaguely chronostratigraphic intervals (Stratigraphic Intervals 1, 2, 3, and 4) based on new and previous radiometric age dates.
3. The range of facies observed in this study indicates that the Elko Formation was deposited across an extensive continental–lacustrine environment that can be subdivided into four spatially distinct depozones, which are, from proximal to distal: (1) alluvial-fluvial, (2) palustrine-lacustrine, (3) littoral-lacustrine, (4) limnetic-lacustrine.
4. The depocenter and locus of limnetic-lacustrine black shale deposition in the Elko Basin progressively shifted southwards along the study transect due to tectonics throughout the Eocene. Black shales were deposited initially in the northern portion of the study area (Coal Mine Canyon; ~53.0–50.0?), then subsequently in the central part (Elko Hills; ~50.0–48.5 Ma), and finally in the south (Tomera Ranch; ~48.5–43.5 Ma). Increasing volcanism, which

enhanced sediment supply and filled available accommodation space, followed black shale deposition in the same north to south progression to “fill in” the lake by ~37.5 Ma.

5. The Elko lake represents a “small” lacustrine system when compared to the roughly time-equivalent Green River lakes, and consequently shows less variability in sedimentary structures and depositional sub-environments. “Small” lacustrine systems cannot be interpreted as “mini” versions of their larger counterparts. The Elko Formation contains its own unique set of depositional controls.
6. Possible source rocks are prevalent throughout the study area as the microbial-mat bearing organic-rich black shale facies (F5). Kerogen content in this facies is interpreted to derive from *in-situ* cyanobacterial communities, rather than from a “rain” of suspended organic material. Consequently, Type-I kerogen is expected as the dominant organic matter type, with some Type-III mixing due to suspension of abundant terrigenous organic material, even in distal portions of the lake.
7. Organic-rich black shales accumulated in an environment that was dominantly oxygenated and in the photic zone. This runs counter to conventional lacustrine source rock models that preclude the possibility for source rock preservation outside of a stratified, anoxic, “deep-water” zone.
8. The central Elko Hills locality contains the thickest accumulations of organic-rich black shales, but features no interfingering brittle and “fraccable” carbonate beds that the northern and southern, more marginal environments of the basin contain. If Elko Formation black shale proves to be too ductile for hydraulic fracturing, exploration efforts should focus on marginal

and more lithologically diverse areas towards the northern and southern portions of this lacustrine system that are more sensitive to lake-level fluctuations.

## 9.0 REFERENCES

- Bauld, J., 1981, Occurrence of benthic microbial mats in saline lakes: Salt Lakes: Developments in Hydrobiology, vol. 5, p. 87–111.
- Bohacs, K. M., 1993, Source quality variations tied to sequence development in the Monterey and associated formations, southwestern California: AAPG Studies in Geology, v. 37, p. 177–204.
- Bohacs, K. M., A. R. Carroll, J. E. Nede, and P. J. Mankiowicz, 2000, Lake-Basin Type, Source Potential, and Hydrocarbon Character: An Integrated Sequence-Stratigraphic-Geochemical Framework, in E. H. Gierlowski-Kordesch and K. R. Kelts, eds., Lake Basins through Space and Time: AAPG Studies in Geology, v. 46, p. 3–32.
- Brock, T. D., and J. Gustafson, 1976, Ferric iron reduction by sulfur- and iron-oxidizing bacteria: Applied and Environmental Microbiology, v. 32, no. 4, p. 567–571.
- Buatois, L. A., M. G. Mângano, X. Wu, and G. Zhang, 1996, Trace fossils from Jurassic Lacustrine Turbidites of the Anyao Formation (Central China) and their Environmental and Evolutionary Significance: Ichnos, v. 4, no. 4, p. 287–303.
- Carroll, A. R., and K. M. Bohacs, 1999, Stratigraphic classification of ancient lakes: Balancing tectonic and climatic controls: Geology, v. 27, no. 2, p. 99–102.
- Christiansen, R. L., and R. S. Yeats, 1992, Post-Laramide geology of the US Cordilleran region, in M. L. Zoback, ed., The Cordilleran Orogen, p. 261–406.
- Coats, R. R., 1964, Geology of the Jarbidge quadrangle, Nevada-Idaho: United States Geological Survey Bulletin, no. 1141-M, scale 1:62,500.
- Coats, R. R., 1987, Geology of Elko County, Nevada: Nevada Bureau of Mines and Geology Bulletin, no. 101, scale 1:250,000.
- Colgan, J. P., and J. R. Metcalf, 2006, Rapid middle Miocene unroofing of the southern Ruby Mountains, Nevada: Geological Society of America Abstracts with Programs, v. 38, no. 7, 417 p.
- DeCelles, P. G., 2004, Late Jurassic to Eocene evolution of the Cordilleran thrust belt and foreland basin system, western USA: American Journal of Science, v. 304, p. 105-168.
- Dunham, R. J., 1962, Classification of Carbonate Rocks According to Depositional Textures, in W. E. Ham, ed., Classification of Carbonate Rocks: American Association of Petroleum Geologists Memoir 1, p. 108–121.

- Dyni, J. R., and J. E. Hawkins, 1981, Lacustrine turbidites in the Green River Formation, northwestern Colorado: *Geology*, v. 9, no. 5, p. 235–238.
- Egenhoff, S. O., and N. S. Fishman, 2013, Traces in the dark-sedimentary processes and facies gradients in the upper shale member of the Upper Devonian-Lower Mississippian Bakken Formation, Williston Basin, North Dakota, U.S.A: *Journal of Sedimentary Research*, v. 83, no. 9, p. 803–824.
- Egenhoff, S. O., N. S. Fishman, and R. J. Hill, 2013, Microbial mats as an indicator for pauses during “shale” deposition; Kimmeridge Clay Formation (Upper Jurassic), offshore UK: Abstracts: Annual Meeting - American Association of Petroleum Geologists, Pittsburgh, 2013.
- Eugster, H. P., and R. C. Surdam, 1973, Depositional Environment of the Green River Formation of Wyoming: A Preliminary Report: *Geological Society of America Bulletin*, v. 84, no. 4, p. 1115–1120.
- Fisher, R. V., 1971, Features of Coarse-Grained, High-Concentration Fluids and Their Deposits: *Journal of Sedimentary Research*, v. 41, no. 4, p. 916-927.
- Flügel, E., 2010, *Microfacies of Carbonate Rocks: Analysis, Interpretation and Application*: Berlin-Heidelberg, Springer Science & Business Media, 1006 p.
- Fouch, T. D., J. H. Hanley, and R. M. Forester, 1979, Preliminary Correlation of Cretaceous and Paleogene Lacustrine and Related Nonmarine Sedimentary and Volcanic Rocks in Parts of the Eastern Great Basin of Nevada and Utah, in G.W. Newman and H.D. Goode, eds., Basin and Range symposium and Great Basin field conference: *Rocky Mountain Association of Petroleum Geologists*, p. 305-312.
- Friedman, G. M., J. E. Sanders, and D. C. Kopaska-Merkel, 1992, *Principles of Sedimentary Deposits*: New York, Wiley, 792 p.
- Gray, M. B., and R. P. Nickelsen, 1989, Pedogenic slickensides, indicators of strain and deformation processes in redbed sequences of the Appalachian foreland: *Geology*, v. 17, no. 1, p. 72–75.
- Haynes, S. R., 2003, Development of the Eocene Elko basin, northeastern Nevada: Implications for paleogeography and regional tectonism: M.S. thesis, The University of British Columbia, Vancouver, British Columbia, 159 p.
- Henry, C. D., 2008, Ash-flow tuffs and paleovalleys in northeastern Nevada: Implications for Eocene paleogeography and extension in the Sevier hinterland, northern Great Basin: *Geosphere*, v. 4, no. 1, p. 1–35.
- Henry, C. D., and J. E. Faulds, 1999, Geologic map of the Emigrant Pass quadrangle, Nevada: Nevada Bureau of Mines and Geology Open-File Report, no. 99-9, scale 1:24,000.

- Janecke, S. U., B. F. Hammond, L. W. Snee, and J. W. Geissman, 1997, Rapid extension in an Eocene volcanic arc: Structure and paleogeography of an intra-arc half graben in central Idaho: *Geological Society of America Bulletin*, v. 109, no. 3, p. 253–267.
- Katz, B. J., and F. Lin, 2014, Lacustrine basin unconventional resource plays; key differences: *Marine and Petroleum Geology*, v. 56, p. 255–265.
- Keighley, D., S. Flint, J. Howell, and A. Moscariello, 2003, Sequence Stratigraphy in Lacustrine Basins: A Model for part of the Green River Formation (Eocene), Southwest Uinta Basin, Utah, U.S.A: *Journal of Sedimentary Research*, v. 73, no. 6, p. 987–1006.
- Ketner, K. B., and A. G. Alpha, 1992, Mesozoic and Tertiary rocks near Elko, Nevada--evidence for Jurassic to Eocene folding and low-angle faulting: *United States Geological Survey Bulletin*, no. 1988C, p. C1-C13.
- Koppers, A. P., 2002, ArArCALC—software for  $^{40}\text{Ar}/^{39}\text{Ar}$  age calculations: *Computers & Geosciences*, v. 28, no. 5, p. 605–619.
- Levi, T., R. Weinberger, T. Aifa, Y. Eyal, and S. Marco, 2006, Earthquake-induced clastic dikes detected by anisotropy of magnetic susceptibility: *Geology*, v. 34, no. 2, p. 69–72.
- Lofgren, G., 1971, Spherulitic textures in glassy and crystalline rocks: *Journal of Geophysical Research*, v. 76, no. 23, p. 5635-5648.
- Macquaker, J. H. S., and A. E. Adams, 2003, Maximizing Information from Fine-Grained Sedimentary Rocks: An Inclusive Nomenclature for Mudstones: *Journal of Sedimentary Research*, v. 73, no. 5, p. 735–744.
- Macquaker, J. H. S., and J. K. Howell, 1999, Small-scale (<5.0 m) vertical heterogeneity in mudstones; implications for high-resolution stratigraphy in siliciclastic mudstone successions: *Journal of the Geological Society of London*, v. 156, no. 1, p. 105–112.
- Macquaker, J. H. S., R. L. Gawthorpe, K. G. Taylor, and M. J. Oates, 1998, Heterogeneity, stacking patterns and sequence stratigraphic interpretation in distal mudstone successions; examples from the Kimmeridge Clay Formation, U.K, in J. Schieber et al., eds., *Shales and Mudstones; v. I, Basin Studies, Sedimentology, and Paleontology*: E. Schweizerbart'sche Verlagsbuchhandlung Naegle u. Obermiller, p. 163–186.
- Macquaker, J. H. S., K. G. Taylor, and R. L. Gawthorpe, 2007, High-resolution facies analyses of mudstones; implications for paleoenvironmental and sequence stratigraphic interpretations of offshore ancient mud-dominated successions: *Journal of Sedimentary Research*, v. 77, no. 4, p. 324–339.
- McGrew, A. J., M. T. Peters, and J. E. Wright, 2000, Thermobarometric constraints on the tectonothermal evolution of the East Humboldt Range metamorphic core complex, Nevada: *Geological Society of America Bulletin*, v. 112, p. 45–60.

- McIntyre, D. H., E. B. Ekren, and R. F. Hardyman, 1982, Stratigraphic and structural framework of the Challis volcanics in the eastern half of the Challis 1° by 2° Quadrangle, Idaho: Cenozoic geology of Idaho: Idaho Bureau of Mines and Geology Bulletin 26, p 3-22.
- Moore, S. W., H. B. Madrid, and G. T. Server, 1983, Results of oil-shale investigations in northeastern Nevada: United States Geological Survey Open-File Report, no. 83-586, 56 p.
- Muntean, J. L., C. Tarnocai, M. Coward, D. Rouby, and A. Jackson, 2001, Styles and restorations of Tertiary extension in north-central Nevada, in D. R. Shaddrick and D. C. Mathewson, eds., Regional Tectonics and Structural Control of Ore: The Major Gold Trends of Northern Nevada: Geological Society of Nevada Special Publication, no. 33, p. 55-69.
- Nutt, C. J., and S. C. Good, 1998, Recognition and significance of Eocene deformation in the Alligator Ridge area, central Nevada: US Geological Survey Open-File Report, no. 98-338, p. 141-150.
- Obermeier, S. F., 1996, Use of liquefaction-induced features for paleoseismic analysis — An overview of how seismic liquefaction features can be distinguished from other features and how their regional distribution and properties of source sediment can be used to infer the location and strength of Holocene paleo-earthquakes: Engineering Geology, v. 44, no. 1-4, p. 1-76.
- Osleger, D. A., A. C. Heyvaert, J. S. Stoner, and K. L. Verosub, 2009, Lacustrine turbidites as indicators of Holocene storminess and climate: Lake Tahoe, California and Nevada: Journal of Paleolimnology, v. 42, no. 1, p. 103–12.
- Plint, A., 2014, Mud dispersal across a Cretaceous prodelta: Storm-generated, wave-enhanced sediment gravity flows inferred from mudstone microtexture and microfacies: Sedimentology, v. 61, no. 3, p. 609–647.
- Renaut, R.W., and E. H. Gierlowski-Kordesch, 2010, Lakes, in N. P. James and R. W. Dalrymple, eds., Facies Models, 4<sup>th</sup> Edition: Geological Association of Canada, p. 541-575.
- Retallack, G. J., 2008, Soils of the Past: An Introduction to Paleopedology: Boston, Unwin Hyman, 548 p.
- Schieber, J., 1998, Sedimentary features indicating erosion, condensation, and hiatuses in the Chattanooga Shale of central Tennessee; relevance for sedimentary and stratigraphic evolution, in J. Schieber et al., eds., Shales and Mudstones; v. I, Basin Studies, Sedimentology, and Paleontology: E. Schweizerbart'sche Verlagsbuchhandlung Naegle u. Obermiller, p. 187-215.
- Schieber, J., 1999, Microbial mats in terrigenous clastics; the challenge of identification in the rock record: PALAIOS, v. 14, no. 1, p. 3–12.

- Schieber, J., J. B. Southard, P. Kissling, B. Rossman, and R. Ginsburg, 2013, Experimental deposition of carbonate mud from moving suspensions: Importance of flocculation and implications for modern and ancient carbonate mud deposition: *Journal of Sedimentary Research*, v. 83, p. 1026-1032.
- Schubel, K. A., and B. M. Simonson, 1990, Petrography and Diagenesis of Cherts From Lake Magadi, Kenya: *Journal of Sedimentary Research*, v. 60, no. 5.
- Seckbach, J., and A. Oren, 2010, *Microbial Mats: Modern and Ancient Microorganisms in Stratified Systems*: New York, Springer Science & Business Media, 595 p.
- Server, G.T., and B. J. Solomon, 1983, Geology and oil shale deposits of the Elko Formation, Piñon Range, Elko County, Nevada: United States Geological Survey Miscellaneous Field Studies Map, no. MF-1546, scale 1:24,000.
- Sims, J. D., 2013, Earthquake-induced load casts, pseudonodules, ball-and-pillow structures, and convolute lamination: Additional deformation structures for paleoseismic studies, in R. T. Cox et al., eds., *Geological Society of America Special Papers* 493, p. 191-201.
- Smith, J. F., K. B. Ketner, and D. R. Mabey, 1976, Stratigraphy of post-Paleozoic rocks and summary of resources in the Carlin-Piñon Range area, Nevada, with a section on aeromagnetic survey: *United States Geological Survey Bulletin*, no. 867-B, 47 p.
- Smith, M. E., A. R. Carroll, and B. S. Singer, 2008, Synoptic reconstruction of a major ancient lake system: Eocene Green River Formation, western United States: *Geological Society of America Bulletin*, v. 120, no. 1-2, p. 54-84.
- Solomon, B. J., 1992, The Elko Formation of Eocene and Oligocene (?) age—source rocks and petroleum potential in Elko County, Nevada, in Trexler et al., eds., *Structural Geology and Petroleum Potential of Southwest Elko County, Nevada*: Nevada Petroleum Society 1992 Fieldtrip Guidebook, p. 25-38.
- Solomon, B. J., and S. W. Moore, 1982, Geologic Map and Oil Shale Deposits of the Elko East Quadrangle, Elko County, Nevada: United States Geological Survey Misc. Field Investigations, no. MF-1421, scale 1:24,000.
- Solomon, B. J., E. H. McKee, and D. W. Andersen, 1979, Stratigraphy and Depositional Environments of Paleogene Rocks Near Elko, Nevada, in Armentrout et al., eds., *Cenozoic Paleogeography of the Western United States, Pacific Coast Paleogeography Symposium 3: S.E.P.M.*, p. 75-88.
- Sullivan, R., 1980, A stratigraphic evaluation of the Eocene rocks of southwestern Wyoming: Wyoming Geological Survey Report of Investigations, no. 20, 50 p.
- Surdam, R. C., and K. O. Stanley, 1979, Lacustrine sedimentation during the culminating phase of Eocene Lake Gosiute, Wyoming (Green River Formation): *Geological Society of America Bulletin*, v. 90, no. 1, p. 93-110.

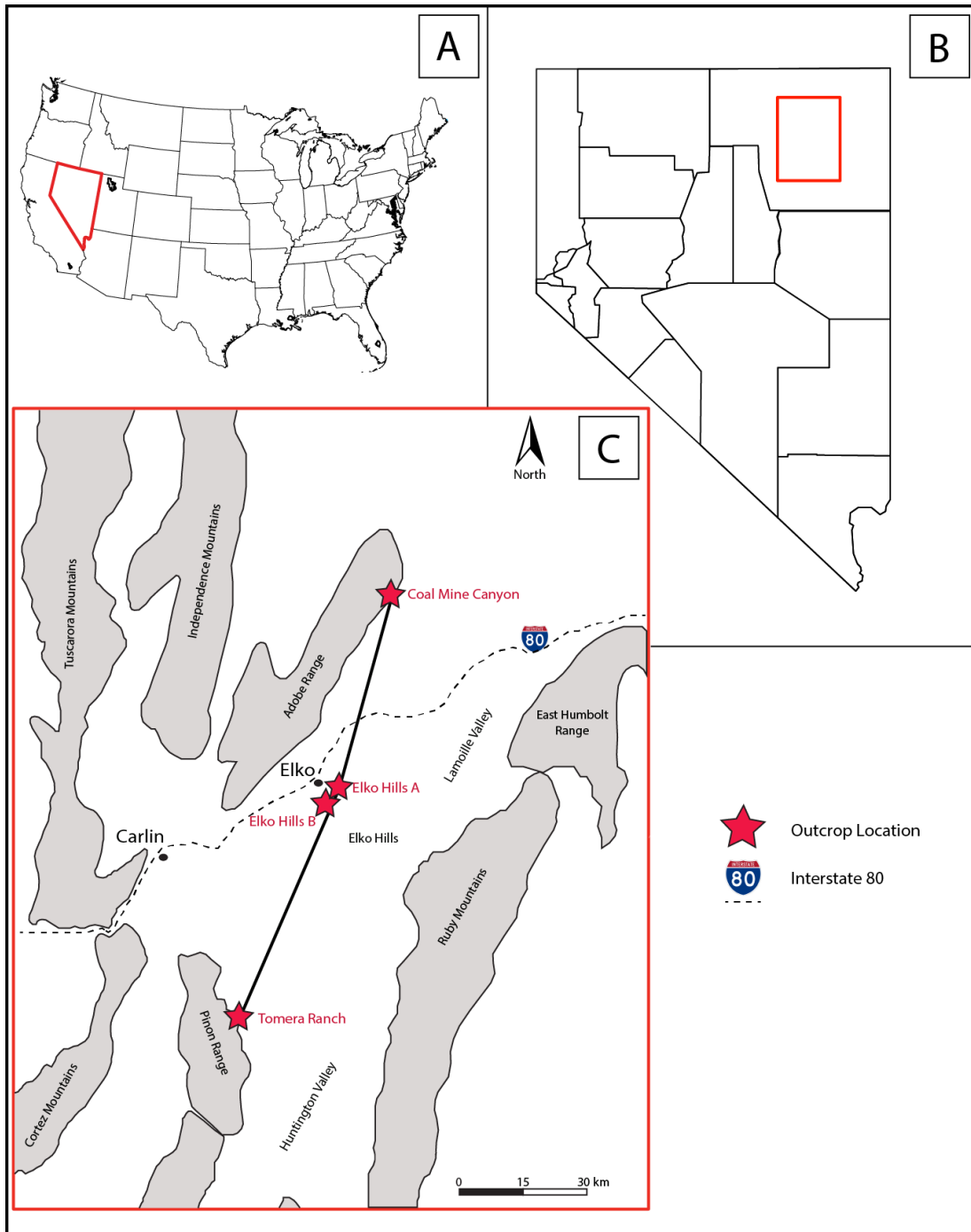
- Surdam, R. C., and C. A. Wolfbauer, 1975, Green River Formation, Wyoming: A Playa-Lake Complex: *Geological Society of America Bulletin*, v. 86, no. 3, p. 335–345.
- Tänavsuu-Milkeviciene, K. A. T. I., and J. F. Sarg, 2012, Evolution of an organic-rich lake basin – stratigraphy, climate and tectonics: Piceance Creek basin, Eocene Green River Formation: *Sedimentology*, v. 59, no. 6, p. 1735–1768.
- Tucker, M. E., 2009, *Sedimentary Petrology: An Introduction to the Origin of Sedimentary Rocks*: New York, Wiley, 291 p.
- Wallace, A. R., M. E. Perkins, and R. J. Fleck, 2008, Late Cenozoic paleogeographic evolution of northeastern Nevada: Evidence from the sedimentary basins: *Geosphere*, v. 4, no. 1, p. 36–74.
- Wignall, P. B., and R. J. Newton, 2001, Black shales on the basin margin; a model based on examples from the Upper Jurassic of the Boulonnais, northern France: *Sedimentary Geology*, v. 144, no. 3-4, p. 335–356.
- Wingate, F. H., 1983, Palynology and age of the Elko Formation (Eocene) near Elko, Nevada: *Palynology*, v. 7, no. 1, p. 93–132.

## **APPENDICES**

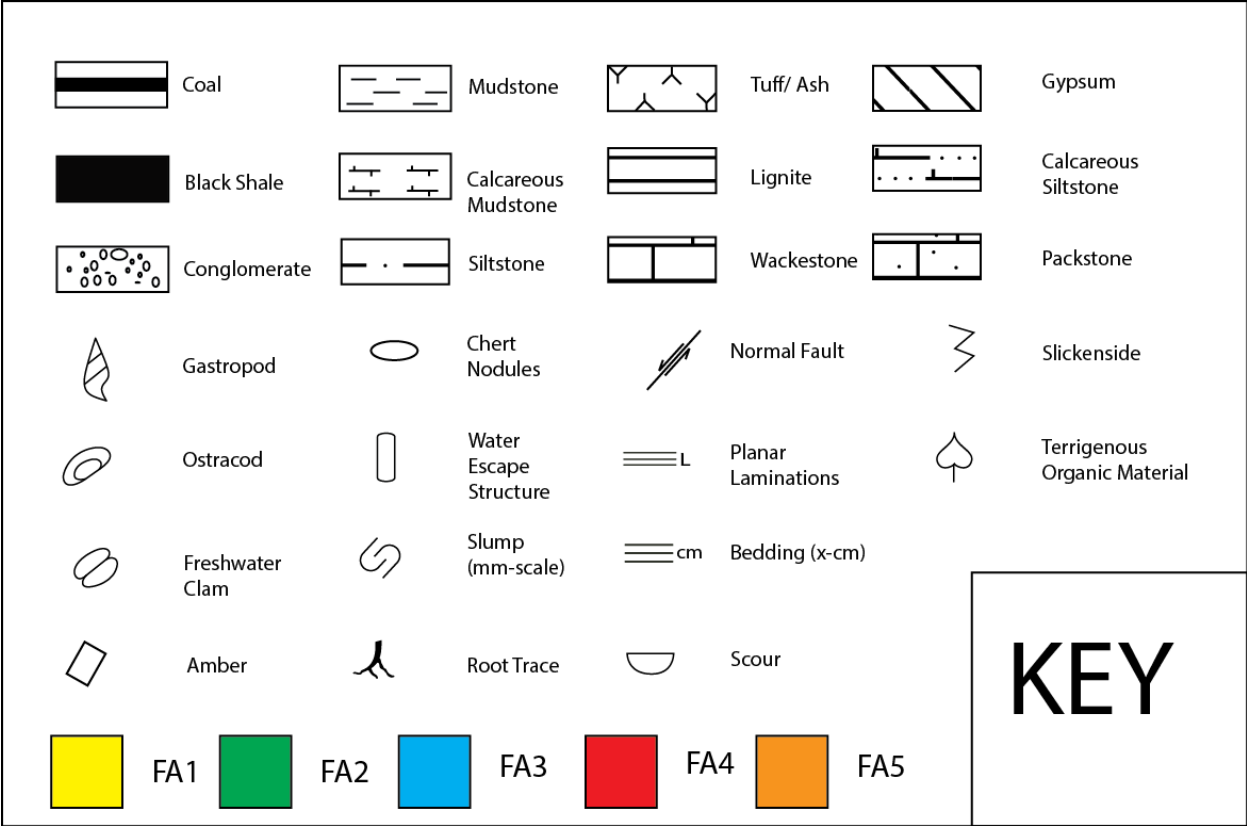
**APPENDIX 1: COMPILATION OF NEW AND PREVIOUSLY PUBLISHED AGES FOR THE ELKO FORMATION REFERENCED IN THIS STUDY**

Chronostratigraphic Interval	Location	Mineral	Age	± error	Source
Top Interval 4	Piñon Range	Biotite- $^{40}\text{K}/^{40}\text{Ar}$	37.1	1.0	Solomon et al., 1979
Top Interval 4	Piñon Range	Biotite- $\text{Ar}^{40}/\text{Ar}^{39}$	37.5	0.10	Haynes, 2003
Top Interval 4	Elko Hills	Zircon- $^{235}\text{U}/^{207}\text{Pb}$	38.9	0.30	Haynes, 2003
Top Interval 4	Coal Mine Canyon	Zircon- $^{235}\text{U}/^{207}\text{Pb}$	41.1	0.20	Haynes, 2003
Interval 3	Elko Hills	Biotite- $^{40}\text{K}/^{40}\text{Ar}$	43.3	0.40	Solomon et al., 1979
Interval 4	Piñon Range	Biotite- $\text{Ar}^{40}/\text{Ar}^{39}$	43.5	0.02	This Study
Interval 1	Elko Hills	Zircon- $^{235}\text{U}/^{207}\text{Pb}$	46.1	0.20	Haynes, 2003
Interval 2	Coal Mine Canyon	Biotite- $\text{Ar}^{40}/\text{Ar}^{39}$	48.2	0.02	This Study

**APPENDIX 2: MEASURED AND DIGITIZED SECTIONS OF THE UPPER ELKO FORMATION, NORTHEAST NEVADA**



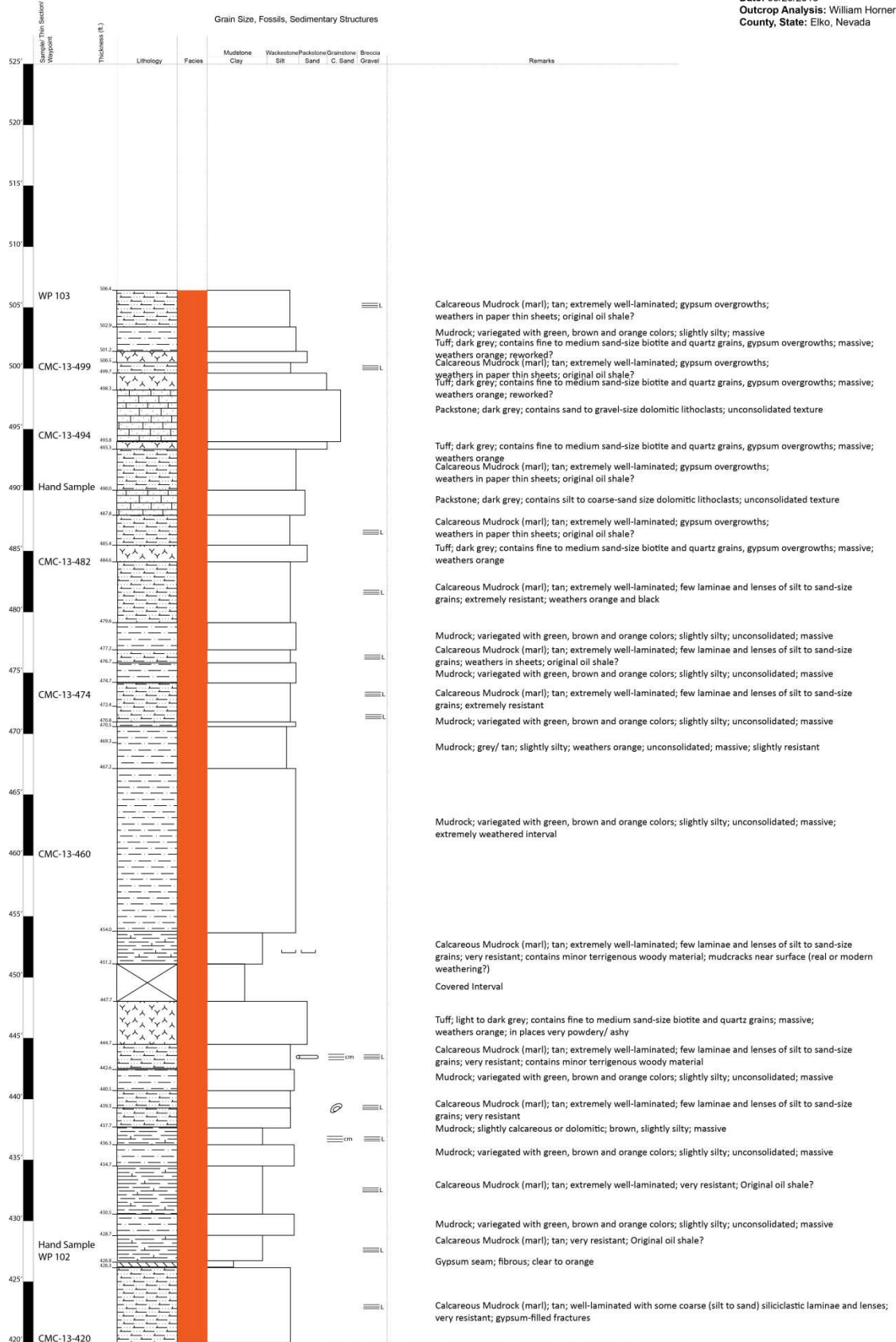
Study Area Map with north-south Transect



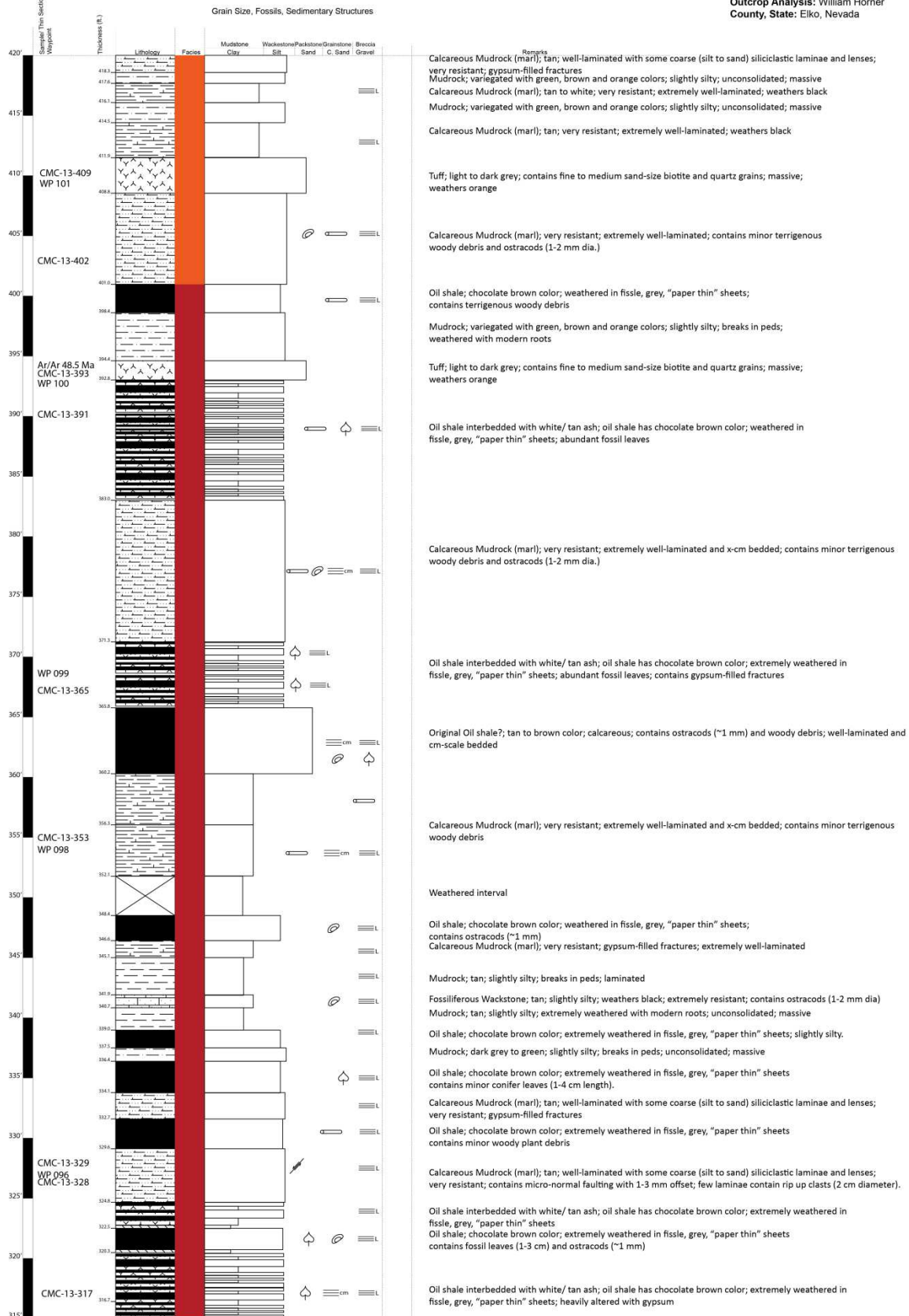
Legend for Digitized Outcrop Sections

## **Coal Mine Canyon**

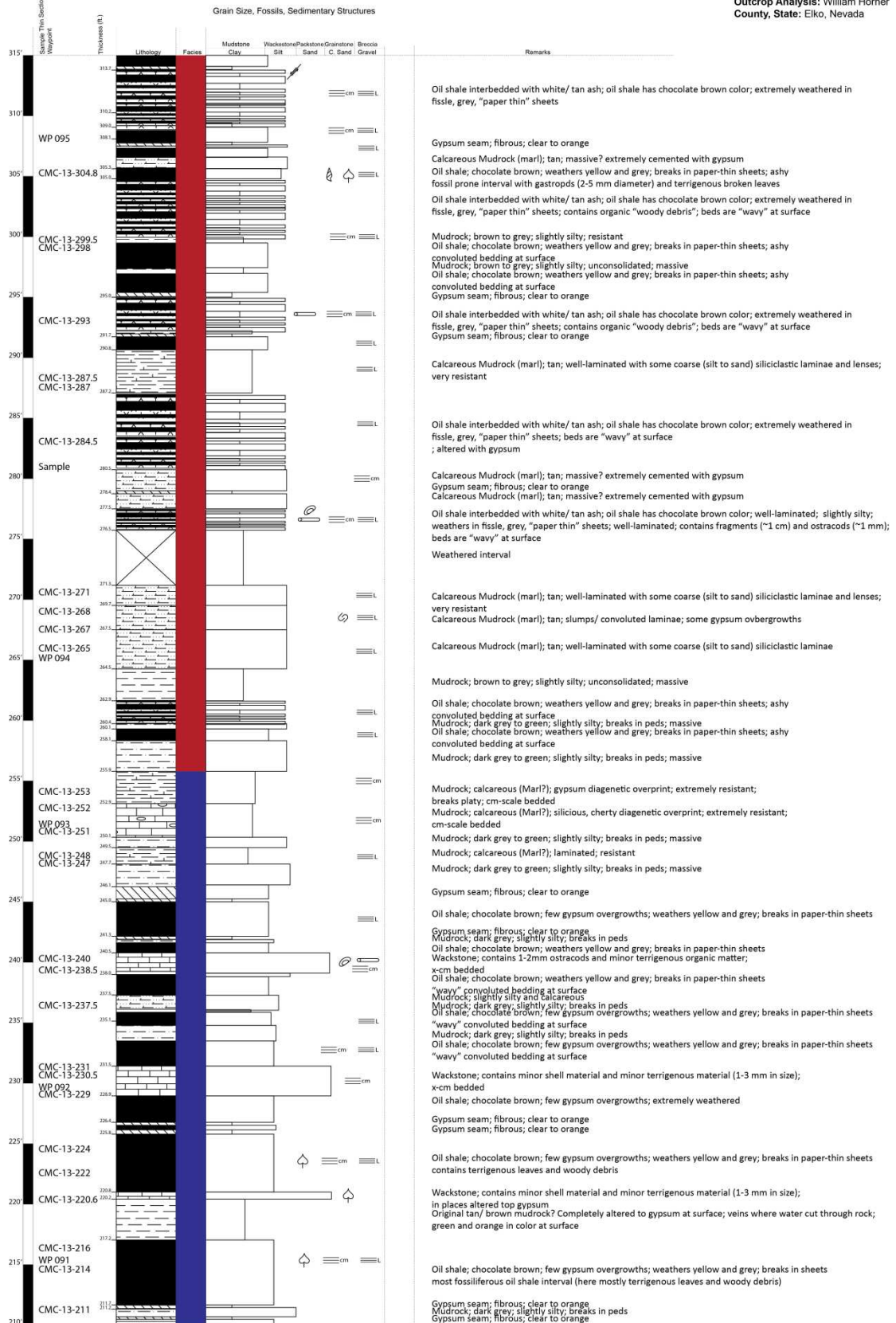
Outcrop: Coal Mine Canyon  
 Stratigraphic Interval: Elko Fm.  
 Date: 05/25/2013  
 Outcrop Analysis: William Horner  
 County, State: Elko, Nevada



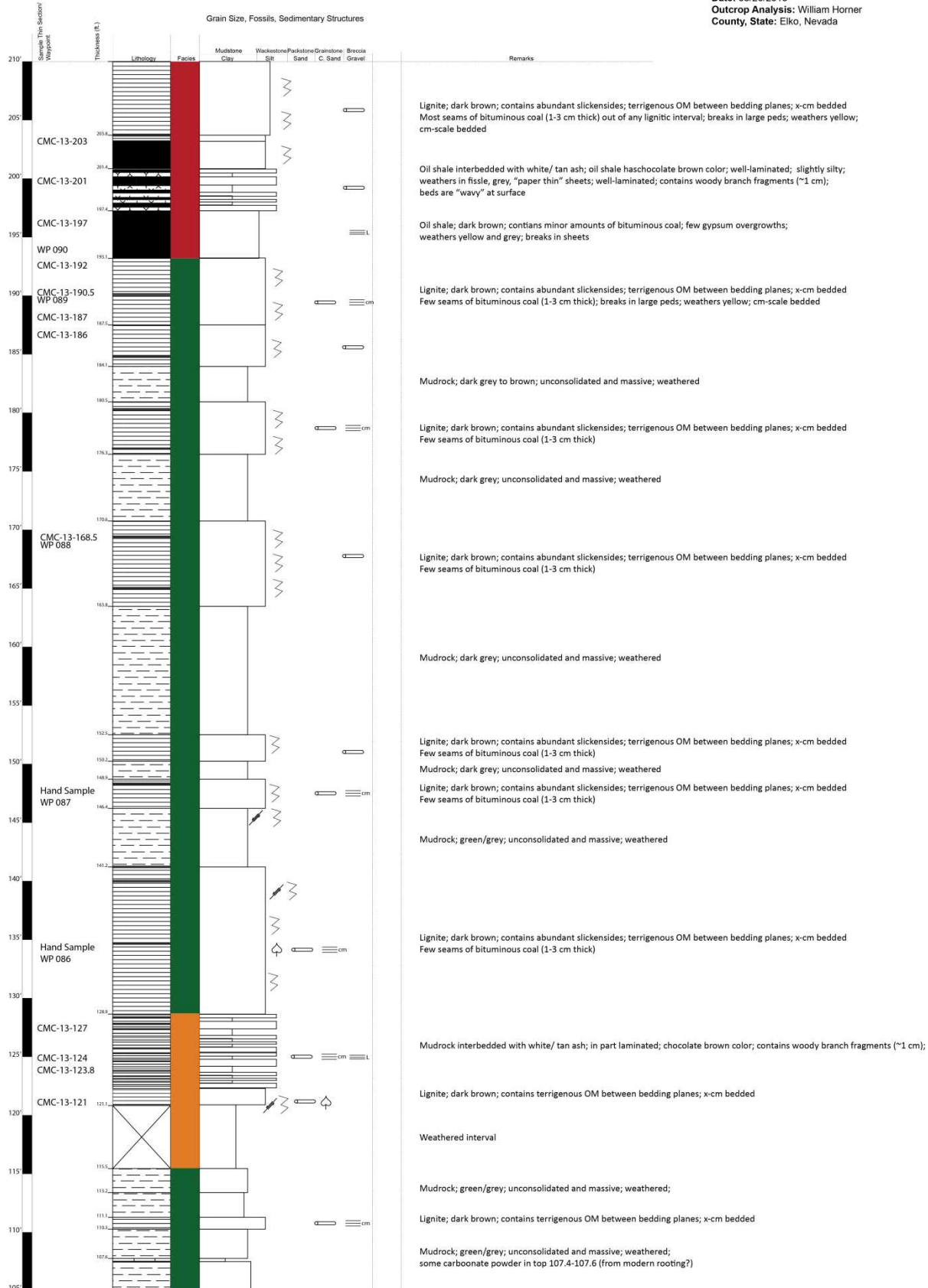
**Outcrop:** Coal Mine Canyon  
**Stratigraphic Interval:** Elko Fm.  
**Date:** 05/23/2013  
**Outcrop Analysis:** William Horner  
**County, State:** Elko, Nevada



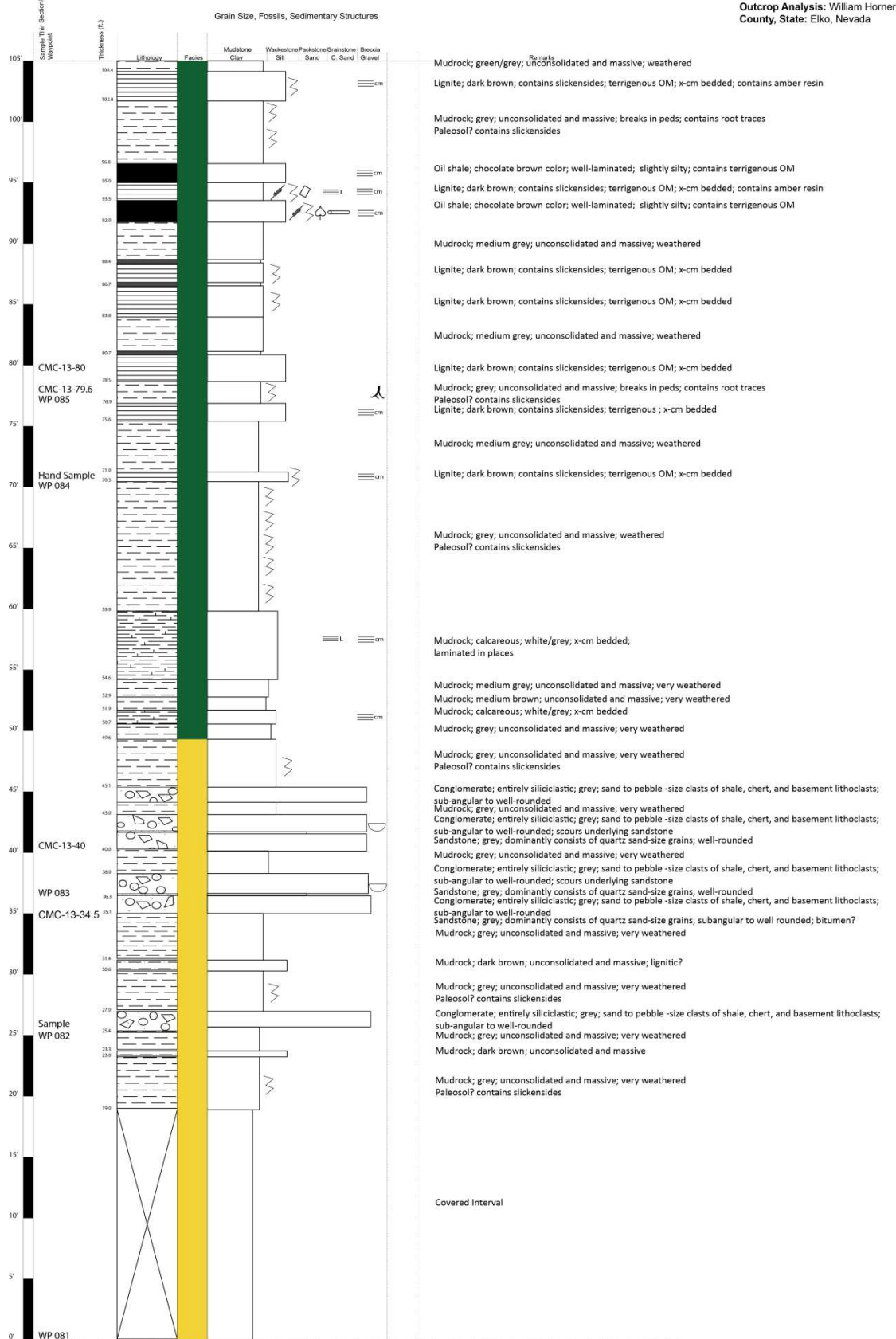
**Outcrop:** Coal Mine Canyon  
**Stratigraphic Interval:** Elko Fm.  
**Date:** 05/24/2013  
**Outcrop Analysis:** William Horner  
**County, State:** Elko, Nevada



Outcrop: Coal Mine Canyon  
 Stratigraphic Interval: Elko Fm.  
 Date: 03/26/2013  
 Outcrop Analysis: William Horner  
 County, State: Elko, Nevada

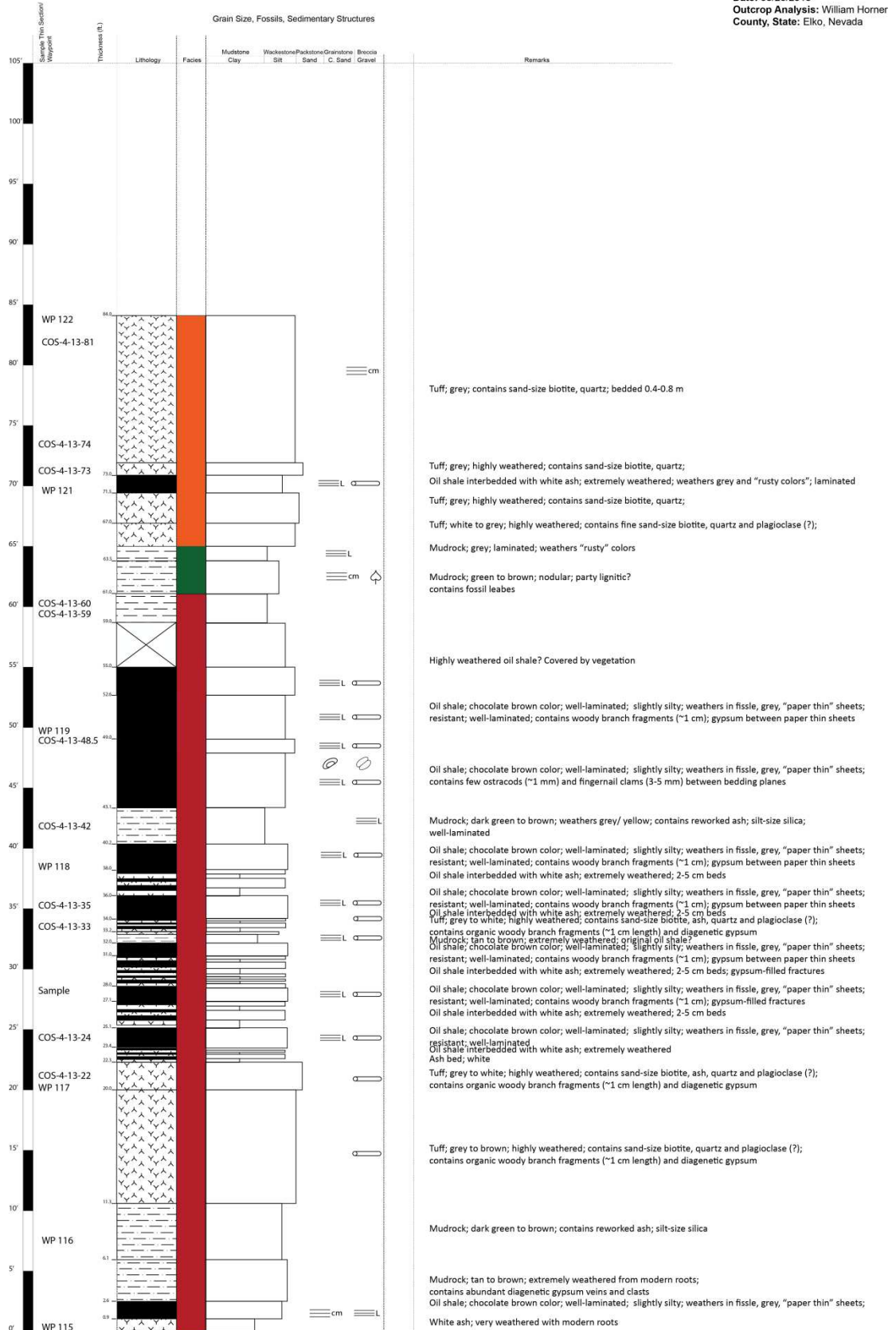


Outcrop: Coal Mine Canyon  
 Stratigraphic Interval: Elko Fm.  
 Date: 03/26/2013  
 Outcrop Analysis: William Horner  
 County, State: Elko, Nevada

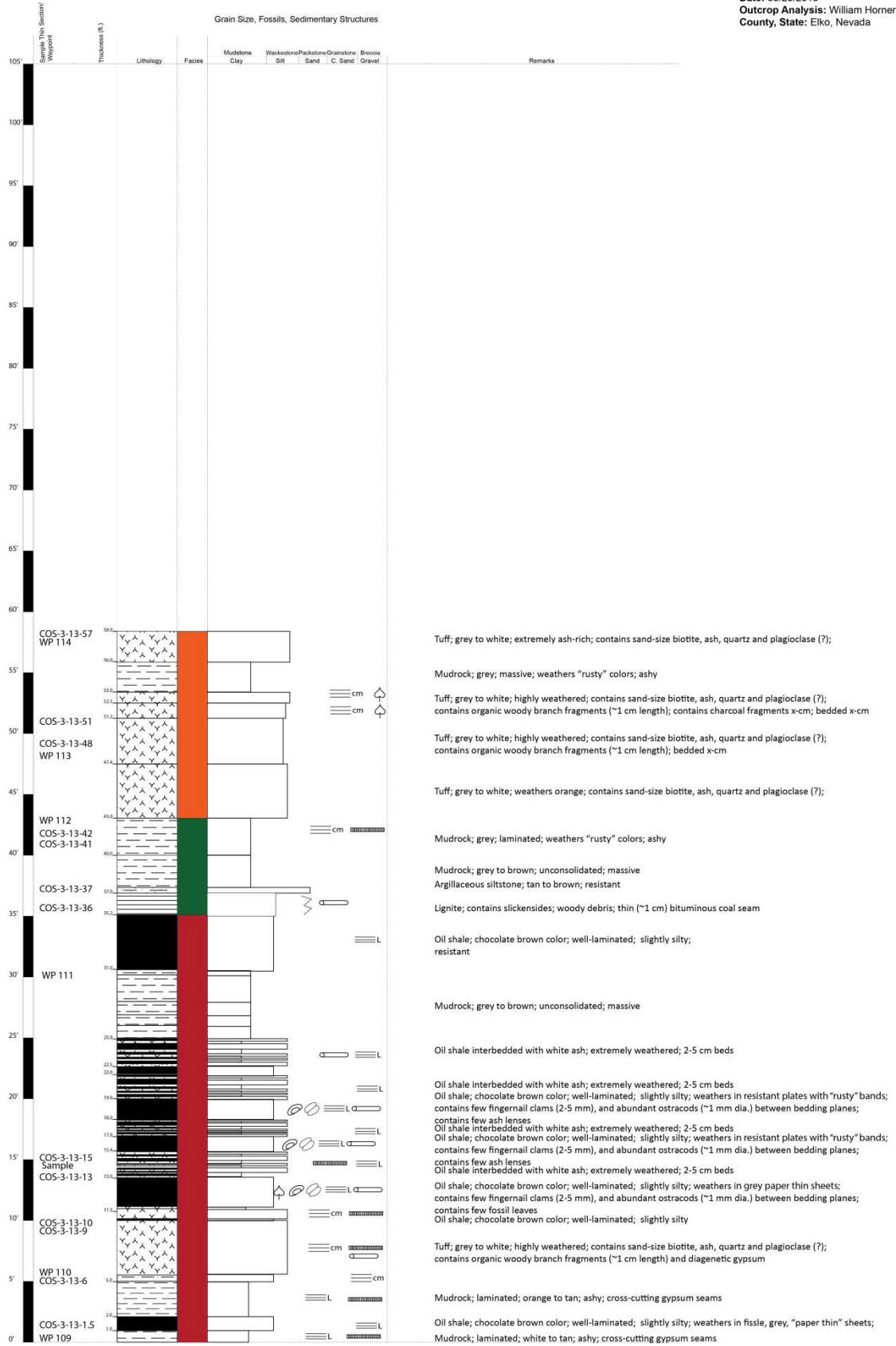


**Elko Hills A and B**

**Outcrop:** Elko Hills A (Elko Hills)  
**Stratigraphic Interval:** Elko Fm.  
**Date:** 05/23/2013  
**Outcrop Analysis:** William Horner  
**County, State:** Elko, Nevada

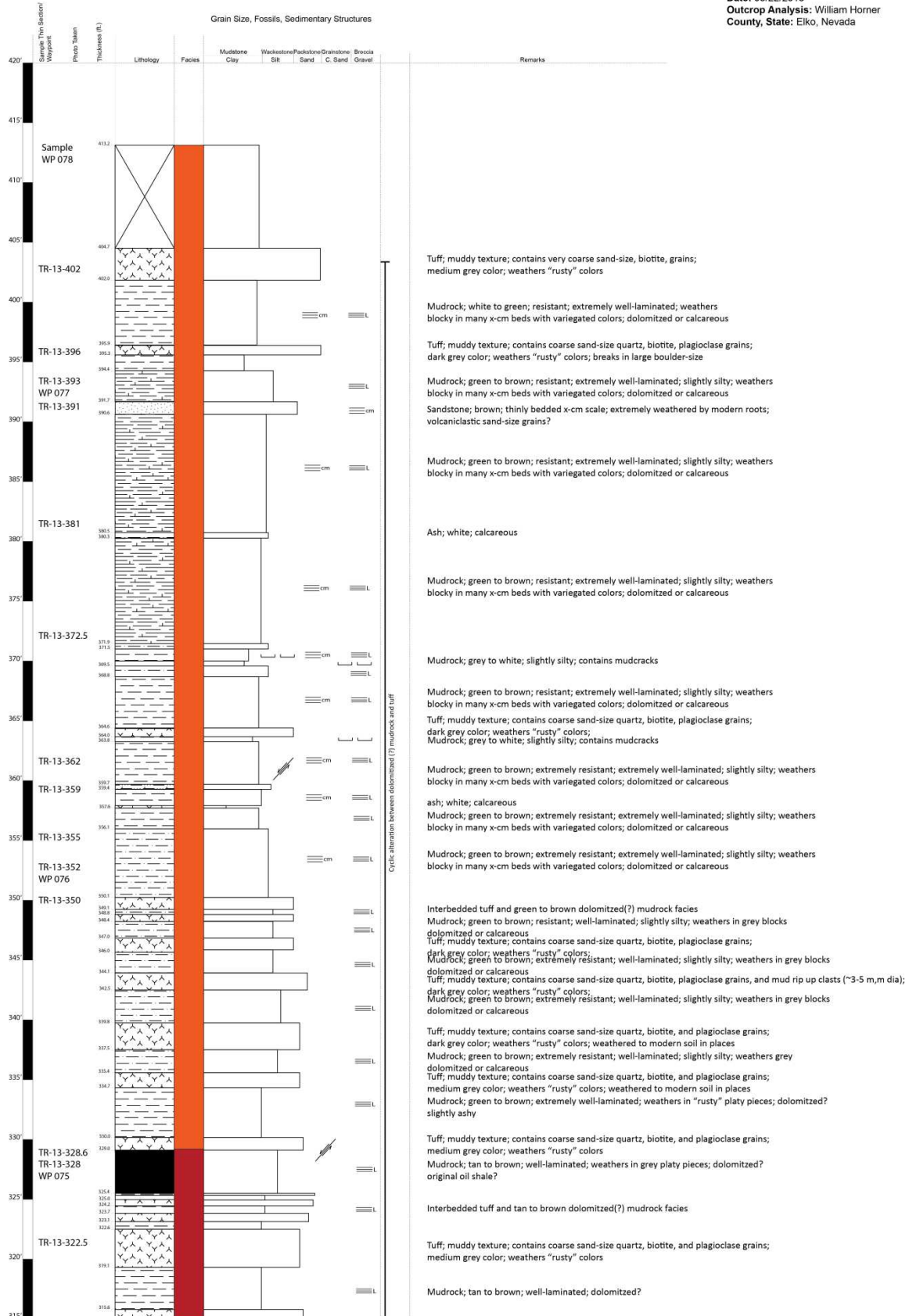


**Outcrop:** Elko Hills B (Elko Hills)  
**Stratigraphic Interval:** Elko Fm.  
**Date:** 05/23/2013  
**Outcrop Analysis:** William Horner  
**County, State:** Elko, Nevada

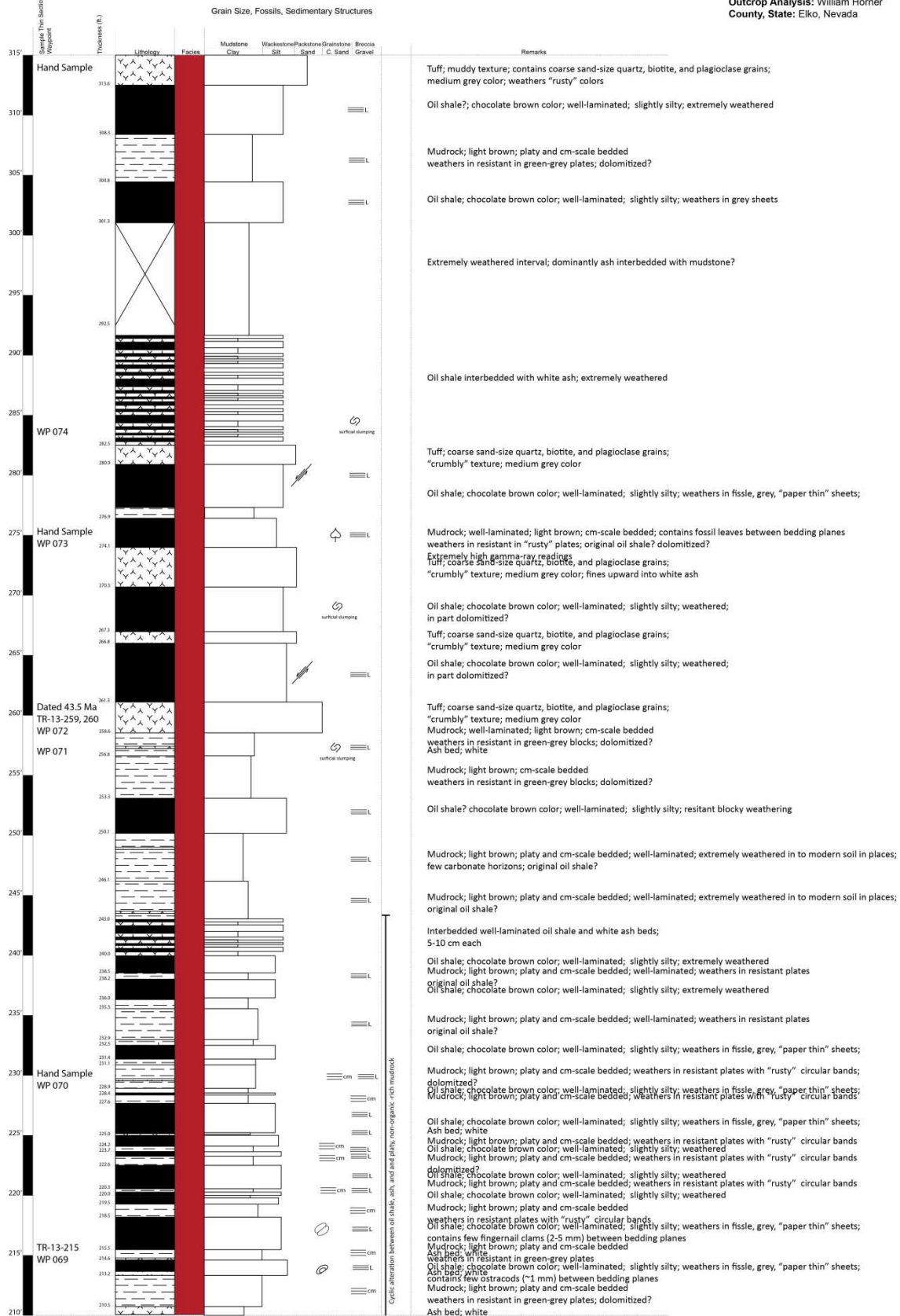


## **Tomera Ranch**

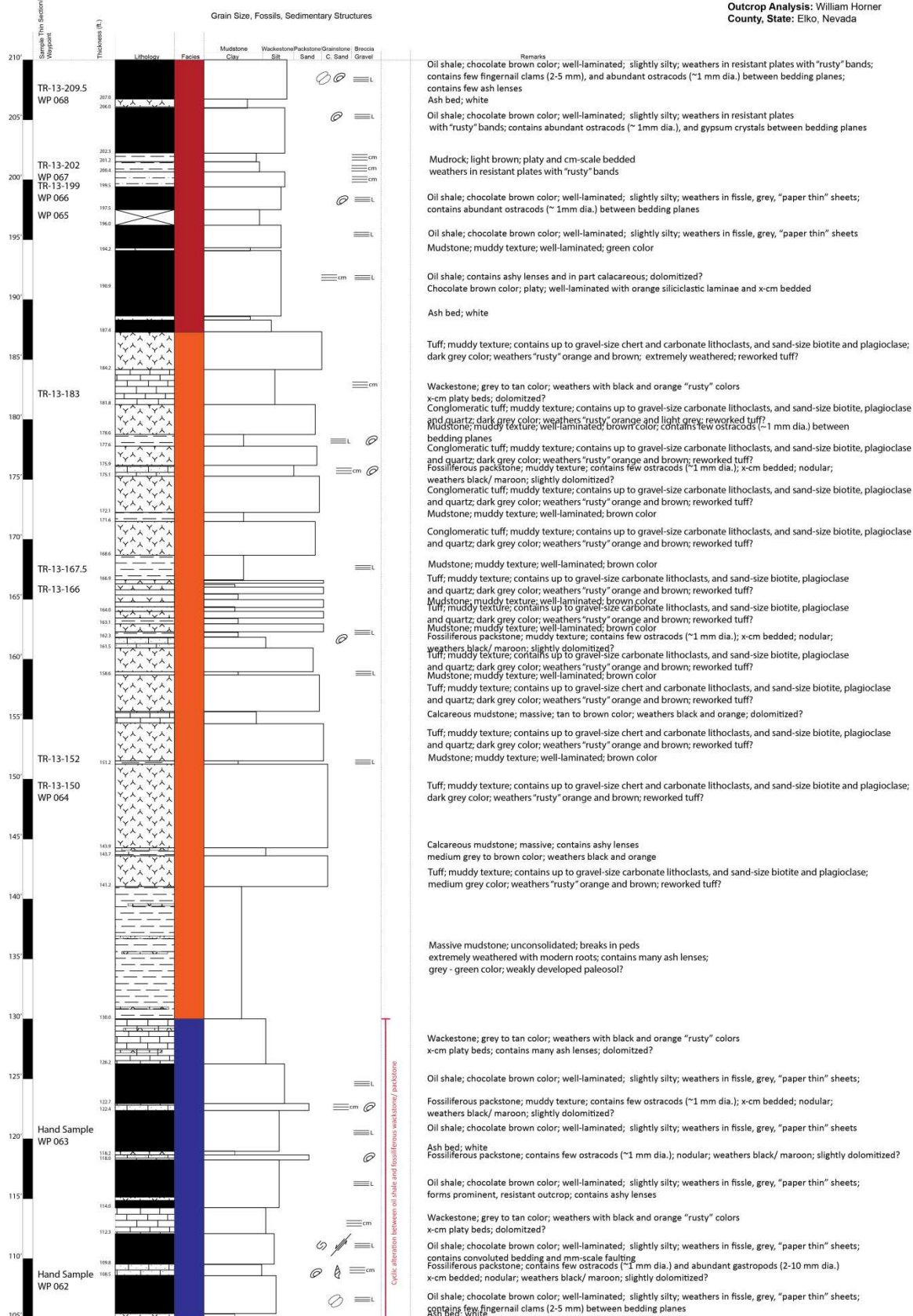
Outcrop: Tomera Ranch  
 Stratigraphic Interval: Elko Fm.  
 Date: 05/22/2013  
 Outcrop Analysis: William Horner  
 County, State: Elko, Nevada



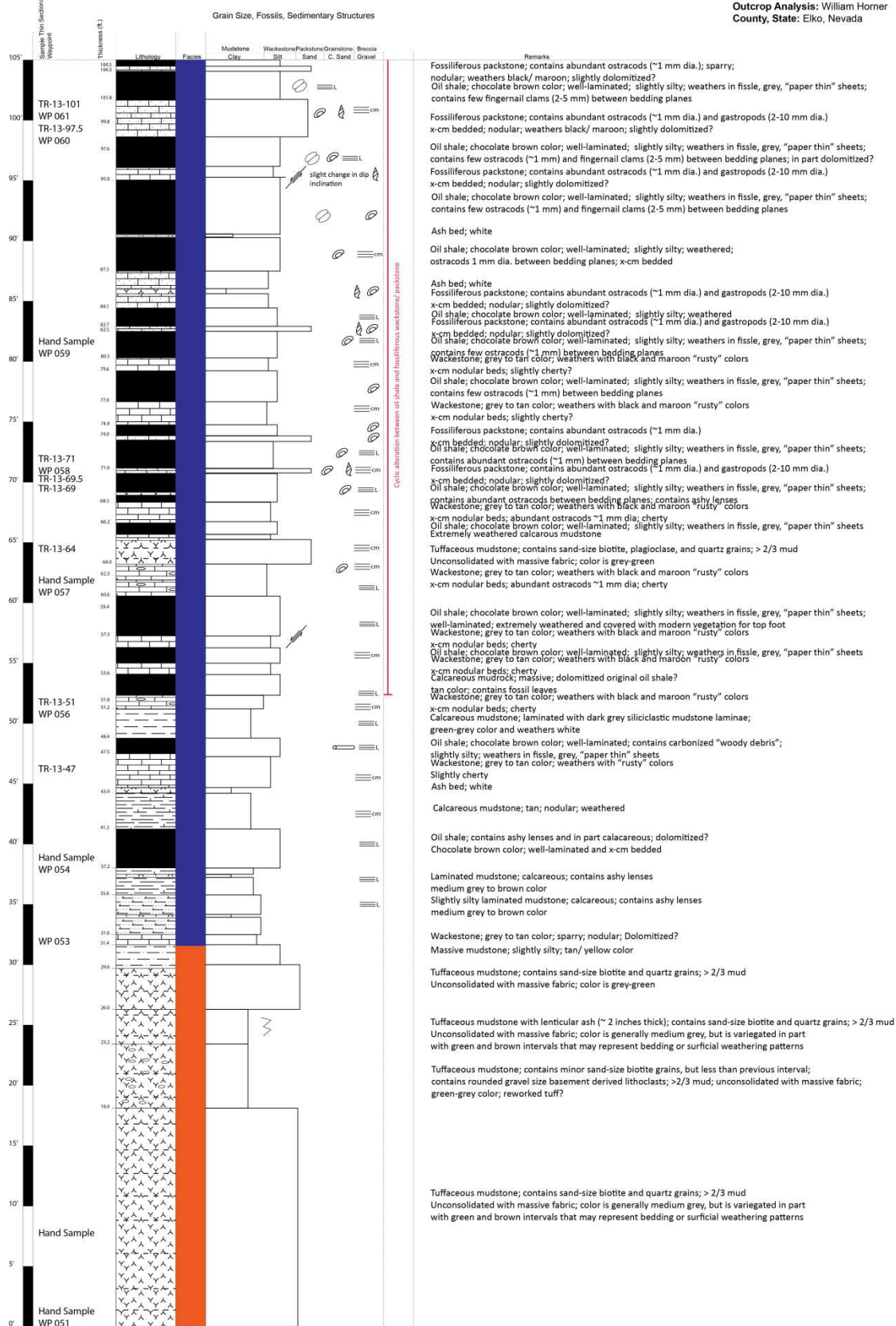
Outcrop: Tomera Ranch  
 Stratigraphic Interval: Elko Fm.  
 Date: 05/22/2013  
 Outcrop Analysis: William Horner  
 County, State: Elko, Nevada



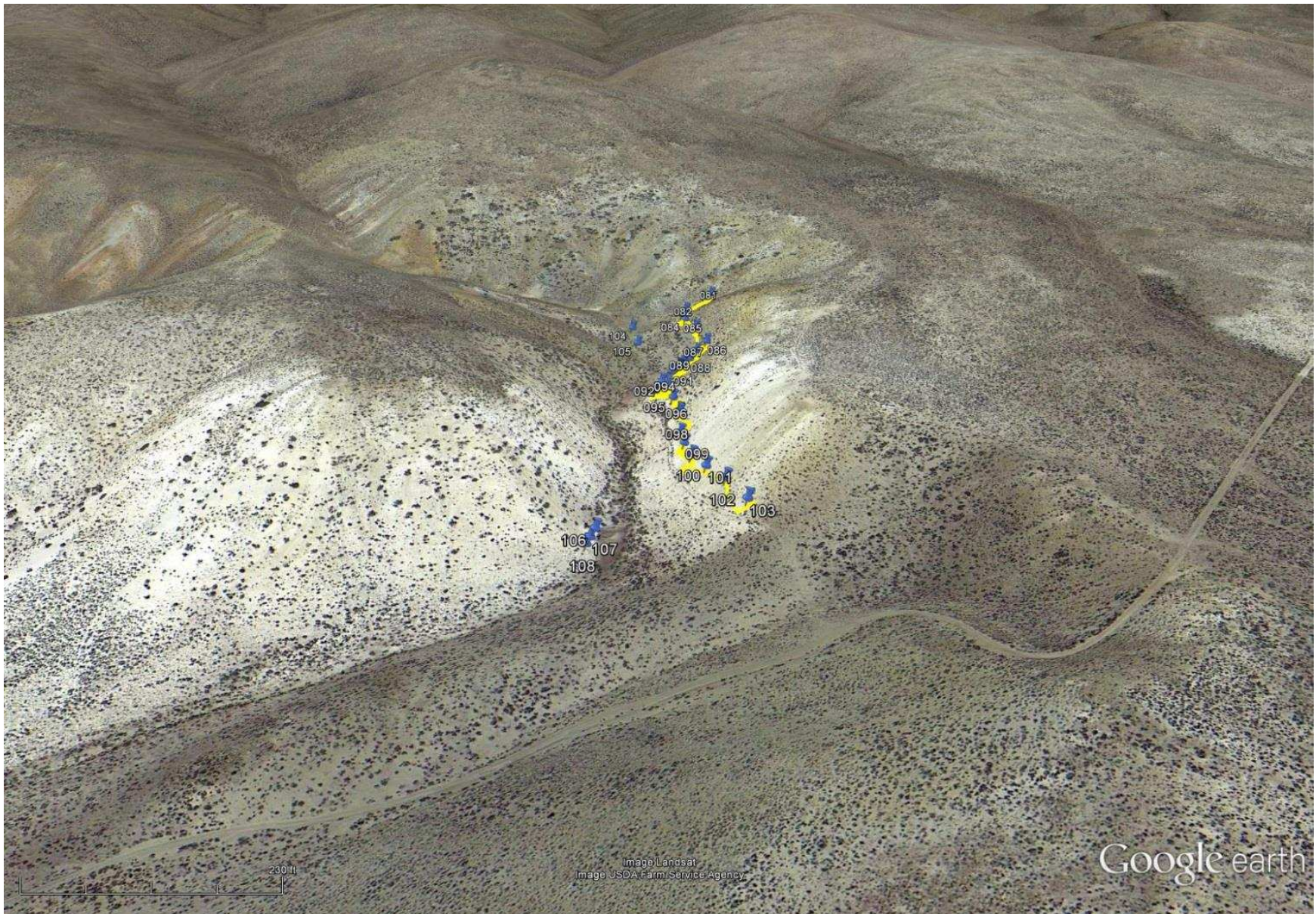
**Outcrop:** Tomera Ranch  
**Stratigraphic Interval:** Elko Fm.  
**Date:** 05/21/2013  
**Outcrop Analysis:** William Horner  
**County, State:** Elko, Nevada



**Outcrop:** Tomera Ranch  
**Stratigraphic Interval:** Elko Fm.  
**Date:** 05/23/2013  
**Outcrop Analysis:** William Horner  
**County, State:** Elko, Nevada



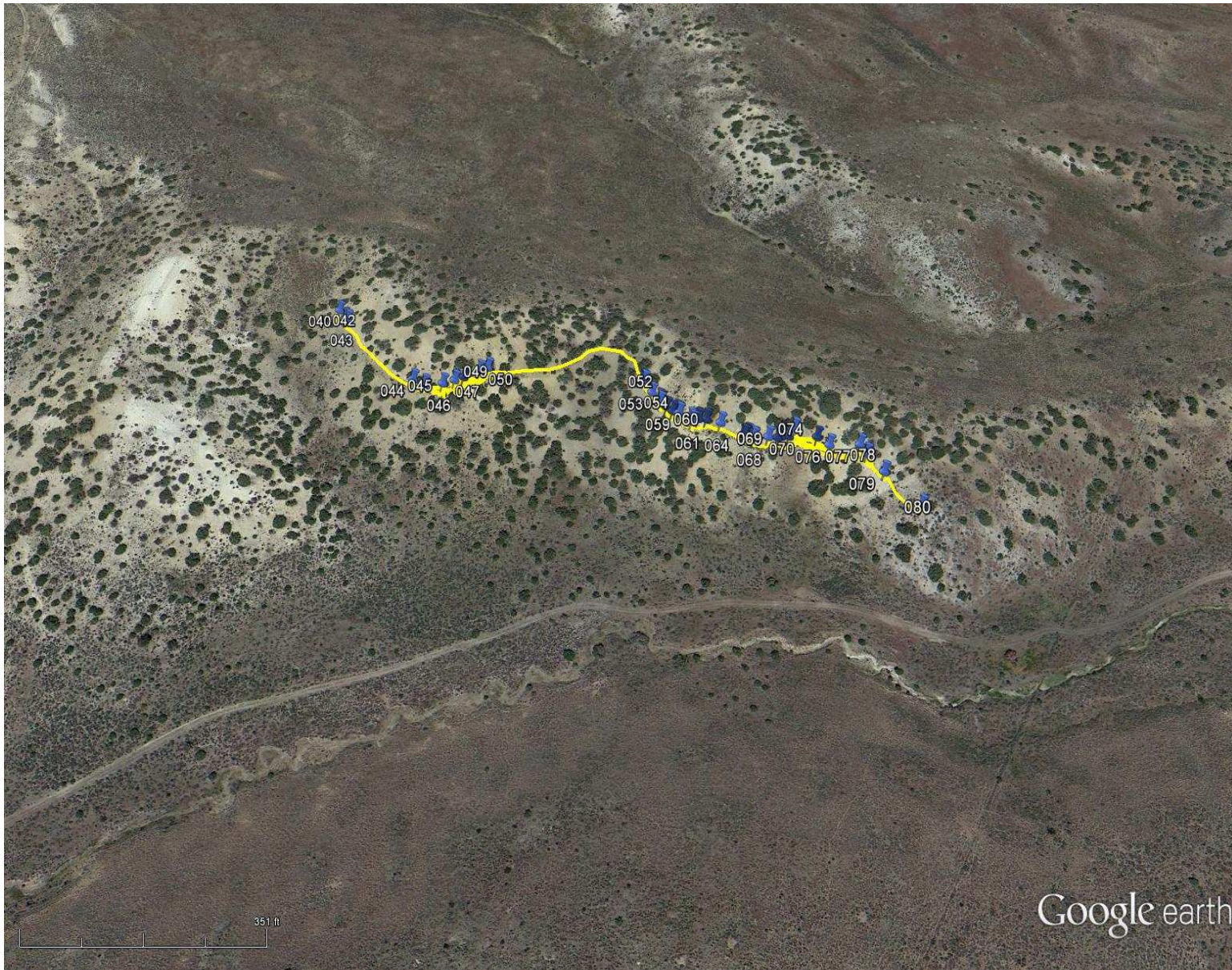
### **APPENDIX 3: OUTCROP SATELLITE VIEWS WITH WAYPOINTS**



Coal Mine Canyon



Elko Hills (A)



Tomera Ranch

## APPENDIX 4: SEM DATA OF MICROBIAL-MAT-BEARING ORGANIC-RICH MUDSTONE (F5)

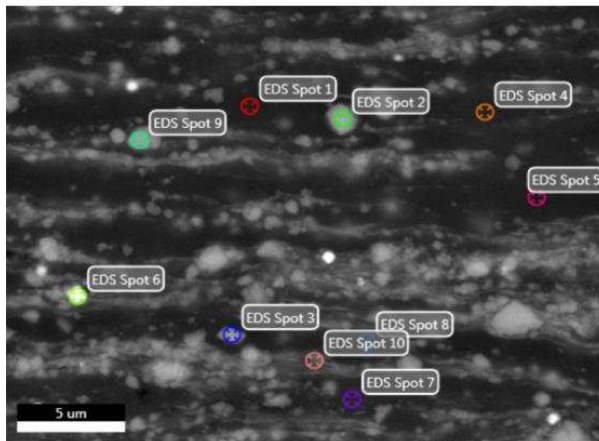
EDAX TEAM

Page 1

EOCENE

Author: segenhoff  
Creation: 8/15/2013  
Sample Name: COS-3-13-1.5

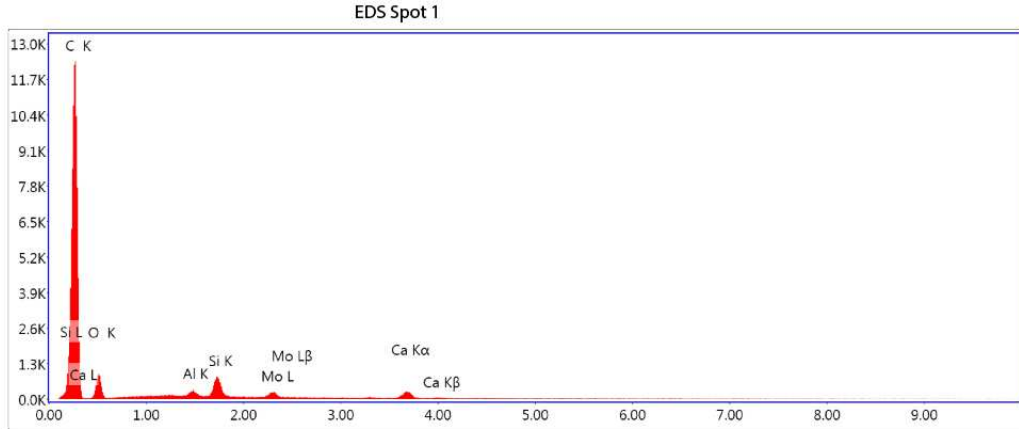
### Area 3



Notes:

EDS Spot 1

kV: 15      Mag: 5870      Takeoff: 35.5      Live Time(s): 30      Amp Time(μs): 3.2      Resolution:(eV) 128



Lsec: 30.0 0 Cnts 0.000 keV Det: Apollo X-SDD Det

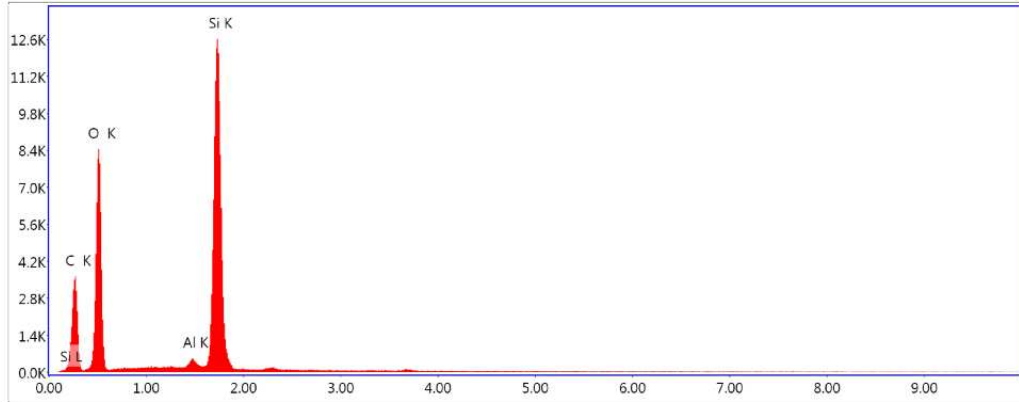
eZAF Smart Quant Results

Element	Weight %	Atomic %	Net Int.	Error %
C K	81.29	87.79	2662.79	4.72
O K	12.36	10.02	188.29	11.34
Al K	0.76	0.37	79.6	6.2
Si K	2.07	0.96	221.71	4
Mo L	1.45	0.2	63.2	8.86
Ca K	2.07	0.67	97.95	5.82

EDS Spot 2

kV: 15      Mag: 5870      Takeoff: 35.5      Live Time(s): 30      Amp Time(μs): 3.2      Resolution:(eV) 128

EDS Spot 2



Lsec: 30.0 0 Cnts 0.000 keV Det: Apollo X-SDD Det

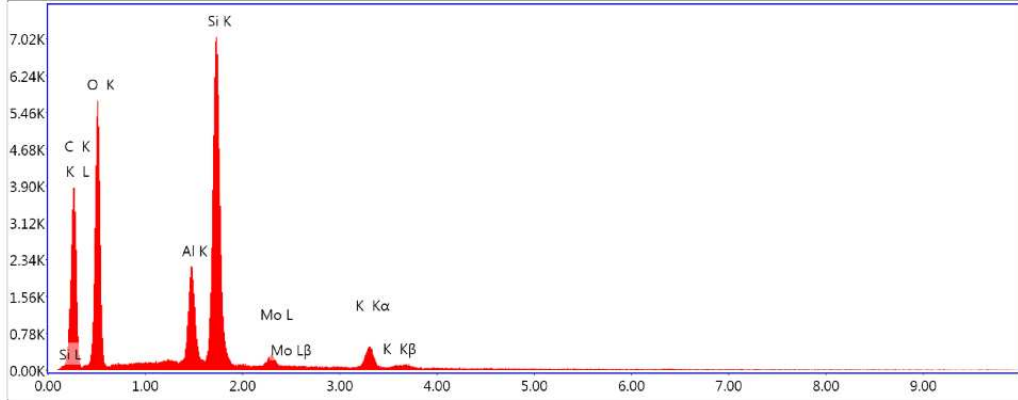
eZAF Smart Quant Results

Element	Weight %	Atomic %	Net Int.	Error %
C K	38.75	49.73	812.25	9.27
O K	40.14	38.67	1800.71	8.78
Al K	0.72	0.41	122.68	6.21
Si K	20.39	11.19	3565.81	2.62

EDS Spot 3

kV: 15      Mag: 5870      Takeoff: 35.5      Live Time(s): 30      Amp Time(μs): 3.2      Resolution:(eV) 128

EDS Spot 3



Lsec: 30.0 0 Cnts 0.000 keV Det: Apollo X-SDD Det

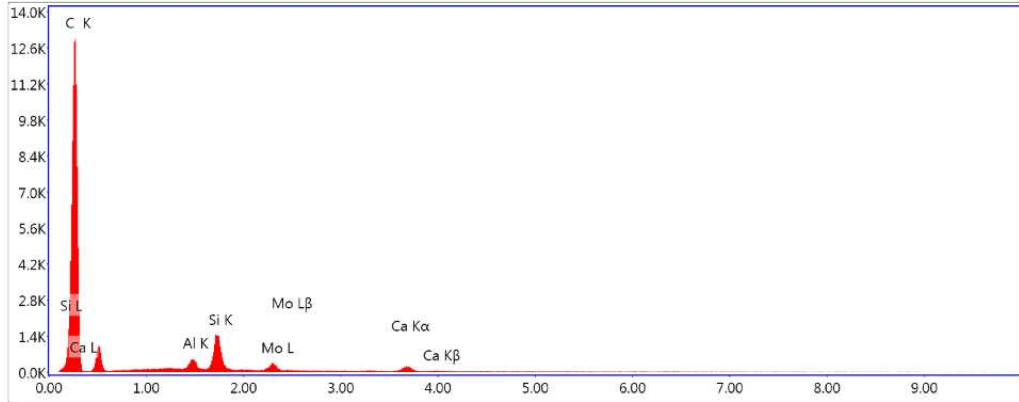
eZAF Smart Quant Results

Element	Weight %	Atomic %	Net Int.	Error %
C K	42.41	54.34	835.85	8.94
O K	35.91	34.54	1202.24	9.26
Al K	4.11	2.34	582.7	4
Si K	14.1	7.73	2008.93	3
Mo L	1.38	0.22	77.37	7.27
K K	2.09	0.82	165.23	4.51

EDS Spot 4

kV: 15      Mag: 5870      Takeoff: 35.5      Live Time(s): 30      Amp Time(μs): 3.2      Resolution:(eV) 128

EDS Spot 4



Lsec: 30.0 0 Cnts 0.000 keV Det: Apollo X-SDD Det

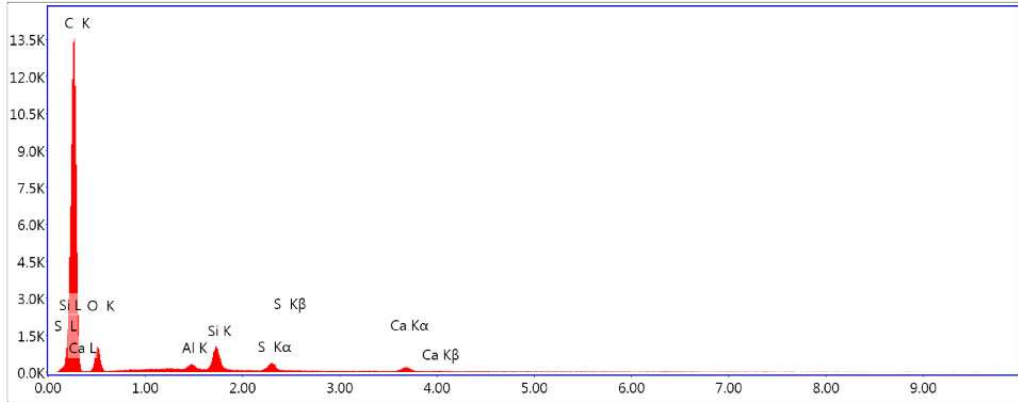
eZAF Smart Quant Results

Element	Weight %	Atomic %	Net Int.	Error %
C K	91.39	96.9	2800.69	5.13
AlK	1.23	0.58	132.17	4.9
SiK	3.84	1.74	418.01	2.92
MoL	1.89	0.25	81.95	7.69
CaK	1.65	0.52	77.8	6.95

EDS Spot 5

kV: 15      Mag: 5870      Takeoff: 35.5      Live Time(s): 30      Amp Time(μs): 3.2      Resolution:(eV) 128

EDS Spot 5



Lsec: 30.0 0 Cnts 0.000 keV Det: Apollo X-SDD Det

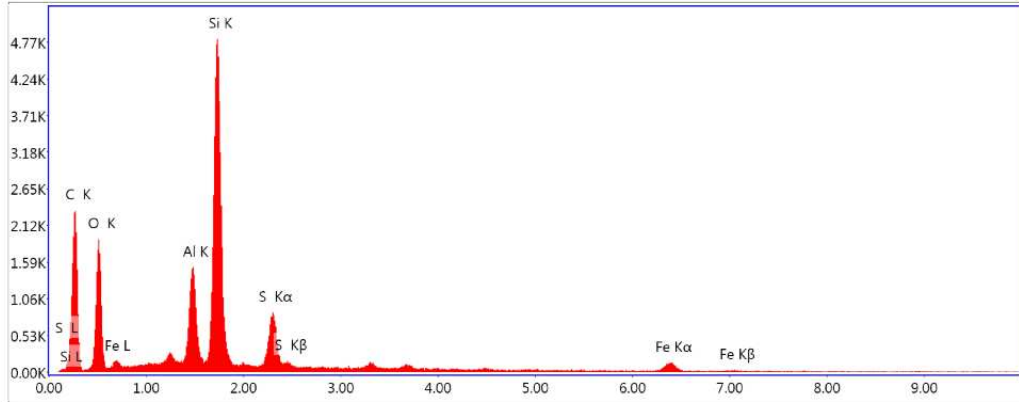
eZAF Smart Quant Results

Element	Weight %	Atomic %	Net Int.	Error %
C K	82.05	87.67	2789.9	5.12
O K	12.6	10.11	215.66	11.23
AlK	0.66	0.32	76.83	6.73
SiK	2.31	1.06	275.26	3.63
S K	1.11	0.44	104.73	6.63
CaK	1.27	0.41	66.31	8.25

EDS Spot 6

kV: 15      Mag: 5870      Takeoff: 35.5      Live Time(s): 30      Amp Time(μs): 3.2      Resolution:(eV) 128

EDS Spot 6



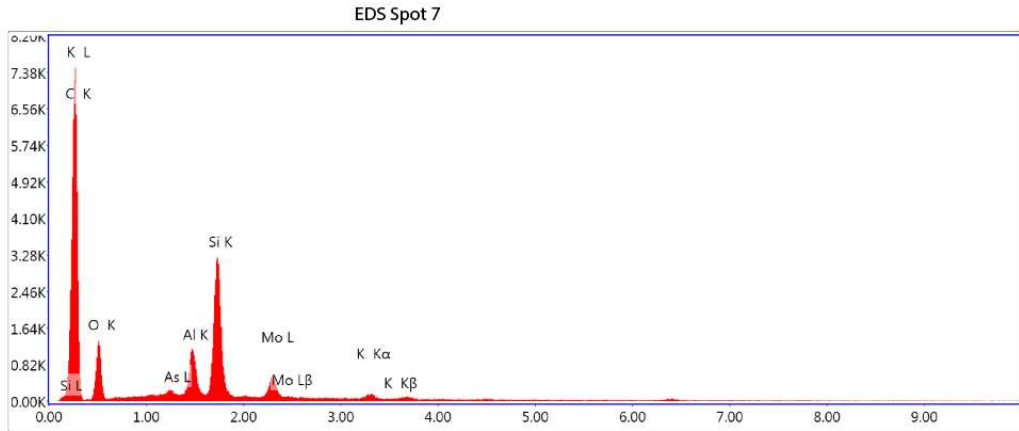
Lsec: 30.0 0 Cnts 0.000 keV Det: Apollo X-SDD Det

eZAF Smart Quant Results

Element	Weight %	Atomic %	Net Int.	Error %
C K	49.85	64.45	472.57	9.78
O K	21.77	21.13	390.01	10.03
Al K	4.63	2.66	401.97	4.28
Si K	15.72	8.69	1357.29	3.08
S K	4.08	1.97	267.78	4.06
Fe K	3.96	1.1	54.92	10.16

EDS Spot 7

kV: 15      Mag: 5870      Takeoff: 35.5      Live Time(s): 30      Amp Time(μs): 3.2      Resolution:(eV) 128



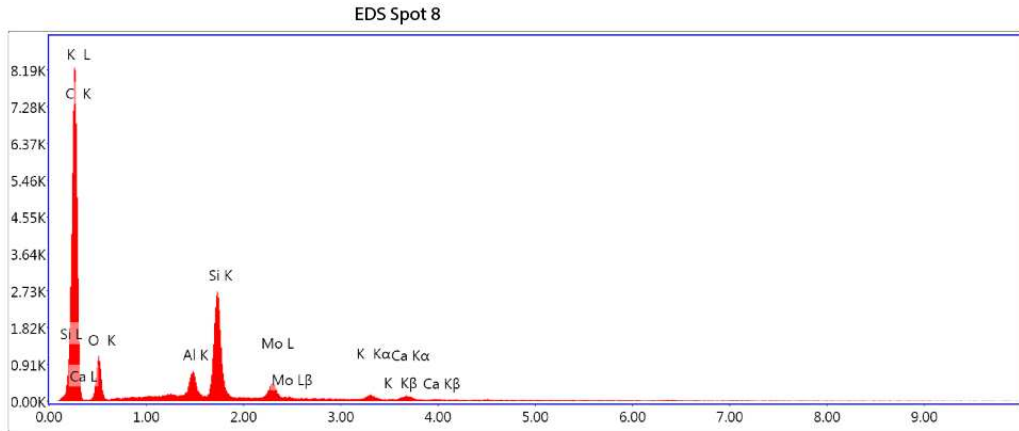
Lsec: 30.0 0 Cnts 0.000 keV Det: Apollo X-SDD Det

eZAF Smart Quant Results

Element	Weight %	Atomic %	Net Int.	Error %
C K	70.22	81.31	1566.96	7.54
O K	14.41	12.52	269.62	10.72
AsL	0.94	0.17	43.41	8.41
AlK	2.63	1.36	306.55	4.25
SiK	7.81	3.87	918.78	2.91
MoL	3.07	0.45	143.72	6.44
K K	0.92	0.33	58.6	9.65

EDS Spot 8

kV: 15      Mag: 5870      Takeoff: 35.5      Live Time(s): 30      Amp Time(μs): 3.2      Resolution:(eV) 128



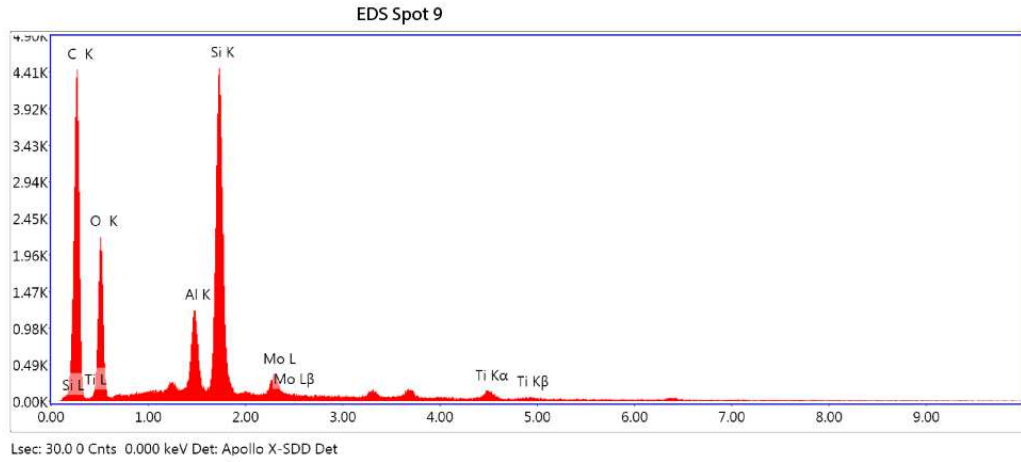
Lsec: 30.0 0 Cnts 0.000 keV Det: Apollo X-SDD Det

eZAF Smart Quant Results

Element	Weight %	Atomic %	Net Int.	Error %
CK	74.11	83.69	1752.87	6.89
OK	13.34	11.3	221.63	11.16
AlK	1.74	0.87	189.12	4.67
SiK	6.74	3.26	743.93	2.89
MoL	2.56	0.36	112.43	6.97
KK	0.74	0.26	43.81	11.07
CaK	0.77	0.26	37.21	12.71

EDS Spot 9

kV: 15      Mag: 5870      Takeoff: 35.5      Live Time(s): 30      Amp Time(μs): 3.2      Resolution:(eV) 128

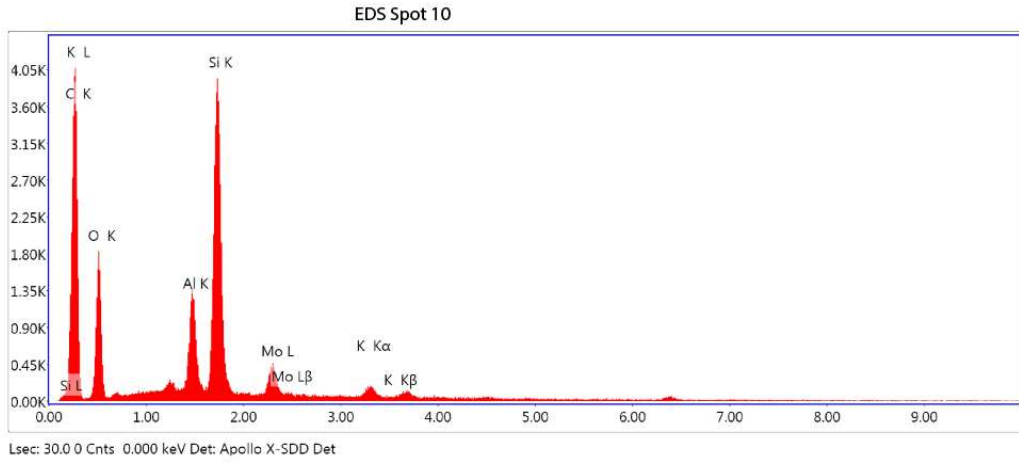


eZAF Smart Quant Results

Element	Weight %	Atomic %	Net Int.	Error %
CK	58.47	70.6	941.51	8.43
OK	22.99	20.84	434.58	10.16
AlK	3.06	1.65	313.74	4.3
SiK	12	6.19	1235.18	2.89
MoL	2.22	0.34	89.26	7.13
TiK	1.27	0.38	45.32	12.48

EDS Spot 10

kV: 15      Mag: 5870      Takeoff: 35.5      Live Time(s): 30      Amp Time(μs): 3.2      Resolution:(eV) 128



eZAF Smart Quant Results

Element	Weight %	Atomic %	Net Int.	Error %
CK	59.27	71.85	853.42	8.51
OK	21.03	19.14	352.66	10.33
AlK	3.7	2	345.8	4.2
SiK	11.78	6.11	1099.36	2.94
MoL	3.03	0.46	110.63	6.5
KK	1.19	0.44	60.36	9.72